JULIUS-MAXIMILIANS-UNIVERSITÄT WÜRZBURG

FAKULTÄT FÜR CHEMIE UND PHARMAZIE

GRADUATE SCHOOL OF BIOMEDICINE

INSTITUT FÜR PHARMAKOLOGIE UND TOXIKOLOGIE

Entwicklung und Anwendung fluoreszierender Biosensoren für cAMP und cGMP

Dissertation zur Erlangung des

naturwissenschaftlichen Doktorgrades

des Bayerischen Julius-Maximilians-Universität Würzburg

Vorgelegt von

Viacheslav Nikolaev

aus Sankt-Petersburg

Würzburg 2005

JULIUS-MAXIMILIANS-UNIVERSITÄT WÜRZBURG

FAKULTÄT FÜR CHEMIE UND PHARMAZIE

GRADUATE SCHOOL OF BIOMEDICINE

INSTITUT FÜR PHARMAKOLOGIE UND TOXIKOLOGIE

Development and application of fluorescent cAMP und cGMP biosensors

Dissertation to obtain

the academic grade in natural sciences

of the Bavarian Julius-Maximilians-University of Würzburg

Submitted by

Viacheslav Nikolaev

from Saint-Petersburg

Würzburg 2005

Eingereicht am: ... September 2005

bei der Fakultät für Chemie und Pharmazie

1. Gutachter: Prof. Dr. Martin J. Lohse

2. Gutachter: Prof. Dr. Ulrike Holzgrabe

der Dissertation

1. Prüfer: Prof. Dr. Martin J. Lohse

2. Prüfer: Prof. Dr. Ulrike Holzgrabe

3. Prüfer: Dr. Moritz Bünemann

des öffentlichen Promotionskolloquiums

Tag des öffentlichen Promotionskolloquiums: ……………………..

Doktorurkunde ausgehändigt am: ………………………………..

Erklärung

Hiermit erkläre ich an Eides statt, dass ich die Dissertation „Entwicklung und Anwendung fluoreszierender Biosensoren für cAMP and cGMP" selbständig angefertigt habe und keine anderen als die von mir angegebenen Quellen und Hilfsmittel benutzt habe.

Ich erkläre außerdem, dass diese Dissertation weder in gleicher oder anderer Form bereits in einem anderen Prüfungsverfahren vorgelegen hat.

Ich habe früher außer den mit dem Zulassungsgesuch urkundlich vorgelegten Graden keine weiteren akademischen Grade erworben oder zu erwerben versucht.

Würzburg, den 12. September 2005

Contents

Abbreviations

AC	Adenylyl cyclase
ACTH	Adrenocorticotropic hormone
AKAP	A-kinase anchoring protein
Alpren	Alprenolol
cAMP	Adenosine-3',5'-cyclic monophosphate
ANP	Atrial natriuretic peptide
Anti-β_1-AR	Anti-β_1-adrenergic receptor antibodies
ATP	Adenosine triphosphate
β_1-AR	β_1-adrenergic receptor
BFP	Blue fluorescent protein
Biso	Bisoprolol
Carved	Carvedilol
CFP	Enhanced cyan fluorescent protein
CICR	Calcium-induced calcium release
CNBD	Cyclic nucleotide-binding domain
CREB	cAMP response element-binding protein
DMEM	Dulbecco's modified Eagle's medium
E.coli	Escherichia coli
EDTA	Ethylenediaminetetraacetic acid
EHNA	Erythro-9-(2-hydroxy-3-nonyl)-adenine
Epac	Exchange protein directly activated by cAMP
FCS	Fetal calf serum
Fig.	Figure
FRET	Fluorescence resonance energy transfer
GAF	CNBDs in c**G**MP-regulated phosphodiesterases, bacterial **A**denylyl cyclases and transcription activator **F**lhA
GC	Guanylyl cyclase

GFP	Green fluorescent protein
GK	cGMP-dependent protein kinase
cGMP	Guanosine-3',5'-cyclic monophosphate
GPCR	G-protein coupled receptors
h	Hour
HCN	Hyperpolarization-activated cyclic nucleotide-gated channel
HEPES	4-(2-hydroxyethyl)-1-piperazineethanesulfonic acid
IgG	Immunoglobulin G
IP_3	Inositoltrisphosphate
Iso	Isoproterenol
Meto	Metoprolol
min	Minute
NE	Norepinephrine
NPRA	Natriuretic peptide receptors
NTE	Neuropathy target esterase
PBS	Phosphate buffered saline
PDE	Phosphodiesterase
PCR	Polymerase chain reaction
PKA	cAMP-dependent protein kinase
RGS	Regulators of G-protein signaling
RIA	Radioimmuno assay
s	Second
S.D.	Standard deviation
S.E.	Standard error
SMC	Smooth muscle cells
SNP	Sodium nitroprusside
Tris	Tris-(hydroxymethyl)-aminomethan
VASP	Vasodilator-stimulated phosphoprotein
YFP	Enhanced cyan fluorescent protein
ZG	Adrenal *zona glomerulosa*

1 Introduction

Membrane G-protein coupled receptors (GPCR) and intracellular second messengers such as calcium, phosphoinositides, cAMP and cGMP play a central role in the communication between numerous cells of an organism, providing a fast response to rapidly changing physiological conditions in order to maintain homeostasis and finely regulate multiple functions inside a cell.

Biochemical science of the 20th century made it possible to understand and thoroughly characterize basic principles of intracellular signalling. Despite their ease of use, good performance and availability, standard biochemical methods have only a relatively low temporal resolution, i.e. they can measure a certain biochemical parameter or biological function on the scale of seconds, whereas the most important processes of cellular signalling have emerged to occur as rapidly as on the millisecond scale. Moreover, standard techniques required a batch of cells to be destroyed in order to yield a small amount of the cytosol to measure the concentrations or activity of the molecules of interest. This does not allow to achieve a higher, subcellular spatial resolution and to study the behaviour of a single live cell.

At the end of the last century novel microscopic techniques were developed, which combined with fluorescence have for the first time allowed to monitor biochemical events inside a single live cell. They gave an opportunity to study

intracellular processes with a high temporal (millisecond scale) and spatial (nanometre range) resolution and to increase our understanding of cell physiology. Single cell fluorescence microscopy has also made it possible to get new insights into the pathophysiology of different diseases and to search for therapeutic agents that have a distinct molecular mechanism of action at the level of the molecules involved in intracellular signalling.

1.1   cAMP and cGMP cascades and their physiological significance

Cyclic adenosine monophosphate (cAMP) was discovered in the early 1950s as an intracellular regulator of glucose metabolism, which was responsible for the modulation of the glycogen phosphorylation in response to noradrenalin stimulation[1-3]. Later on it was appreciated that β-adrenergic receptors couple to the class of G proteins called G_s (*s* for stimulatory), which in turn are capable of activating adenylyl cyclases located in the plasma membrane and producing cAMP from ATP[4-9] (Fig. 1). The complexity of the cascade from the receptor to cAMP-production has at least two biological functions. First, it enables multiple mechanisms and modalities of regulation of the signalling through the modulation of receptor activity (e.g. by receptor kinases, phosphatases and arrestins)[10], G-protein cycle (e.g. by RGS proteins)[11,12] and adenylyl cyclase (e.g. by other receptors through G_i-proteins, *i* for inhibitory)[13]. Secondly, there is an

amplification of the signal, which occurs in the cascade. One activated receptor can switch on several G-proteins, each of which activates an adenylyl cyclase, producing thousands of cAMPs per second. This amplification results in a production of micromolar amounts of the second messenger in response to nanomolar hormone concentrations, and this leads to a high sensitivity of a cell towards the constantly changing physiological conditions in order to provide a fast and adequate response[14].
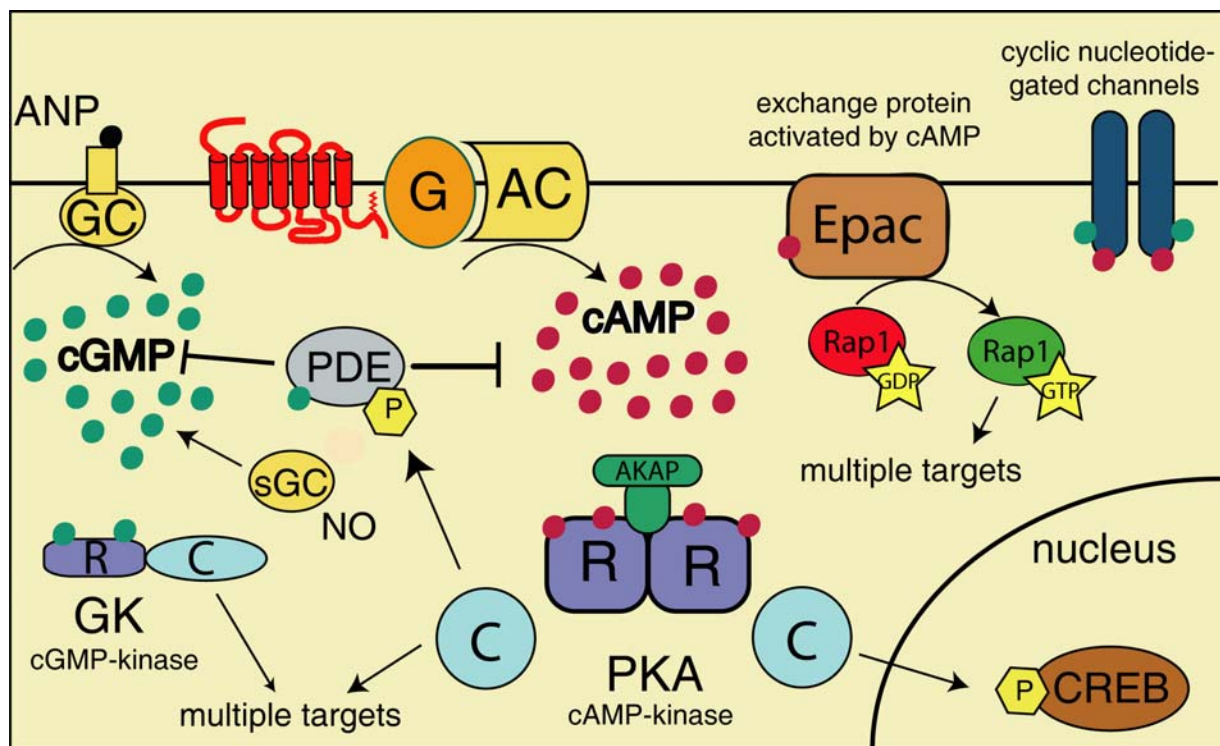
Fig. 1. cAMP and cGMP signalling cascades in a typical animal cell and their interactions. cAMP is produced by the family of G-protein-regulated adenylyl cyclases and elicits its effects in a cell by activating three kinds of effectors: PKA, Epac and cyclic nucleotide-gated channels. cGMP is a second messenger, which is synthesized by soluble NO-activated (sGC) or a membrane-bound (particulate) guanylyl cyclase (GC), located in the intracellular domain of an ANP-receptor. Three classes of cGMP targets are cGMP-dependent protein kinases (GK), cGMP-activated phosphodiesterases (PDE) and cGMP-gated channels.

Being an ubiquitous second messenger cAMP regulates a wide variety of cellular events and biological processes from metabolism and gene expression[15], cell division[16] and migration[17], exocytosis[18] and insulin secretion[19] to immune defence[20], memory formation[21] and cardiac frequency[22]. How can such a small molecule account for hundreds of biological effects? Since its discovery in the 1950s until the end of the last century only one single effector of cAMP, namely cAMP-dependent protein kinase (PKA), was supposed to convey all cAMP effects in different cells[1,23]. PKA is a complex enzyme, which in higher animals consists of four subunits, two regulatory and two catalytic, brought together by a series of intermolecular interactions[23,24]. In protozoa, such as *Dictyostelium discoideum*, PKA is a complex of only one regulatory and one catalytic subunit. The catalytic subunits are only active when they are released from the regulatory subunits as a result of the complex activation by cAMP (Fig. 1, Fig. 2). Each regulatory subunit has two binding sites, which bind cAMP with different affinities. Cooperative occupation of both leads through a series of conformational rearrangements to the release of the catalytic subunits from the complex[23-25]. Free catalytic subunits are then active and can phosphorylate a myriad of substrates regulating diverse intracellular functions until it becomes proteolytically degraded or binds again to a regulatory subunit[23,26]. The catalytic subunit can freely diffuse through the pores into the nucleus, where it activates CREB, which is a protein that regulates transcription of many different genes[15]. Another classical example of a PKA substrate is an L-type calcium channel,

which accounts for calcium influx and enhanced contractility of cardiac myocytes after adrenergic stimulation[27,28].

In 1998 it became evident that PKA represents not the only target of cAMP. At that time new avenues for cAMP research were opened up by the discovery of exchange protein directly activated by cAMP (Epac)[29,30], which is expressed in the brain[31], heart, liver and some further tissues[32]. In addition to PKA, Epac serves as an important intracellular effector for cAMP[33]. Epac is a protein consisting of a regulatory cAMP binding site and a catalytic domain (Fig. 2), which has the function of GTP-loading of a small G-protein, Rap1, and maintaining its active state (Fig. 1). Rap1 has several functions including the modulation of MAPK-kinase cascade through Raf-1[33,34] and cell adhesion through the regulation of integrin expression[35,36]. Another important function of Rap1 is the stimulation of exocytosis. It was demonstrated that Epac binds to Rim (Rab3-interacting molecule, Rab3 being a small G protein), which is a putative regulator of fusion of vesicles to the plasma membrane. Epac, through its interaction with Rim2, mediates in neuron-like PC12 and insulin-secreting cells cAMP-induced, calcium-dependent secretion that cannot be blocked by an inhibitor of PKA[18]. Epac-dependent regulation seems also to play a central role in insulin secretion. 8-(4-chloro-phenylthio)-2'-*O*-methyladenosine-3',5'-cyclic monophosphate (8-pCPT-2'-*O*-Me-cAMP), which is a selective Epac activator, acts in human pancreatic beta-cells and INS-1 insulin-secreting cells to mobilize calcium from intracellular stores via Epac-mediated calcium-induced calcium

release (CICR). The cAMP-dependent increase of intracellular calcium that accompanies CICR is shown to be coupled to exocytosis. Interaction of cAMP and Epac to trigger CICR explained the blood glucose-lowering properties of an insulinotropic hormone (glucagon-like peptide-1), which is now under investigation for use in the treatment of type-2 diabetes mellitus[37,38].

The third intracellular target of cAMP that has been identified around two decades ago are the cyclic nucleotide-gated channels which are present in olfactory epithelium of the nose and in semen. The family of hyperpolarization-activated, cyclic nucleotide-modulated (HCN) channels are crucial for a range of electrical signalling, including cardiac and neuronal pacemaker activity, setting resting membrane electrical properties and dendritic integration[39]. These non-selective cation channels are activated by membrane hyperpolarization and modulated by the binding of cyclic nucleotides such as cAMP and cGMP (Fig. 2)[40]. The cAMP-mediated enhancement of channel activity is largely responsible for the increase in heart rate caused by β-adrenergic agonists[41].

Computer-based analysis of the protein sequence databases has allowed to find some further candidates to bind cAMP and maybe responsible for some yet unknown functions of this second messenger[42]. One such candidate is neuropathy target esterase (NTE), which is a large transmembrane protein with a serine esterase activity, catalysing hydrolysis of lysophospholipids. It is abundantly expressed in neurons of the brain, but also in a variety of non-neuronal tissues including intestine, placenta, testis and kidney. NTE inhibition

by organic phosphorus esters is responsible for the delayed neuropathy characterised by a paralysis of the lower limbs due to degeneration of long axons in the spinal cord and in peripheral nerves. The catalytic domain of NTE is located in the C-terminal part of the protein; the N-terminal part, which contains the three putative cNMP-binding domains, may serve as a regulatory domain[42].

In summary, three classes of functionally significant cAMP targets have been demonstrated so far. cAMP conveys its effect in cells by activating PKA, Epac and cAMP-gated channels.
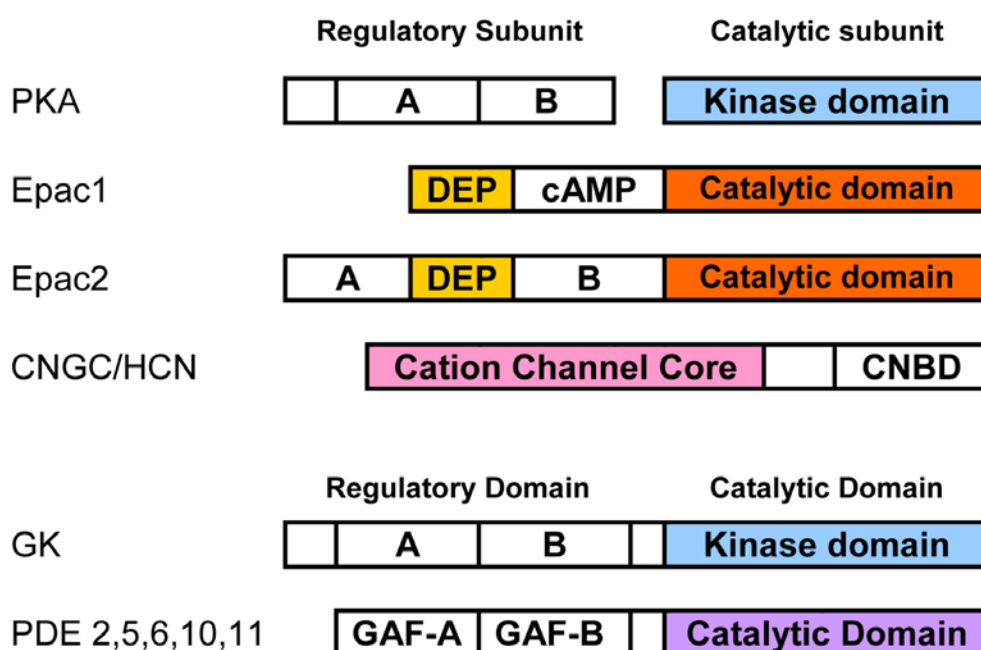
Fig. 2. Cartoon depiction of modular structures of cellular proteins that interact with cAMP and cGMP. cAMP binds to A and B domains of regulatory subunit of PKA, as well as to regulatory domains of Epacs and CNG/HCN channels. cGMP interacts with high affinity A and low affinity B domains of GK, with regulatory GAF domains of PDEs and also with CNBD of the channels. DEP – Dishevelled, Egl-10, Pleckstrin domain, responsible for membrane targeting of Epac.

Another ubiquitous and important second messenger is **cyclic guanosine monophosphate** (cGMP), which is produced by two kinds of guanylyl cyclases (Fig. 1). **Membrane-bound guanylyl cyclase** is represented by an intracellular domain of natriuretic peptide receptors (NPR)[43,44]. These receptors, unlike GPCR comprised of seven transmembrane helices, consist of 3 distinct domains: extracellular domain, transmembrane region and intracellular domain. The extracellular domain is supposed to bind peptide ligands, members of the natriuretic peptide family ANP (atrial), BNP (brain) or CNP (C-type) natriuretic peptides. These are peptide hormones (22-27 amino acids), which are produced by specialized secretory cells in response to elevated blood volume. For example, in cardiac atrium secretion of ANP is induced by hypervolemia[45]. The physiological role of ANP is to reduce blood volume by stimulating kidney excretion sodium and, hence, water through inhibition of aldosterone production, which is under the control of cAMP-stimulating adrenocorticotropic hormone (ACTH). Such a negative feed-back loop of hormone regulation ends up in the aldosterone producing cells of the adrenal *zona glomerulosa.* Activation of ANP-receptors in these cells induces their conformational change[46], activating through the transmembrane helix the intracellular domain of the receptor bearing the guanylyl cyclase, which starts to synthesize cGMP. The latter is a freely diffusible second messenger that activates a specific phosphodiesterase PDE2, which hydrolyzes cAMP and this in turn reduces aldosterone production[47,48]. There have been three types of NPR receptors

described, which differ in their ligand binding properties and domain architecture. NPR-A receptors bind ANP and BNP, NPR-B - only CNP. NPR-C receptor binds all three peptides but lacks the intracellular guanylyl cyclase domain. Its function is to bind and degrade the peptides, reducing their concentrations in the blood and in tissues[44].

The second type of guanylyl cyclases is a **soluble guanylyl cyclase**[49], which is located in the cytosol of almost all mammalian cells and mediates a wide range of important physiological functions, such as inhibition of platelet aggregation, relaxation of smooth muscle, vasodilatation, neuronal signal transduction, and immunomodulation[50]. This enzyme is a heterodimeric protein consisting of α- and β-subunits, and expression of both subunits is required for catalytic activity[51-53]. Each subunit has an N-terminal regulatory domain and a C-terminal catalytic domain that shares sequence homology with the corresponding domains in membrane-bound guanylyl and adenylyl cyclases[54-56]. Soluble GC is activated by nitric oxide (NO), a paracrine vasorelaxant initially termed EDRF, for endothelium derived relaxant factor[57] (Fig. 1). In experiments as well as in clinical therapy this GC could be switch on by the so-called NO-donors, substances that release NO once having appeared in the cytosol of a cell, e.g. sodium nitroprusside (SNP) and nitroglycerine .

cGMP is a key player in the regulation of various physiological processes, including smooth muscle tone[58], neuronal excitability[59], epithelial electrolyte transport[60], phototransduction in the retina[61-63], and cell adhesion[64]. The effects

9

of cGMP in cells are exerted by activation of three different effectors (Fig. 1):

cGMP-dependent protein kinase (GK), cGMP-activated isoforms of PDE[58] and cyclic-nucleotide-gated ion channels[65,66].

GK is a well characterized protein kinase, which is activated by cGMP and phosphorylates numerous target proteins. In contrast to PKA, GK is a single chain kinase, containing regulatory and catalytic domains in one protein of around 700 amino acids (Fig. 2). Elevation of intracellular cGMP induces a binding-dependent activation of GK leading to the catalytic transfer of the phosphate from ATP to a serine or threonine residue on the target protein. This phosphorylated protein then mediates the translation of an extracellular stimulus into a specific biological function. Two different genes for GK have been identified in mammals. One gene is located on human chromosome 10 and codes for the Ia and Ib isoforms, which arise from alternative splicing of the N-terminal region[67]. The other is located on human chromosome 4 and encodes GK II [68]. GKI is a cytosolic 76-kDa homodimer widely expressed in mammalian tissues, especially in cerebellum, platelets, and smooth muscle[69]. The difference in the N-terminal domain between two GK subtypes confers different binding affinities for cGMP. GKIa has high and low affinity binding sites that display positive cooperative behaviour. GKIb has two cGMP binding sites characterized by lower affinity and cooperativity[59,67]. GKIa is mainly detected in the vascular system, kidney, and adrenal gland, whereas GKIb is expressed in the uterus[67]. GKII is an 86-kDa membrane-bound homodimer. It is absent from the

cardiovascular system, abundant in brain and intestine, and is also expressed in lung, kidney, and bone[69-71]. The amino acid sequence of GKII differs from that of GKI principally at the N-terminus, where unique sites direct intracellular localization of the enzyme. GKII contains a myristoylation site that is required for membrane association[69]. A major difference between the two GKs is that the cGMP binding sites in GKII have much lower affinity and cooperativity. Another difference is a significant divergence in their substrate selectivity[59]. Moreover, the two forms of GK are expressed in different cells, with the exception of chondrocytes in the growth plate in the tibia of newborn mice[72]. All known GKs are composed of N-terminal, regulatory, and catalytic domains. The N-terminal domain contains five regulatory sites: (1) the subunit dimerization site, consisting of an α-helix with a conserved leucine/isoleucine repeat; (2) autoinhibitory sites, involved in the inhibition of the catalytic domain in the absence of cGMP; (3) autophosphorylation sites, which in the presence of cGMP may increase the basal catalytic activity and the affinity of GKs for cAMP; (4) a site regulating the affinity and the cooperative behaviour of the cGMP binding sites; and (5) the intracellular localization site, which determines the interaction of the enzyme with specific subcellular structures. The regulatory domain contains two cyclic nucleotide binding sites termed "A" and "B" that allow for full activation of the enzyme after specific binding of two molecules of cGMP (Fig. 2). Finally, the catalytic domain, located at the C-terminus, contains the binding sites for Mg-ATP and the target protein[59,60,69].

A broad range of **proteins** are **phosphorylated by GKs**. GKI is supposed to primarily regulate intracellular calcium in the cytosol, while GKII modulates fluid homeostasis at the cell membrane. Biological substrates for GKI may be conceptually subdivided into three main groups, "classical," "new," and "hypothetical" targets. *"Classical" targets* are clearly recognized as substrates, *in vitro* and/or *in vivo*, are phosphorylated by GKI, and have well established functions. This group includes: (1) the inositoltrisphosphate (IP$_3$) receptor and phospholamban (cGMP-mediated phosphorylation leads to calcium sequestration in the endoplasmatic reticulum), which are primarily implicated in smooth muscle cell (SMC) relaxation[73,74]; (2) the vasodilator-stimulated phosphoprotein (VASP) and vimentin, which are involved in platelet and neutrophil activation, respectively[75,76]; (3) the G substrate, which is strongly expressed in cerebellar Purkinje cells where it acts as a phosphatase inhibitor[77]; and (4) the thromboxane A2 receptor, whose activation was found to be inhibited by GK-mediated phosphorylation in platelets[78]. *"New" target proteins* are GKI substrates that either have been described recently or have conflicting evidence regarding their phosphorylation by GKI. This group includes: (1) the L-type calcium channel and the calcium-activated K1 channel which, upon phosphorylation, contribute to the regulation of vascular smooth muscle tone and cardiac contractility[79,80]; (2) the calcium-dependent cytosolic phospholipase A2, implicated in intestinal smooth muscle relaxation[81]; (3) a tyrosine hydroxylase whose activity in intact bovine chromaffin cells was observed to

increase after GKI-mediated phosphorylation[82]; and (4) the myosin-binding subunit of myosin light chain phosphatase, which mediates SMC relaxation and vasodilation[83]. Most, if not all, of these substrates are phosphorylated by the GKIa. *"Hypothetical" target proteins* have been suggested, but not demonstrated, to be phosphorylated by GKIb. This group contains putative substrates predicted on the basis of experimental demonstrations of cGMP/GKI mediated processes. For example, cytoskeletal and contractile proteins (i.e., myosin light chain, calponin, desmin, connexins) are thought to be GKIb target molecules in the regulation of vascular remodelling and neoangiogenesis[64,84]. Similarly, synaptic vesicle proteins (i.e., rabphilin-3A) may be phosphorylated by GKI and mediate synaptic plasticity and neurotransmission[85-87]. The cGMP/GKI pathway has been implicated in the control of gene expression of various promoter response elements (i.e., serum response element, AP-1 binding site, and CREB)[88,89]. In contrast to GKI, the only recognized classical substrate that is phosphorylated by GKII is the cystic fibrosis transmembrane conductance regulator in intestinal mucosal cells[90]. Localization of GKII in the apical membranes of the enterocytes of the small intestine permits it to phosphorylate this protein in response to cGMP formation. The phosphorylation of transmembrane conductance regulator induces an electrogenic chloride current and subsequent water secretion in the intestine. Co-localization and co-regulation of the expression of GKII and a chloride channel in the inner medulla of rat kidney suggest that a similar mechanism may regulate renal function[91,92].

GKII may also control the renin system and endochondral ossification and growth of bone[72,93]. However, the target molecules in these latter processes are unknown.

The second important class of cGMP effectors are phosphodiesterases (**PDEs**). This is a class of enzymes consisting of 11 families including multiple isoforms hydrolysing cyclic nucleotides[94,95]. Each member contains a conserved catalytic domain of around 270 amino acids located on the C-terminus (Fig. 2). This domain cleaves the phosphodiester bond, hydrolyzing the 3', 5'-cyclic nucleotide to its corresponding nucleotide, 5'- monophosphate. PDE families 1, 2, 3, 10, and 11 hydrolyze both cGMP and cAMP; PDE families 4, 7, and 8 preferentially cleave cAMP; and PDE families 5, 6, and 9 specifically hydrolyze cGMP. The activity of PDEs is crucial for cellular signalling because metabolism of cyclic nucleotides modulates their intracellular concentrations and affects subsequent cellular and behavioural responses. PDEs regulate for example cardiac functions, adrenal steroidogenesis, the male erectile response, and phototransduction[58]. Specific PDE targeting sites may localize the enzyme in close proximity to selected proteins, thereby modulating cyclic nucleotide levels in specific compartments.

Cyclic GMP regulates PDEs through three different mechanisms: (1) increasing activity through mass action (PDE5, 6, and 9), (2) altering the rate of hydrolysis of cAMP through competition at the catalytic site (PDE1, 2, and 3), and (3)

regulating enzymatic activity through direct binding to specific allosteric sites (PDE2, 5, 6, 10, and 11)[96].

The cGMP binding domain in PDE2, 5, 6, and 10 contains two in-tandem homologous sites of about 110 amino acids located at the N terminus (Fig. 2, regulatory GAF-domains, from c**G**MP-regulated phosphodiesterases, bacterial **A**denylyl cyclases, and transcription activator **F**lhA, where such domains were identified). They contain an amino acid sequence different from that of cyclic nucleotide-dependent kinases and HCN channels, representing a separate class of cGMP-regulated proteins[96]. PDE10 catalyzes the hydrolysis of both cyclic nucleotides, but its physiological function is still unclear. PDE2 is widely distributed, exists as homodimers and catalyzes the hydrolysis of cGMP and cAMP. Cyclic GMP binds to allosteric sites, stimulates PDE2 activity, and increases cGMP hydrolysis, forming a negative-feedback mechanism regulating intracellular cGMP. Similarly, cGMP enhances the PDE2-mediated degradation of cAMP, thus cross-regulating its intracellular concentration[97,98]. PDE5 is a homodimer which specifically degrades cGMP. Direct binding of cGMP to allosteric sites promotes phosphorylation of PDE5 by either GK or PKA, thereby indirectly stimulating enzyme activity. It has been suggested that binding of cGMP to the allosteric sites directly activates PDE5, but this effect has not been demonstrated *in vivo* [99]. Finally, PDE6 in rod (PDE6A and B) and cone (PDE6C) photoreceptors is comprised of two large catalytically active subunits associated with various smaller inhibitory and a regulatory subunit. It is

believed that cGMP binding to allosteric sites of PDE6 regulates the interaction between catalytic subunits, inhibitory subunits, and transducin, an important step in phototransduction[61].

cAMP and cGMP represent two different signalling cascades. However, they interact at different levels in order to orchestrate multiple biochemical events, which occur in cells at the same time. One possible modality of the interaction is on the level of target proteins that are, for instance, phosphorylated by both PKA and GK. One can give many examples of those proteins such as VASP, phospholamban, L-type calcium channel, IP_3 receptor, some GPCR (references cited above). GK and PKA inhibit IP_3-dependent release of calcium and induce relaxation in dispersed rabbit and guinea pig gastric muscle cells[81]. Similarly, isoproterenol or SNP induce the phosphorylation of cytosolic calcium-dependent phospholipase A2 by activating PKA or GK, respectively, in SMCs from the longitudinal muscle layer of rabbit intestine[81]. The same effect is achieved by simultaneous stimulation of both kinases by VIP and isoproterenol, contributing to the relaxation response of these cells. In vertebrates, cGMP and cAMP relax vascular smooth muscle, inhibit platelet activation, and regulate chloride and water secretion in the intestine.

Another level of cAMP/cGMP interaction is represented by PDEs. They are located at an intersection of cAMP and cGMP cascades. At their level cGMP is capable of directly regulating cAMP concentrations in a cell (Fig. 1). Several PDEs, e.g. PDE2 are activated by cGMP in order to reduce the intracellular

concentrations of cAMP and cGMP. This mechanism plays a key role in regulation of aldosterone secretion (see above) and is an example of antagonistic action of cAMP and cGMP. On the other hand, cGMP-inhibited PDE3 is involved in cAMP-signalling in cardiac myocytes[100] or regulates electrogenic chloride secretion in the small and large intestine by cGMP-dependent increases in intracellular cAMP, and activation of PKA[101]. The reverse situation, i.r. a direct effect of the cAMP cascade on the hydrolysis of cGMP, has not been observed. This suggests that the cAMP-system influences the cGMP-cascade primarily on the level of common target proteins and their corresponding effectors. cAMP-specific but not cGMP-specific isoforms such as PDE4 can be activated by PKA phosphorylation and hydrolyze exclusively cAMP[102]. Two signalling systems therefore exist in cells, which are subject to multiple interactions that have not yet been fully elucidated. In the present work this issue was addressed by the development and use of fluorescent biosensors.

1.2. Biosensors, GFP-technology, FRET

In recent decades has become possible to visualize biochemical events in single live cell by fluorescence microscopy techniques. These techniques are based on using special reporter proteins, which change their physicochemical properties (e.g. fluorescence spectrum) in response to particular intracellular molecules (ions, small second messengers such as cAMP or cGMP, various proteins or

even DNA). A strong contribution to the development of bioimaging techniques has come from the molecular cloning and subsequent engineering of the **green fluorescent protein** (GFP) from the bioluminescent jellyfish *Aequorea victoria*[103]. GFP is a middle size (~ 20 kDa, containing ~ 240 amino acids) protein with a β-barrel structure, bearing an internal chromophore group consisting of several interacting amino acids (Fig. 3A). GFP has several qualities that make it ideal for *in vivo* imaging. First, GFP can be expressed in a variety of cells, where it becomes spontaneously fluorescent without the need for any cofactors. Second, because it is a protein, GFP can be tagged with many signalling peptides or fused to other proteins targeted to specific organelles, such as the mitochondria, the nucleus, or the endoplasmic reticulum. Finally, mutagenesis of GFP has generated many mutants with varying spectral properties, thus allowing imaging of several different fluorescent proteins simultaneously[104-107].

GFP has been successfully used for several years as a marker for studying gene expression as well as protein folding, trafficking, and localization. Recently, however, more sophisticated applications have been developed by using several GFP-mutants to generate biosensors capable of monitoring complex processes, such as intracellular second messenger dynamics, enzyme activation, and protein-protein interactions[105,108-110].

Development of GFP-based biosensors became possible when various GFP-mutants were cloned. They exhibited - compared to GFP - changed fluorescent

spectrum properties, most importantly shifted excitation and emission spectra. Combining two fluorescent GFP-mutants with appropriate spectra makes it possible to monitor intra- or intermolecular distances between them in live cells based on **fluorescence resonance energy transfer** (FRET).

FRET is a quantum mechanical phenomenon that occurs between a fluorescence donor and a fluorescence acceptor that are in molecular proximity of each other if the emission spectrum of the donor overlaps the excitation spectrum of the acceptor. Examples for this are enhanced cyan fluorescent protein (CFP) and enhanced yellow fluorescent protein (YFP) (Fig. 3B). Under these conditions, energy is transferred non-radiatively from the donor to the acceptor with an efficiency E defined by the equation (Fig. 2A), where r is the distance between two fluorophores and R_0 (Förster distance) is the distance at which 50 % energy transfer takes place (typically 20-60 Å). The latter is dependent on the extent of spectral overlap, the quantum yield of the donor and the relative orientation of the donor and acceptor[105]. In FRET experiments, the donor is excited by incident light, and, if an acceptor is in close proximity, the excited state energy from the donor can be transferred. This leads to a reduction in the donor's fluorescence intensity and excited lifetime and an increase in the acceptor's emission intensity. According to the Förster equation, a doubling of the distance between the two fluorophores, for example from R_0 to $2R_0$, may decrease the efficiency of transfer from 50 % to 1.5 %. Therefore, FRET provides a very sensitive measure of intermolecular distances and conformational changes.

The generation of GFP mutants with distinct excitation and emission spectra, as well as the molecular cloning of new fluorescent proteins from *Fungia concinna* (orange fluorescent protein)[111] and coelenterate marine organisms[112] has provided several fluorophores that can serve as FRET donor/acceptor pairs.

When selecting fluorescent proteins to use as workable FRET pairs, three spectroscopic properties of the donor and acceptor should be considered. First, there needs to be sufficient separation in excitation spectra to achieve a selective stimulation of the donor. Second, there needs to be an overlap between the emission spectrum of the donor and the excitation spectrum of the acceptor to obtain efficient energy transfer. Third, reasonable separation in emission spectra between donor and acceptor fluorophores is required to allow the fluorescence of each fluorophore to be measured independently[113]. To date, the mostly and successfully used donor-acceptor pair is the CFP–YFP combination (Fig. 3B).

A lot of effort is being placed on the search for more red-shifted fluorescent proteins (RFPs) to be used as FRET acceptors in combination with a GFP donor. RFPs would provide greater tissue penetration and minimize tissue autofluorescence background; however, additional improvement of the existing proteins will be necessary for their useful application in FRET experiments. The major limitation of the original dsRed protein is that it forms tetramers and can therefore tetramerize a cellular protein to which it is fused, leading to large aggregation of the fusions. By a combination of site-directed and random mutagenesis, a monomeric variant of this RFP has been generated (mRFP1) in
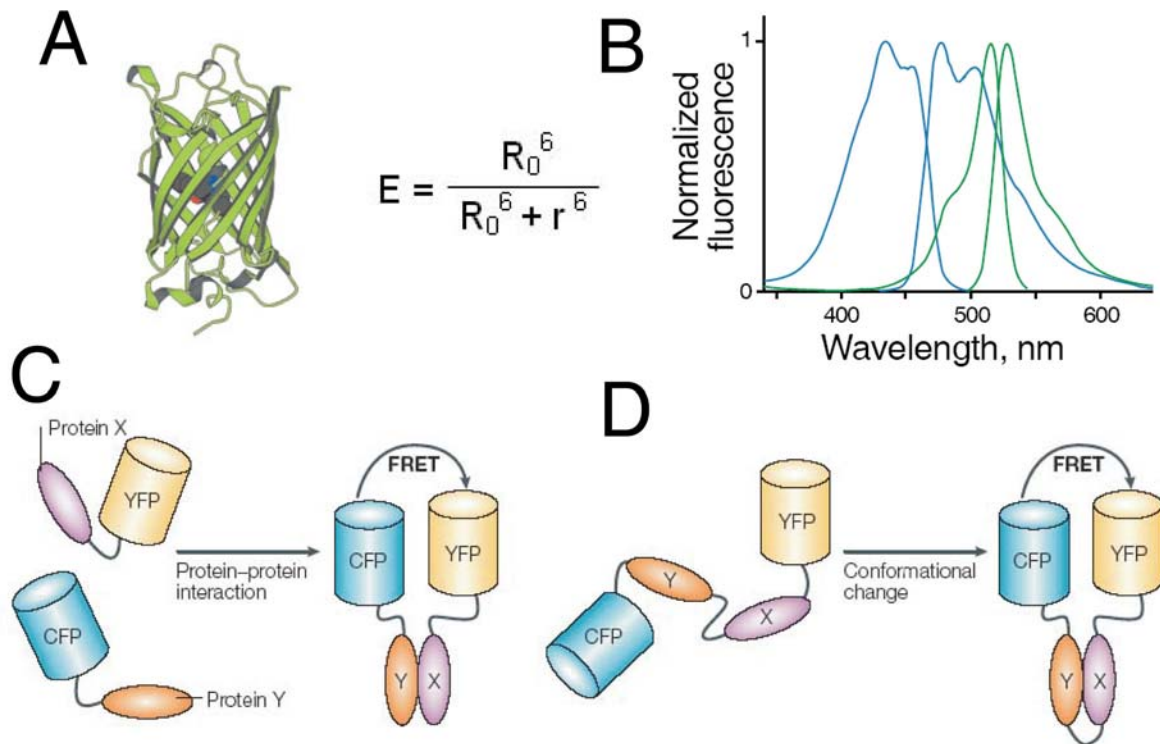
Fig. 3. General principles of GFP-based fluorescent biosensors. **A.** Crystal structure of GFP, which is composed of numerous β-sheets forming the so-called β-barrel. The chromophore is a group of amino acids interacting in the core of the barrel (in grey). On the right – a general equation to calculate Förster resonance energy transfer efficiency (explained in text). **B.** Normalized excitation (left) and emission (right) spectra of CFP (cyan) and YFP (green) fluorescent proteins commonly used as a FRET-pair. Extensive overlap of the CFP emission and YFP excitation spectra is a basis for FRET. **C.** Schematic representation of a bimolecular biosensor, consisting of two proteins X and Y fused to YFP and CFP, respectively. Intermolecular FRET appears when the proteins are interacting. D. Principle of a monomolecular biosensor, where a protein sequence (here containing two different domains X and Y) is sandwiched between CFP and YFP. Interaction between the domains leads to a conformational change monitored by a change in intramolecular FRET.

which most of the problems of dsRed have been overcome. However, mRFP-1 performance as a FRET acceptor remained seriously hampered by the very long tail of its excitation spectrum on the short wavelength side, leading to direct

excitation of the acceptor when exciting the donor[113]. For this reason, very recently a series of new red-shifted fluorescent proteins was developed by subjecting mRFP1 to many rounds of directed evolution. The properties of the resulting variants include several new colours (banana, strawberry, tomato, honeydew, and cherry) and improvements of extinction coefficients, quantum yields and photostability[106].

GFP-based FRET biosensors follow two basic designs. One option is to use *bimolecular probes*, in which the fluorophores are fused to two independent domains or proteins whose interaction depends on ligand binding or a conformational change in the separate domains. In this case the *intermolecular FRET* is measured, which increases when two proteins interact or decreases upon protein dissociation (Fig. 3C). *Monomolecular probes* are based on *intramolecular FRET* between CFP and YFP fused to a protein sequence interacting with a molecule of interest. Binding of the specific ligand to this sequence leads to a conformational change, which is monitored by FRET (Fig. 3D). In general, monomolecular sensors may be preferable because a single, monomolecular probe is less likely to interact with bystanding partners. Such interaction may interfere with endogenous reactions and thus affect cell physiology and reduce the probe sensitivity. Monomolecular constructs have an additional advantage of containing equimolar amounts of the donor and acceptor fluorophores, therefore allowing maximal exploitation of the dynamic range of FRET changes and facilitating quantification.

Up to date, there have been tens of biosensors developed covering multiple intracellular processes[109]. Just a few examples of monomolecular sensors are: *cameleons* to monitor intracellular calcium[114,115], sensors for phospholipase C activation[116] and phosphoinositides[117], reporters of activity of different protein kinases (where a target sequence for a particular kinase is sandwiched between GFP variants)[118-120]. Bimolecular biosensors are tools to monitor interactions between proteins, for example between the subunits of trimetric G-proteins[121,122] or between regulatory of catalytic subunit of the PKA[123,124]. They will be discussed in detail in the following two parts of the introduction (see 1.3 and 1.4).

Several **FRET microscopy techniques** are available for measuring biosensors in live cells. Wide-field microscopy is the simplest and most widely used technique[110]. FRET is typically measured as the ratio of acceptor emission to donor emission on excitation of the donor, giving a value that is proportional to the degree of physical association between the two fluorophores. One of the major drawbacks of wide-field microscopy is the generation of an out-of-focus signal. This can be a serious problem, especially when relatively thick samples are inspected and when the goal of the experiment is to study molecular events that take place in restricted volumes within the cell. Laser scanning confocal microscopy[125] solves this problem and, by collecting serial optical sections from thick specimens, allows resolving FRET signals in 3 dimensions. A major limitation of confocal microscopy is the availability of standard laser lines of

defined wavelength that normally do not allow one to resolve FRET. A recent technological advance, however, has introduced multiphoton confocal microscopy that, by using a tuneable laser in the 700- to 1000-nm range, allows the excitation of a wide variety of fluorophores with higher axial resolution, greater sample penetration, limited photobleaching of the fluorophores, and reduced damage of the sample[125].

The intensity-based FRET techniques described above suffer from contamination of the FRET images with unwanted bleedthrough components because of the incomplete separation of the donor and acceptor excitation and emission spectra. When using CFP/YFP, for example, excitation of CFP is associated with partial direct excitation of YFP, which therefore will emit independently of FRET. Even more important is the bleedthrough of CFP emission in the YFP channel, which can contribute up to 80 % of the FRET image. The degree of crosstalk between fluorophores must be assessed for each individual imaging system, and careful choice of filter sets can minimize bleedthrough. Moreover, the degree of crosstalk should be carefully measured and be accounted for in the offline image processing phase[126], which should include corrections for bleedthrough and direct YFP excitation. Recently, a new algorithm has been developed that removes both the donor and acceptor bleedthrough signals and corrects the variation in fluorophore expression level, generating a true FRET signal[125].

Fluorophore crosstalk is a particularly serious problem when looking at steady-state, intermolecular FRET. In this situation, the intracellular molar ratio between donor and acceptor is difficult to control, and different concentrations of the two fluorophores may be misinterpreted as FRET. Such a problem is completely overcome if an intermolecular FRET sensor and the experimental set up allow monitoring of dynamic FRET. In this case, it is possible to establish whether a change in donor to acceptor fluorescence is a true change in FRET by monitoring donor and acceptor fluorescence intensity over time. A true FRET change corresponds to a symmetric change of donor and acceptor fluorescence intensity (e.g. in case of an increase in FRET – simultaneous increase in the donor and decrease in acceptor fluorescence). Another approach for imaging steady-state FRET consists in collecting the donor emission before and after photobleaching of the acceptor. If FRET is present, elimination of the acceptor by photodestruction releases the energy transferred from donor to acceptor with consequent brighter emission from the donor. This method is very simple and can be used in any laboratory equipped with a simple fluorescence microscope. However, the correct interpretation of the results obtained is not always straightforward, especially if FRET efficiency is low[127,128]. An alternative method for measuring FRET is via donor photobleaching[129]. This technique exploits the fact that photobleaching is proportional to the excited-state lifetime of the fluorophore. Because FRET reduces the lifetime of the donor's excited state, its photobleaching rate decreases proportionally.

Apart from the intensity-based methods described above, more sophisticated technologies for measuring FRET are also available. Fluorescence lifetime imaging microscopy takes advantage of the fact that FRET results in a shortening of the donor's lifetime; by subtracting the fluorescence lifetime of the donor alone from the lifetime of the donor in the presence of the acceptor, the efficiency of FRET can be measured[130,131]. Another technique is fluorescence correlation spectroscopy, in which spontaneous fluorescence intensity fluctuations are measured in a microscopic volume and energy transfer efficiency of freely diffusing single molecules can be accurately measured[132,133].

1.3. Biosensors for receptors, G-proteins and second messengers

In this section, the most important biosensors will be characterized, which are used to monitor the activity of different players in a typical GPCR-pathway (Fig. 1). These include the probes designed for monitoring GPCR activation, G-protein activation and cAMP production in live cells.

Binding of specific ligands to a family of seven-transmembrane receptors is supposed to induce an intracellular response through activation of G-proteins and downstream enzymes such as adenylyl cyclase and phospholipase, which produce second messengers (cAMP, phosphoinositides and calcium) triggering numerous biochemical events in a cell. This multistep mechanism provides amplification of the signal and different modalities of regulation (see 1.1). Using

numerous fluorescent biosensors it became possible to monitor such signaling events in a single live cell.

GPCR activation could be monitored as a change of FRET using a monomolecular sensor consisting of the receptor fused to two fluorophores: CFP as a donor on the C-terminus of the receptor and YFP or Flash as an acceptor in the 3rd intracellular loop of the receptor (Fig. 4A)[134,135]. A ligand-induced conformational change in the receptor leads to an increase of distance between the 3rd intracellular loop and the C-terminus of the receptor, which could be easily monitored in live cells as a decrease in intramolecular FRET of the biosensor. Initially such chimeric receptors were created using the CFP-YFP FRET pair to watch activation of α_{2A}-adrenergic and parathyroid hormone receptors[134]. Later on YFP was replaced by the smaller organic Flash fluorophore, which has a small size and improves the signaling properties of the chimeric receptor (in terms of coupling to G-proteins), which physiologically becomes now undistinguishable from a normal untagged receptor[135]. Flash is a fluorescein derivative containing two AsH groups, which shows no fluorescence until it is covalently bound to a specific helical amino acid motif (CCPGCC), which can be introduced into different proteins for their specific labeling[136,137]. Flash bound to the 3rd intracellular loop of the receptor (such sensors have been reported for adenosine A_{2A}- and adrenergic α_{2A}-receptors) serves as a fluorescence acceptor of CFP. Receptor conformational switch upon activation leads to a decrease of FRET between CFP and Flash occurring within a few tens
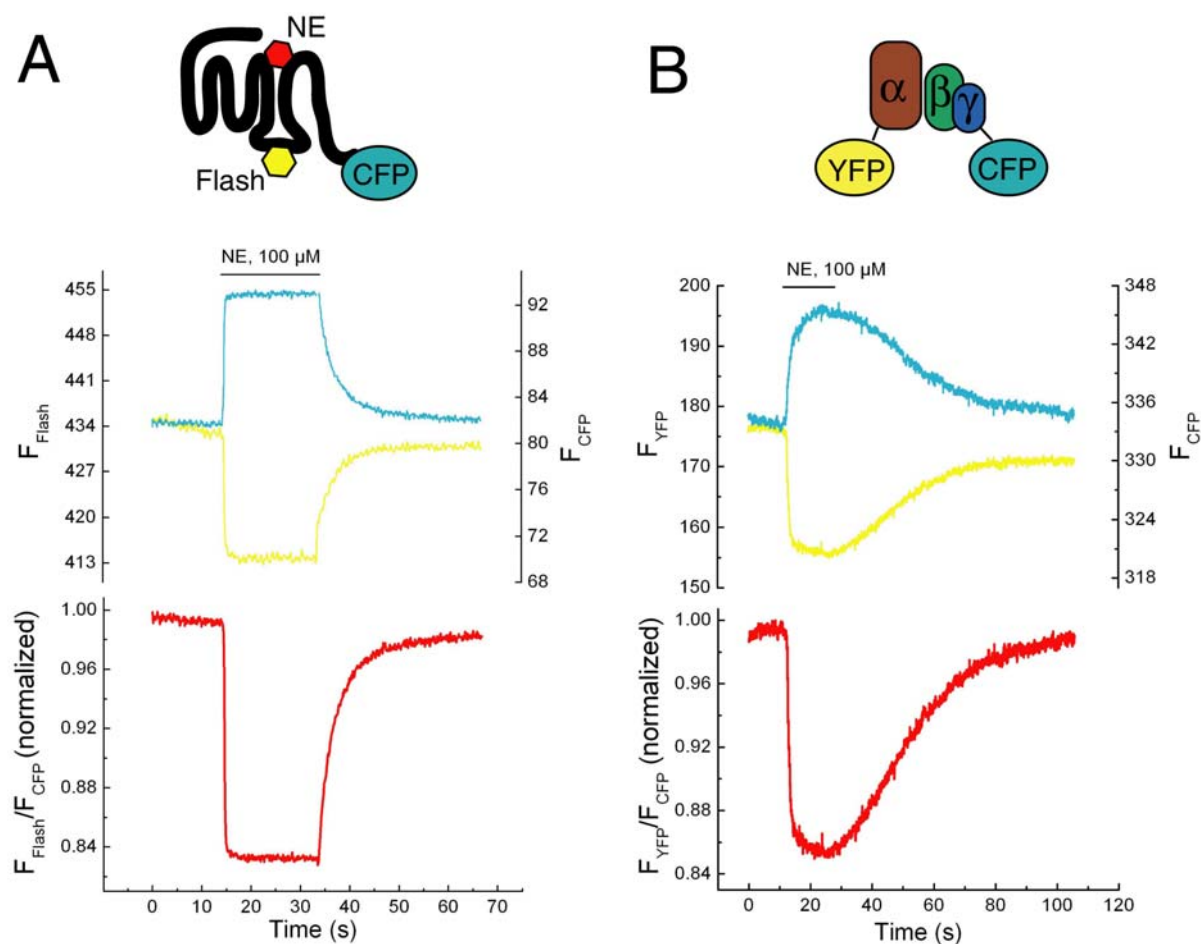
*Fig. 4. Examples of fluorescent biosensors for GPCR and G-proteins. **A.** A monomolecular sensor for monitoring of the receptor activation switch. Adrenergic α_{2A}-receptor is fused to CFP on the C-terminus and has an inserted six amino acid sequence to bind the acceptor fluorophore Flash in the 3rd intracellular loop. Due to a conformational change in the receptor upon binding of norepinephrine (NE) a rapid decrease in intramolecular FRET was monitored as a measure of receptor activation. Live cell experiment. Fluorescence intensities in single Flash and YFP channels and their ratio are presented. B. System for monitoring G_i-protein activation consists of an α_i2 subunit tagged with YFP, γ_2-subunit fused to CFP and unlabeled β_1-subunit[122]. A decrease in intermolecular FRET is observed in cells stably expressing α_{2A}-adrenergic receptor upon activation with NE.*

of milliseconds (Fig. 4A). Withdrawal of the ligand returns the receptor in the initial conformation (Fig. 4A). A pharmacological application of this biosensor

is to study and screen compounds acting on the level of GPCRs (these represent around one third of all currently used drugs), because the sensor can effectively differentiate between full agonists, antagonists/reverse agonists and inverse agonists of the receptors[134].

Another group of biosensors was designed to monitor **G-protein activation**. This field was pioneered by Janetopoulos and colleagues who analyzed receptor-induced G-protein activation in live *Dictyostelium discoideum* cells by monitoring FRET between α- and β-subunits of G-protein fused to CFP and YFP. The G-protein heterotrimer rapidly dissociated and reassociated upon addition and removal of chemoattractant[121]. Later on similar sensors were developed for mammalian G_i proteins and it was demonstrated that those subunits do not dissociate upon activation, but rather undergo a conformational rearrangement. When fusing YFP to $\alpha_i 2$ and CFP to the C-terminus of the γ_2 subunit, a predicable decrease in FRET was observed (Fig. 4B). However, if the CFP was placed at the N-terminus of the γ_2- or β_1-subunit, an increase in FRET was observed indicating that the G_i subunits stay together and that a conformational rearrangement takes place within the complex[122]. The described biosensor allows monitoring G-proteins activation in single live cells, which in the case of G_i occurs within ~ 1 second (Fig. 4B)[122].

The next level of signalling that could be analyzed using fluorescent biosensors is the **production and intracellular distribution of second messengers**. One very important second messenger is calcium which is accumulated in cells as a

result of L-type calcium channel activation, CICR or released from intracellular stores (see 1.1). The classical way to image calcium in live cells is to use cell-permeable fluorescent dyes such as *Fluo, BAPTA* or *Fura*[138]. Over the last 8 years, several protein-based probes have been developed that are based on FRET between CFP and YFP fused to a protein sequence containing a calcium-binding protein, calmodulin. Calcium induces a conformational change in the sensor, which is monitored as a change of intramolecular FRET[114,115,138,139]. The protein-based sensors due to the possibility to target them to distinct intracellular locations allowed for the first time monitoring of calcium in living animals and at the subcellular level, e.g. visualizing of calcium uptake into the mitochondria during skeletal muscle contraction[140].

Another second messenger, which regulates CICR through its receptors on the endoplasmatic reticulum, is IP_3. This second messenger is produced by phospholipase C after the stimulation of G_q-protein coupled receptors. To visualize IP_3 in live cells a biosensor was developed based on a sequence of the IP_3-receptor sandwiched between YFP and CFP[141]. Another approach to monitor the signal transduction through the G_q-pathway is to image the activation of phospholipase C by means of FRET-biosensor, which consists of the PH-domain of this enzyme fused to CFP or YFP. The activation results in a translocation of the fluorescent probes to the plasma membrane with an increase in FRET[116].

1.4 FRET-sensors for cAMP and cGMP based on protein kinases and their disadvantages

Measurements of cAMP and cGMP using FRET-based biosensors first became possible by monitoring the activation of the main intracellular targets for these second messengers, namely PKA and GK, which were initially thought to be exclusive effectors of cyclic nucleotides.

The first attempts to visualized cAMP in live cells based on the **dissociation of PKA** go back to the early 1990-es, when the first biosensor for cAMP was created. The sensor consisted of a PKA in which the catalytic (C) and regulatory (R) subunits were each labelled with a different fluorescent dye such as fluorescein or rhodamine capable of FRET in the holoenzyme complex R_2C_2. When cAMP molecules bind to the regulatory subunits, the catalytic subunits dissociate, thereby eliminating energy transfer. The change in the fluorescence emission spectrum allowed cAMP concentrations and the activation of the kinase to be nondestructively visualized in single living cells microinjected with the labelled holoenzyme[142]. At that time, when GFP-technology was not yet established, it was the only way to label proteins with organic fluorophores to construct a biosensor. This first cAMP biosensor was successfully used to image cAMP in sensory neurons[143] and neural circuits[144], but the sensor was not widely applied due to several limitations such as the need to use purified proteins, microinjections and instability of the probes. Later on, when the GFP-technolo-

PKA-based FRET sensor for cAMP
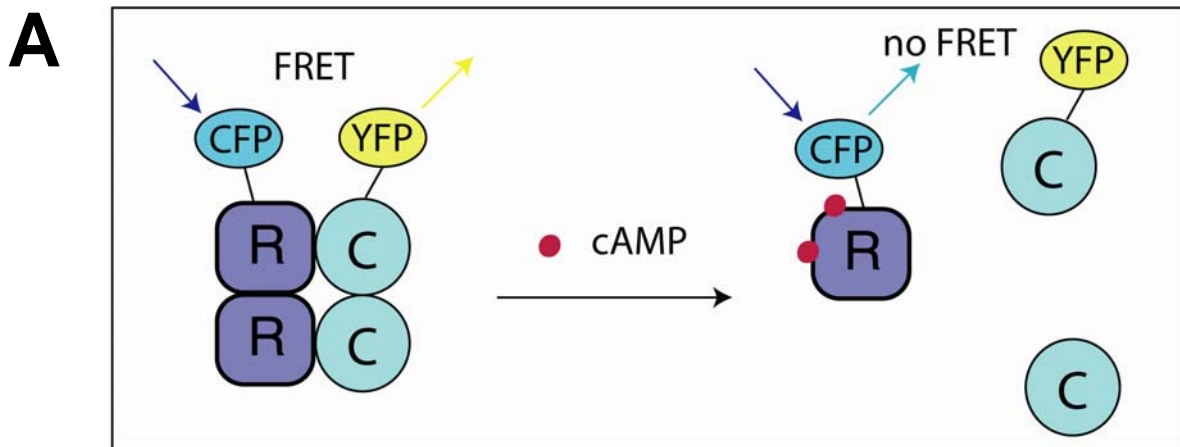
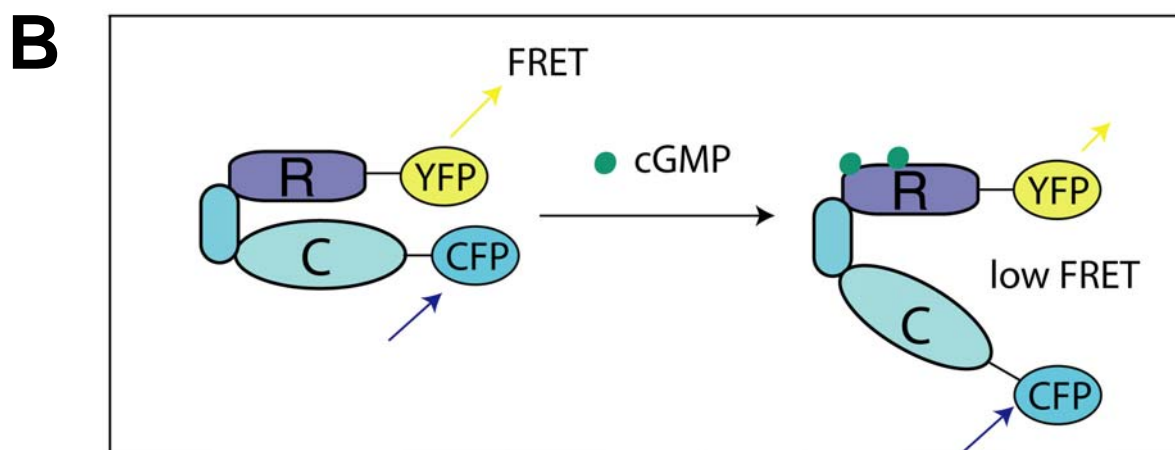# cGMP-kinase-based FRET sensor for cGMP

*Fig. 5. Schematic representation and principles of kinase-based sensors for cAMP and cGMP. **A.** cAMP is measured as the dissociation of the PKA holoenzyme. In the* absence of cAMP, PKA-sensor is a complex of two regulatory (R) and two catalytic (C) subunits fused to CFP and YFP, respectively, and high FRET is observed. After cAMP binding to the two sites in each regulatory subunit, catalytic subunits are released from the complex, which results in the loss of FRET. ***B.*** *cGMP-biosensor* based on GK (*cygnet*) consists of a mutant N-terminally truncated by 70 amino acids of the kinase still bearing regulatory (R) and catalytic (C, or mutated catalytically dead) domains sandwiched between CFP and YFP. Binding of cGMP to the two regulatory sites induces a conformational change, which is monitored as a decrease in FRET.

gy has been developed, the organic fluorophores on the PKA were replaced first by blue fluorescent protein (BFP) and GFP[123], and subsequently with a more convenient FRET-pair, CFP-YFP[124] (Fig. 5A). Despite being now genetically encoded due to using GFP-mutants (i.e. the sensor could be expressed in live cells by transfecting them with two DNA constructs encoding for R-CFP and C-YFP subunits), the sensor had several important disadvantages limiting its application for measuring cAMP:

1. The PKA-sensor is comprised of two large proteins (R-CFP and C-YFP) that have to be equally expressed in cells to form a functional tetramer.

2. Excess of catalytic subunit expression leads to detrimental consequences for a cell. When overexpressed alone C-subunit leads to cell death[26].

3. cAMP binding to 4 different binding sites of different affinities is a multistep cooperative process occurring through a series of conformational changes before C-subunits are released (see 1.5 for details)[23-25]. The FRET-signal reported by the sensor reflects the apparent complex dissociation, rather than acute changes in cAMP concentrations.

4. Once being activated the sensor due to its C subunit exhibits catalytic activity, which leads to activation of PDE4 (an enzyme hydrolyzing cAMP); this makes, therefore, accurate cAMP measurements impossible (Fig. 1) [102].

5. The PKA-sensor could itself be anchored to distinct subcellular sites through interaction with A-kinase anchoring proteins (AKAPs, Fig. 1), so that the sensor is not equally distributed in the cytosol and might be directly affected by AKAPs or its interacting partners[124,145].

These limitations greatly hamper and complicate correct cAMP measurements by this PKA-sensor or their correct interpretation.

A FRET approach to measure changes in intracellular cGMP has been developed using **GKI as a backbone for a monomolecular sensor**[146,147]. This protein changes its overall conformation upon cGMP binding to the two sites on the GK regulatory domain, which results in a decrease in FRET between CFP and YFP (Fig. 5B). Compared to the PKA-sensor for cAMP, this cGMP indicator is large but a single-chain protein, where the N-terminal anchoring, dimerization and autophosphorylation sites are deleted and the catalytic activity is switched off by a point mutation. However, the sensor still contains two binding sites with a complicated mechanism of activation. The major drawback of *cygnets* is a poor temporal performance in terms of physiological cGMP signaling. Although the sensor has a relatively high affinity for cGMP (~ 1 µM) it reports cGMP in live cells with an enormous delay of 50-150 seconds after the application of a natriuretic peptide or of a NO-donor[146]. Only very high (1 mM)

concentrations of SNP were once demonstrated to induce a rapid response[148]. This has prevented the sensor from being further applied in cGMP research.

The aim of the present study was to develop novel biosensors for cAMP and cGMP which would overcome the disadvantages of the kinase-based probes and would contain a single cyclic nucleotide binding domain (CNBD).

1.5. Structure of cyclic nucleotide binding domains. Conformational change as a mechanism of activation

To date there have been numerous cAMP-binding domains characterized and crystallized in absence or presence of cAMP. For cGMP only one regulatory binding domain of PDE2 has been described and crystallized in presence of the ligand[98], whereas structures of GKs and cGMP-channels are still unresolved, making reliable predictions on the mechanism of the ligand induced activation difficult. However, using small angle X-ray scattering technique a cGMP-dependent conformational change in the GK has been described[149], which has also been proven by creating monomolecular FRET-based cGMP sensors using GK as a backbone[146,147]. The structure of the CNBD of PDE2 revealed a high degree of similarities with cAMP-binding domains, suggesting that they might exhibit similar mechanisms of activation, namely a cyclic-nucleotide induced conformational change[98,150,151].

In case of Epac the change in conformation leads to the release of the allosteric inhibition of the catalytic domain, which becomes active after binding of cAMP

in the regulatory part of the protein[33]. In the PKA, binding of cAMP to the high-affinity site B induces a conformational change, giving cAMP access also to the A-site, which upon cAMP binding changes its conformation, leading to the release of the catalytic subunit[24,25]. In the HCN2-channel, the cAMP-induced conformational change is supposed to regulate the orientations of transmembrane domains, thereby changing the gating properties of the channel[22]. The first structural evidence for a conformational change in CNBD was provided by a crystal structure of Epac2, which was the first apo-structure of a CNBD (i.e. without cAMP)[152]. Comparing this structure to the known ones of PKA binding domains the authors took note of the different orientation of the helix α6:B (hinge) and proposed a conformational change as a mechanism of ligand-induced activation (Fig. 6A).

Another more direct evidence for a conformational change in the B-site of the PKA came more recently when the cAMP-bound and ligand-free structures were presented for the same CNBD, the regulatory I subunit of the PKA. A major conformational rearrangement was observed that involved mainly the movement of the C-terminal hinge helix[153]. The next more complicated structure was provided for the A-domain of the same PKA in the complex with either catalytic subunit or cAMP (Fig. 6B). This has, for the first time, demonstrated the interplay between cAMP and catalytic subunit at the molecular level and revealed the mechanism how the cAMP-induced structural rearrangement leads to the release of the catalytic subunit[24].
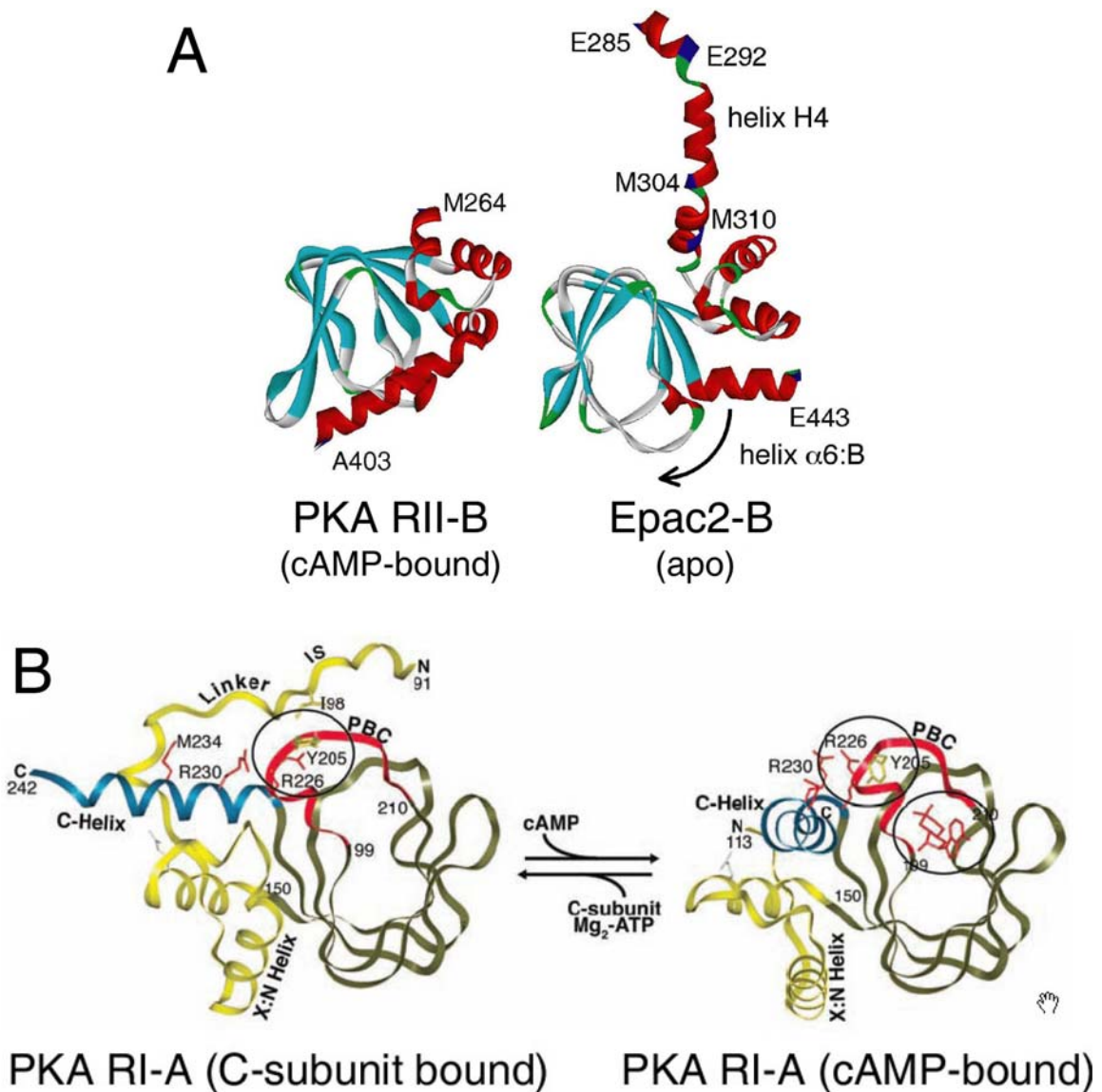
Fig. 6. cAMP-induced conformational change in CNBDs of Epac and PKA. ***A.*** Crystal structures of the cAMP-bound B cAMP-binding domain of PKA regulatory II subunit (left)[25] compared to a cAMP-free structure of the B-domain of Epac2[152]. The movement of the helix α6:B is proposed (black arrow) as a mechanism of activation. The phosphate binding cassette (PBC) is in blue. ***B.*** Mechanisms of the interplay between cAMP and the catalytic subunit on the A binding domain of the regulatory I subunit of the PKA. cAMP binding induces the release of the catalytic subunit (not shown) and a conformational rearrangement, characterized by a major movement of the C-helix (analogous to the hinge in Epac2) shown in blue. The PBC is colored in red[24].

The last two studies have thoroughly characterized the cooperative mechanism of PKA complex activation by cAMP, which occurs through a series of binding events and conformational changes:

1. cAMP is first bound to the B-domain where a conformational change is induced (movement of the hinge helix) .

2. The conformational change in the B-domain provides access of the ligand to the A-domain.

3. cAMP binds to the A-domain where it induces a conformational change (movement of the C-helix).

4. The catalytic subunit is released and becomes active to phosphorylate its substrates.

In summary, analysis of crystal structures of different CNBDs demonstrated that a cyclic nucleotide-induced conformational change seems to be a ubiquitous mechanism for the activation of these domains and corresponding proteins: kinases, Epacs, channels and PDEs. In the present study, advantage was taken of this conformational change at the level of a single CNBD in order to create novel highly sensitive monomolecular biosensors to measure cAMP and cGMP

1.6. Aims of the work

The present study had the following goals:

1. Development of novel biosensors for cAMP and cGMP based on single CNBDs for measurements.

2. Analysis of the temporal and spatial aspects of cyclic nucleotide signaling.

3. Real-time characterization of the activity of the enzymes hydrolyzing cyclic nucleotide (PDEs).

4. Development of physiologically and clinically relevant systems for analysis of cyclic nucleotide signaling.

5. Characterization of the cAMP-induced conformational change in different binding domains using a series of cAMP analogues.

2 Methods and Materials

2.1 Methods

For generation of cAMP and cGMP biosensors, many common well established techniques were applied. They are described in enough details elsewhere to reproduce the experiments presented in the study. Characterization of fluorescent indicators was performed *in vitro* and in different live cells.

2.1.1 Molecular biology techniques

To produce a functional biosensor for cAMP or cGMP, DNA sequences encoding for CNBDs were fused with those of CFP and YFP to produce a chimeric fusion protein, which is supposed to exhibit a cAMP or cGMP-dependent conformational change. The DNA constructs encoding for cAMP-sensing proteins were generated by polymerase chain reaction (PCR) using human Epac1 (Acc.No. AF103905), murine Epac2 (AF115480) or murine PKA regulatory IIβ subunit (M12492) cDNA as a template. cGMP sensors were based on human GKI (NM_006258), murine PDE2A (XM_133606) and human PDE5A (NM_001083). Generally, the sequence of a CNBD was amplified using

primers encoding for EcoRI and XbaI restriction sites on N- and C-termini, respectively. GFP variants were amplified with standard primers from pEYFP- and pECFP plasmids and attached to CNBDs via EcoRI (YFP) and XbaI (CFP) restriction sites to produce genetic constructs encoding for fusion proteins schematically depicted in Figs 7A, 10, 26A, 27A.

First, PCR was performed to amplify the respective DNA fragments. The standard PCR mix contained: Water (in all experiments ultrapure water was used from NANOpure system, Barnstead) ad 100 µl, 10x Pfu polymerase buffer 10 µl, 10 mM desoxyribonucleotide triphosphates mix 2 µl, 20 µM forward primer, 20 µM reverse primer, Pfu polymerase 1 µl. The PCR program was run on Gene Amp2450 (Perkin Elmer): 94°C – 5 min, 20x (94°C – 30 s, 55°C – 30 s, 72°C – t), 72°C – 7 min, 20°C - ∞. t was calculated depending on the length of the fragment amplified, 1000 base pairs per 120 s. The primers were designed to contain a restriction site and a DNA sequence of CNBD or GFP-mutant with a length corresponding to the amplification temperature.

PCR fragments were run on a 1% **agarose gel** prepared on TAE puffer (40 mM Tris, 0.1 mM EDTA, 1 mM $(CH_3COO)Na$, pH=8.54) using the same as a running puffer. DNA was **purified** directly from the gel using *Qiaquick Gel Extraction Kit* according to the manufacturer protocol. The DNA fragments were then cut using the appropriate restriction enzymes and subcloned into pcDNA3 expression vector for mammalian cell expression, pVL1393 for insect

cells or pET3d for bacterial expression. For protein purification from insect cells or bacteria, a sequence encoding for a hexahistidine tag was inserted into the constructs directly at the N-terminus using oligonucleotides

5'-GATCCATGCATCATCATCATCATCATGGTATGGCTAGCT-3' and

5'-CTAGAGCTAGCCATACCATGATGATGATGATGATGCATG-3'.

Cloning of PCR fragments or oligonucleotides was performed by **ligation** of the cut fragments into the restriction sites of the vector for 20 min at room temperature using T4 DNA ligase.

The ligation mix was, next, introduced into competent *E. coli* XL1-Blue bacteria using a KCM buffer: 15 µl ligation mix, 65 µl water, 20 µl 5x KCM buffer, 100 µl competent cells (competence $1x10^6$ - $1x10^7$ colonies/µg DNA), incubated 20 min on ice, 10 min at room temperature, shaken 50 min at 37°C (Thermomixer 5436, Eppendorf) with 1 ml added LB medium and plated on a selective LB-medium plate, containing 1.5 % agar and 100 µg/ml ampicillin. 5x KCM buffer was prepared as follows: 150 mM $CaCl_2$, 250 mM $MgCl_2$, 500 mM KCl. LB medium was sterilized by autoclaving *ex tempore* (Varioklav) and contained (m/v): 1% NaCl, 1% trypton and 0.5% yeast extract. Bacterial colonies were grown overnight and checked for the presence of the cloned construct by plasmid DNA isolation (*Qiagen Plasmid Mini Kit*) with subsequent restriction analysis. Positive colonies were then grown overnight in 200 ml LB medium

plus 100 µg/ml ampicillin and used for plasmid DNA purification (*Qiagen Plasmid Maxi Kit*).

Concentration of plasmid DNA was calculated from the light absorption at 260 nm measured in spectrophotometer with 1 cm path length (Shimadzu). Absorption of 1 corresponds to a plasmid DNA concentration of 50 µg/µl.

2.1.2 Protein purification

Sensor proteins were expressed in and purified from either insect *Spodoptera frugiperda Sf9* cells or *E.coli* BL21-DE3.

Insect cells were grown at 27°C in TC100 medium supplemented with 10 % fetal calf serum (FCS), 4 mM L-glutamine, 100 U/ml penicillin, and 100 µg/ml streptomycin. The construct of interest cloned into pVL1393 vector was expressed using the baculovirus system (Baculogold, Pharmingen). Cells were washed twice with chilled phosphate buffered saline (PBS), resuspended in buffer A (5 mM Tris buffer, pH=7.4), supplemented with 0.1 mM benzamidine and 0.1 mM phenylmethylsulphonylfluoride (protease inhibitors). Cell membranes were then disrupted by 20 s Ultra-Turrax T8 (IKA Labortechnik) and centrifuged at 40000 g (Beckman Ultracentrifuge LE70, Ti70 rotor). Cell lysates were purified by Ni-NTA chromatography (Qiagen) according to the

manufacturer's instruction. Buffer A was used at the washing step and for 0-100 mM imidazol gradient preparation.

For **bacterial expression** competent BL21-DE3 cells were transformed with sensor constructs in pET3d vector. Bacteria were grown at 37°C to achieve an optical density of 0.6-0.8 measured at 600 nm, and protein synthesis was induced by addition of 0.5 mM isopropyl-ß-D-thiogalactopyranosid. Next, proteins were expressed for 18 h at 22°C. Bacteria were centrifuged for 10 min at 5000 rpm (Beckman Avanti J-25, JA-14 rotor), washed once with buffer A and resuspended in the same buffer plus protease inhibitor cocktail. Cell walls were then disrupted by 3 freeze/thaw cycles using liquid nitrogen and 5 min ultrasound treatment (Bandelin Sonopuls HD200). Cell lysates were centrifuged and processed for protein purification as described above. Fluorescent proteins were used for in vitro experiments directly after purification or frozen at -20°C for further studies (with no apparent change in functionality).

2.1.3 Cell culture and transfections

HEK293, **HEKβ$_1$** (HEK293 cell stably expressing 0.4 pMol/mg β$_1$-AR) and **TsA201** cells were grown in DMEM medium with 4.5 g/l glucose, 10 % FCS, 2 mM L-glutamine, 100 U/ml penicillin, and 100 µg/ml streptomycin at 37°C and 7 % CO_2. The cells were plated onto 24 mm glass coverslips in 100 mm dishes for live cell experiments or onto 150 mm Petri dishes for cuvette fluorometric

measurements and transfected with 10 µg or 30 µg, respectively, plasmid DNA using the calcium phosphate method. A precipitation mix for a 100 mm dish was as follows: water ad 1 ml, 2.5M $CaCl_2$ 50 µl, plasmid DNA 10 µg (10 µl of 1 µg/µl solution), 2x BBS buffer 500 µl. To transfect 150 mm dishes 2.5x amounts were used. The mixture was incubated 20 min at room temperature and applied onto the cells for 24 h at 37°C 5% CO_2. 2x BBS buffer contained: 1.5 mM Na_2HPO_4, 50 mM N,N-bis-(2-hydroxyethyl)-2-aminoethanesulfonic acid, 280 mM NaCl, pH=6.95. All solutions used in cell culture were filter-sterilized.

CHO and **CHOA2B** (CHO cells stably expressing adenosine A_{2B} receptors) cells were maintained in DMEM/F12 medium with 1.0 g/l glucose, 10 % FCS, 2 mM L-glutamine, 100 U/ml penicillin, and 100 µg/ml streptomycin at 37°C and 5 % CO_2, split onto 24 mm coverslips and transfected by the same procedure.

PC12 cells were grown in DMEM medium (37°C, 5% CO_2) containing 1.0 g/l glucose, 5% FCS, 10% horse serum and other supplements as above. Transfection was performed by electroporation in PBS and using Gene Pulser (BioRad) at 250 V, 500 µF. Cells were then seeded onto coverslips and used for imaging experiments after 24 h.

2.1.4 Primary cells

Peritoneal macrophages were isolated from 10-12 week old FVB/N mice as described[154], resuspended in PBS and immediately transfected by

electroporation using Gene Pulser at 250 V, 500 µF, seeded onto 24 mm glass coverslips and maintained in RPMI 1640 medium, 10 % FCS, 2 mM L-glutamine, 100 U/ml penicillin, and 100 µg/ml streptomycin (37 °C, 5 % CO_2).

Primary dissociated **mouse hippocampus neurons** were isolated from neonatal (P1) C57BL/6 mice and cultured as described previously with some modifications[155]. Hippocampi were dissociated by incubation for 20 min in Tyrode's solution containing ispase (4.8 mg/ml), collagenase (1 mg/ml) and desoxyribonuclease I (0.8 mg/ml). Primary neurons were transiently transfected with the Nucleofector system (Amaxa, Köln). Briefly, 3 x 10^6 freshly dissociated cells were electroporated with 5 µg plasmid DNA and cells were plated on poly-L-lysine and Matrigel-coated glass slides (coating was performed with a few drops of 1 % solution for 1 h) in Neurobasal-A medium for 3-5 days (37 °C, 5 % CO_2). 18 h after transfection, 5 µM cytosine arabinoside was added to prevent proliferation of glial cells. Neurobasal-A medium contains 10 % FCS, 0.5 mM L-glutamine, 100 U/ml penicillin, and 100 µg/ml streptomycin. All animal procedures were approved by the responsible government authorities (Regierung von Unterfranken, protocol No. 621-2531.01-10/98 and 28/01).

Bovine adrenal *zona glomerulosa* (ZG) cells (adrenal glands were obtained from a local slaughterhouse) attached to the adrenal capsule were digested with 1 mg/ml collagenase in Tyrode's solution and mechanically disaggregated as described[156,157]. Isolated cells were suspended in DMEM medium supplemented

with 10% FCS, 100 U/ml penicillin, and 100 µg/ml streptomycin. For microscopic measurements, cells were plated on glass coverslips at a density of 10 000 cells/ml and after 2 days were infected with adenovirus encoding for cAMP biosensor Epac2-camps. Adenovirus was constructed in the laboratory of Dr. Stefan Engelhardt using AdEasy kit and manufacture's protocol (Invitrogen). After tittering adenoviral concentrations by plague assays conducted on monolayer 293 cultures, a multiplicity of infection between 10 and 50 was used to infect primary adrenal ZG cells 48 h prior to FRET-measurements.

Primary rat mesangial cells were isolated from rat kidney glomeruli[158]. Glomeruli were obtained from whole kidneys of newborn rats and were minced finely with a razor blade followed by sequential sieving through 125- and 75-µm pore-size metal sieves and then collected on a 22.5-µm pore size sieve. Cells were cultured in RPMI 1640 medium, containing 20% FCS, 2 mM L-glutamine, 0.1 mM sodium pyruvate, 5 mM HEPES buffer, pH 7.2, 100 units/ml penicillin, 100 µg/ml streptomycin, 0.1% non-essential amino acids, and 0.1% growth supplements (5 µg/ml insulin, 5 µg/ml transferrin, 5 ng/ml sodium selenite). The cells were maintained at 37 °C and 5 % CO_2 and transiently transfected with the Nucleofector system using the Primary Smooth Muscle Cell Kit (Amaxa, Köln). Briefly, 5 x 10^6 cells were electroporated with 5 µg PDE5 sensor plasmid DNA and immediately plated onto sterile glass slides. 18-24 h after transfection cell imaging experiments were performed.

2.1.5   Fluorescence measurements *in vitro*

TsA201 cells 24 h post-transfection were washed thrice with chilled PBS, scraped from the plate and resuspended in buffer B (5 mM Tris-HCl, 2 mM EDTA, pH = 7.4). After disruption with an Ultraturrax device for 40 s on ice and 20 min centrifugation at 80000 rpm (Beckman Opima TLX ultracentrifuge, TLA 120.2 rotor), fluorescence emission spectra of the supernatant (excitation at 436 nm, emission range 460-550 nm) were measured with a fluorescence spectrometer LS50B (Perkin Elmer) before and after addition varying cAMP, cGMP, AMP or ATP concentrations. Saturation curves were plotted using KaleidaGraph 3.0.5 software (Abelbeck).

For high throughput chemical mapping of CNBDs, fluorescent proteins purified from *E.coli* were diluted in buffer B to 50 nM concentration and pipetted onto a black 96-well plate, 98 µl per well. 2 µl of cyclic nucleotide analogue water solution were then added and the FRET ratios were measured using a MITRAS plate reader (Berthold Technologies). The data were analyzed by Microsoft Excel and Origin 6.1 software (Microcal). Concentration-response dependences for each substance were plotted using KaleidaGraph.

2.1.6   Fluorescence measurements in live cells

For fluorescent microscopy and **cell imaging** glass coverslips with adherent cells were transferred to the experimental chamber in buffer C (144 mM NaCl, 5 mM KCl, 1 mM $CaCl_2$, 1 mM $MgCl_2$, 20 mM HEPES, pH = 7.3) at room temperature and placed on a Zeiss Axiovert 200 inverted microscope equipped with an oil immersion 63x Plan-Neofluar objective, beam splitter 505 DCXR and a CoolSNAP HQ CCD-camera (Visitron Systems, Puchheim, Germany). Samples were excited with light from a polychrome IV (TILL Photonics, Planegg, Germany). FRET was monitored using MetaFluor 5.0 software (Visitron Systems) as the emission ratio at 535 ± 20 nm and 480 ± 15 nm upon excitation at 436 ± 10 nm. The imaging data were analyzed by MetaMorph 5.0 (Visitron Systems) and Origin software, corrected for spillover of CFP into the 535 nm channel (57 % of the measured CFP fluorescence as calculated from the cells expressing CFP only), direct YFP-excitation and acceptor photobleaching to give a corrected ratio YFP/CFP. To study agonist-induced changes in FRET, cells were continuously superfused with buffer C plus agonist solutions. For local stimulation of a cell, patch pipettes filled with the respective agonists were accurately positioned onto the plasma membrane by a manipulator (Patchman, Eppendorf). To avoid free agonist diffusion along the membrane, cells were

continuously superfused with laminar flow of buffer C (coming from perfusion system) in the direction opposite to the pipette.

In **fluorometric detection** mode the microscopy was performed by placing cells plated on coverslips on a Zeiss inverted microscope (Axiovert 200) with an oil-immersion x100 objective, dual-emission photodiode system and a polychrome IV (both TILL Photonics). FRET ratios were measured as the ratio of the YFP and CFP emission intensities at 535 ± 15 and 480 ± 20 nm (beam splitter DCLP 505 nm) upon excitation at 436 ± 10 nm (beam splitter DCLP 460 nm). The YFP emission upon excitation at 480 nm was recorded at the beginning of each experiment to subtract direct excitation of YFP (6 % of the measured YFP fluorescence as calculated from the cells expressing YFP only and excited at 436 nm). Spillover of CFP into the 535-nm channel (80%, measured as described above; spillover of YFP into the 480-nm channel was negligible) was subtracted to give a corrected FRET ratio.

FRET between CFP and YFP was also confirmed by donor dequenching after acceptor photobleaching. YFP (acceptor) bleaching was achieved by 5 min illumination at 480 nm. CFP fluorescence was recorded (436-nm excitation) in short intervals during the bleaching process (using the dual-wavelength protocol) to determine the resultant increase of CFP fluorescence. To study agonist-induced changes in FRET, cells were continuously superfused with buffer C and agonist was applied using a computer-assisted solenoid valve–controlled rapid superfusion device (ALA-VM8, ALA Scientific Instruments) (solution exchange

5–10 ms). Signals detected by avalanche photodiodes were digitalized using an AD converter (Digidata1322A, Axon Instruments) and stored on a personal computer using Clampex 8.1 software (Axon Instruments).

2.1.7 Biochemical techniques

VASP phosphorylation. After 3 days in culture the medium of *zona glomerulosa* cells was replaced by serum-free DMEM for 12 h and cells were incubated for 1 h with 10 µM forskolin, 10 nM ANP and 10 nM ACTH 1-24 peptide, then the media was collected for aldosterone radioimmuno assay (RIA) and cells were harvested in SDS gel loading buffer (at 95 °C). PKA activity in the cells was analyzed by Western blot using the phosphorylation of the well-known PKA and PKG substrate VASP detected by monoclonal anti-phospho (Ser239) mouse antibody[159]. Equal loading was controlled by Ponceau-S staining of the membrane and by incubation of the stripped membranes with non-phospho VASP antibody. For visualization of the signal, goat anti-mouse IgG conjugated with horseradish peroxidase was used as secondary antibody (dilution 1:5000), followed by ECL detection.

In the case of mesangial cells, the media was replaced with serum free DMEM for 12 h and they were stimulated for 5 min with 5 nM ANP, 10 µM SNP or 10 µM isoproterenol with subsequent addition of the SDS loading buffer and Western blot analysis.

Aldosterone RIA. Aldosterone concentration in the culture medium of ZG cells was determined by RIA using a commercially available aldosterone kit (DPC Bierman) according to manufacture's instruction.

2.2 Materials

1. **Bacteria strains**

E. coli XL1-Blue	Stratagene
E.coli BL-21 DE3	Stratagene

2. **Plasmid vectors**

pcDNA3.1	Invitrogen
pVL1393	Invitrogen
pET3d	Novagen
pcDNA3-PKA-RII-CFP	M. Zaccolo, Padova
pcDNA3-PKA-CAT-YFP	M. Zaccolo, Padova
pEYFP	Clontech
pECFP	Clontech
pcDNA3-NPRA receptor	M. Kuhn, Würzburg

3. **Template cDNA**

Epac1	H. Rehmann, Dortmund
Epac2	A. Wittinghofer, Dortmund
GKI	S. Gambaryan, Würzburg
PDE2	J. Beavo, Washington
PDE5	C. Arkona, Leipzig

4. **Oligonucleotides**   MWG Biotech GmbH, Ebersberg

5. **Chemicals**

ACTH 1-24	Sigma
Adenosine	Sigma

AMP	Sigma
cAMP	Sigma
ANP	Sigma
ATP	Sigma
Agar	Gibco BRL
Agarose	Peqlab
Alprenolol	Sigma
Ampicillin	Applichem
Benzamidine	Sigma
Bisoprolol	Merck
N,N-bis-(2-hydroxyethyl)-2-aminoethanesulfonic acid	Sigma
Bradford reagent	Biorad
$CaCl_2$ dihydrate	Merck
Carvedilol	Stefan Engelhardt, Würzburg
$(CH_3COO)Na$	Merck
Collagenase	Sigma
Cytosine arabinoside	Sigma
Disoxyribonuclease I	Sigma
Disoxyribonucleotides (dNTPs)	Eppendorf
DNA ladders	New England Biolabs
EDTA	Merck
EHNA	Sigma
Ethanol	J.T. Baker
Forskolin	Sigma
cGMP	Sigma
HEPES	Roth
ICI 118.551	Sigma
Imidazole	Roth

Insulin	Sigma
Isopropanol	J.T. Baker
Isopropyl-ß-D-thiogalactopyranosid	Applichem
Isoproterenol	Sigma
Ispase	GibcoBRL
KCl	Sigma
Metoprolol	Applichem
MgCl$_2$	Merck
NaCl	Applichem
Non-essential amino acids	Sigma
Parathormone	Bachem
Phenylmethylsulphonylfluoride	Sigma
Ponceau-S	Serva
Selenite	Sigma
Sodium pyruvate	Sigma
Transferrin	Sigma
Tris	Merck
Trypton	Applichem
Yeast extract	Applichem

6. **Cyclic nucleotides (cAMP, cGMP) and their analogues for plate reader experiments (see Table 1)** — Biolog Life Science Institute, Bremen

7. **Enzymes and kits**

PKA catalytic subunit	Cornelius Krasel, Würzburg
Pfu DNA-polymerase	Promega
Restriction enzymes	New England Biolabs
T4 DNA-ligase	Promega

Qiagen DNA-Maxiprep	Qiagen
Qiagen Plasmid Mini Kit	Qiagen
Qiaquick Gel Extraction Kit	Qiagen
Ni-NTA protein purifucation kit	Qiagen
Baculovirus expression system	
Baculogold	Pharmingen
Western blot ECL detection kit	Amersham
Aldosterone RIA kit	DPC Biermann

8. **Cell culture**

DMEM, 4.5 % glucose	PAN
DMEM/F12, 1% glucose	PAN
Neurobasal-A medium	Gibco BRL
RPMI 1640	PAN
FCS	Invitrogen
Glutamine	PAN
Horse serum	Invitrogen
Matrigel	Becton-Dickinson
Penicillin/Streptomycin	PAN
Poly-L-lysine	Sigma
TC100	Biochrom

9. **Other materials**

Cell culture dishes and multiwells	NUNC
96-well reader plates	Costar
Glass coverslips 24 mm	Hartenstein
Patch pipette capillaries	Harvard Apparatus
Filter for sterile filtration FP30/0.2	Schleicher&Schuell

3 Results

This section is comprised of four distinct parts. The first two are dedicated to the novel cAMP biosensors and describe their development and biological applications. The last two parts describe the generation and applications of improved single-domain cGMP fluorescent probes.

3.1   Development of cAMP biosensors

3.1.1   Single binding domain of Epac2 as a backbone for a cAMP-sensor

To develop a novel highly sensitive cAMP biosensor advantage was taken of FRET as a tool to measure conformational changes in protein molecules. Based on the crystal structure of the regulatory domain of Epac2 [152] and the predictions on a cAMP-induced conformational change, fusions of truncation mutants of Epac2 with YFP and CFP were generated to be able to monitor the cAMP-driven structural rearrangement (Fig. 7A, B). Among the constructs containing either a single low affinity domain A or both low and high affinity (B) domains, none demonstrated a detectable change in FRET upon saturation with cAMP. Next, fusions of a single high affinity B-domain were generated, which produced a decrease in FRET upon activation (Fig. 7A, B, C).
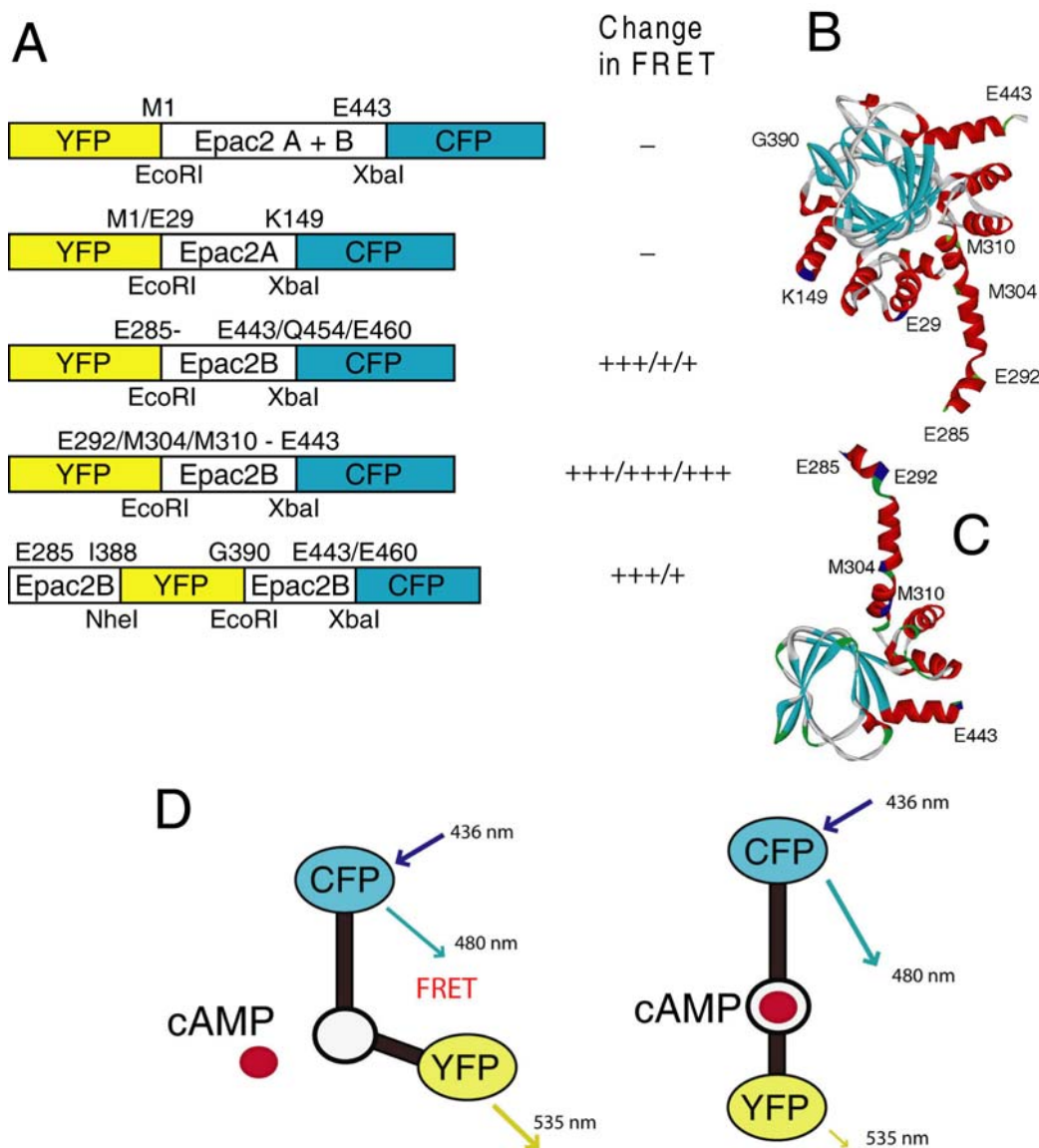
Fig. 7. Development of the single-chain cAMP biosensors based on a single binding domain of Epac2. **A.** Schematic representation of the constructs designed to measure cAMP. These are fusion proteins, containing a sequence of the regulatory domain of Epac2 (encompassed by amino acids M1-E443, M1-K149, E29-K149, E285-E443, E285-Q454 et c.) fused to YFP and CFP. A relative change in FRET measured in CHOA2B cells upon full receptor activation (with adenosine, 100 µM) is presented by + signs (significance of one, two, three +). Under each of the constructs the restriction sites are marked which were used to obtain a fusion construct. **B.** Crystal structure of the whole regulatory domain of Epac2[152]. Positions of fluorophore insertions are marked blue and labelled. **C.** Structure of a single high affinity binding domain B of Epac2 with positions indicated for fusions giving functional biosensors. **D.** The principle of the cAMP biosensor. cAMP induced conformational change determines a decrease in FRET between CFP and YFP.

Here CFP and YFP sequences were inserted directly on the α-helices B (at E 285) and α6 (the so-called hinge helix, at E443) covering the phosphate binding cassette depicted in blue (Fig. 6C). In this case, it was possible to achieve an efficient initial FRET-signal (high emission of YFP upon CFP excitation), indicating a close spatial proximity of the fluorescent proteins (Fig. 7D). This signal underwent a dynamic change in presence of cAMP indicative of a cAMP-induced conformational change, moving the described α-helices and the GFP-variants fused on them apart from each other and resulting in a decrease of FRET (Fig. 7D). The first functional construct of the Epac2 binding domain B contained a sequence E285-E443 of Epac sandwiched between YFP and CFP and was called **Epac2-camps** (camps for *cAMP s*ensor). To further characterize the fluorescent properties of the sensor, dynamic changes in cAMP were measured *in vitro* and in live cells.

Expression of Epac2-camps in *E.coli* gave a highly soluble fluorescent protein, which was purified using the Ni-NTA method. The spectra of the purified protein demonstrated a high efficiency of FRET between CFP and YFP upon excitation at 436 nm (Fig. 8A). The FRET peak at 525 nm was reduced concentration-dependently by addition of cAMP, accompanied by a simultaneous increase in CFP fluorescence. The maximal change in FRET ratio observed in this case was over 40%, which is suitable for effective measurements in live cells (Fig. 8A). To compare the novel biosensor with the previously used technique based on PKA
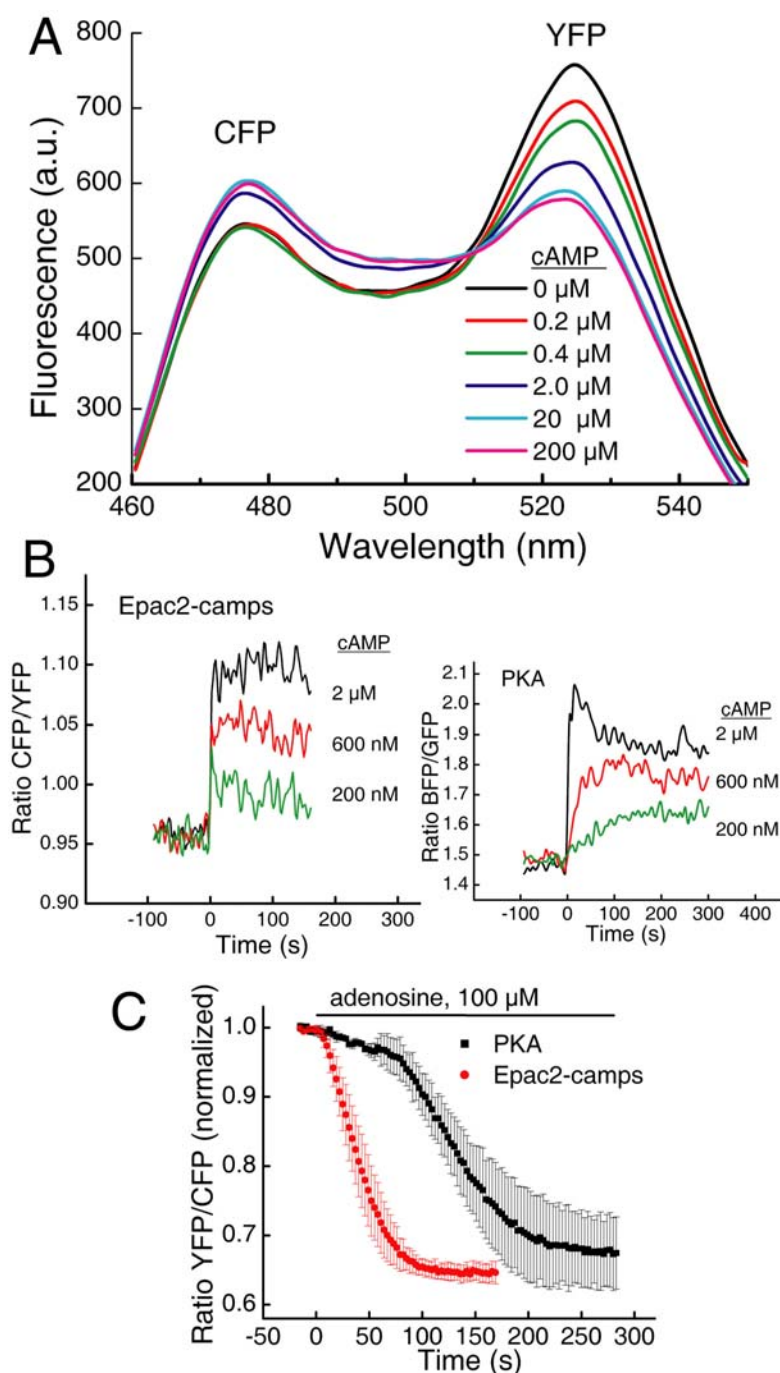
Fig. 8. Measuring cAMP by Epac2-camps. **A.** Fluorescent spectra of Epac2-camps purified from *E.coli*. Growing cAMP concentrations lead to a progressive decrease in FRET. Representative spectra from 4 independent experiments are shown. **B.** *In vitro* kinetic measurements of Epac2-camps activation by cAMP compared to the PKA-based sensor using proteins purified from *Sf9* insect cells at 50 nM concentration. Epac2 demonstrates a rapid change in FRET at different cAMP concentrations, whereas the speed of PKA dissociation decreases at lower cAMP. Representative traces from 4 independent experiments are shown **C.** Kinetics of cAMP measured by Epac2-camps vs. PKA-probe in transiently transfected CHOA2B cells upon activation

of the A_{2B} receptor with 100 µM adenosine. Data are mean ± S.D. are from 5 independent experiments.

dissociation (see 1.4) the kinetics of cAMP binding to both sensors were studied *in vitro* using the proteins expressed in insect cells and purified by the Ni-NTA method. Epac2-camps was switched on very rapidly (within 2 seconds, which is the limit of detection of our instrument) at different cAMP concentrations. PKA holotetramer, however, dissociated much slower, especially upon addition of the lower cAMP concentrations (Fig. 8B). This experiment demonstrates a much faster speed of Epac2-camps, which is limited solely by one-step binding of cAMP to the regulatory domain, whereas the dissociation of the PKA seems to be limited by multiple factors, such as cooperative sequential occupation of the 4 cAMP binding sites and a series of conformational changes occurring prior to the dissociation of the complex (see 1.4 and 1.5). In this case one might get a delay when measuring cAMP, because the sensor is not capable of rapidly reporting a change in the concentration of the second messenger. Epac2-camps, however, provides a higher temporal resolution and increased sensitivity (Fig. 8C), reporting the minor changes in cAMP as fast as never before.

Comparing both approaches in live cells again demonstrated a higher performance of Epac2-camps compared to the PKA. Just a few seconds after the addition of adenosine to CHO cells stably expressing adenosine A_{2B} receptors, Epac2-camps was activated reporting an increase in cAMP represented as a

decrease in FRET-ratio (Fig. 8C). The PKA-based sensor demonstrated a greater delay and a slower FRET-signal.

Next, an attempt was undertaken to optimize the position of CFP and YFP insertion on the binding domain of Epac2 in order to improve Epac2-camps in terms of the amplitude of FRET-signal. Shortening of the helix B on the N-terminus by 7 amino acids (fusion of YFP to E292) resulted in an increase of the amplitude without altering the kinetic properties of the sensor. Further N-terminal truncations over the helix B (to M304, M310) did not significantly affect the signal (Fig. 7A, 9A). Taking longer sequences on the C-terminus (till Q454, E460 on the hinge helix of Epac2) dramatically decreased the amplitude of response in live cells, so that the optimal amino acid range to produce a highly sensitive sensor was determined to lie between E285 and E443. The best amplitude at almost 40% ratio change was achieved using the E292-E443 construct (Fig. 9A). Fig. 9B demonstrates original traces of a cAMP measurement using this sensor in CHOA2B cells upon full activation of cAMP production. Like in a fluorometer cuvette (Fig. 8B), the sensor in live cells exhibited a rapid decrease in YFP and increase in CFP fluorescence, representative of the loss of FRET (Fig. 9B).

The decrease in YFP/CFP ratio could be also monitored with high temporal and spatial resolution using cell imaging techniques, representing the rise in intracellular cAMP by false colours changing from red to blue (Fig. 9C).
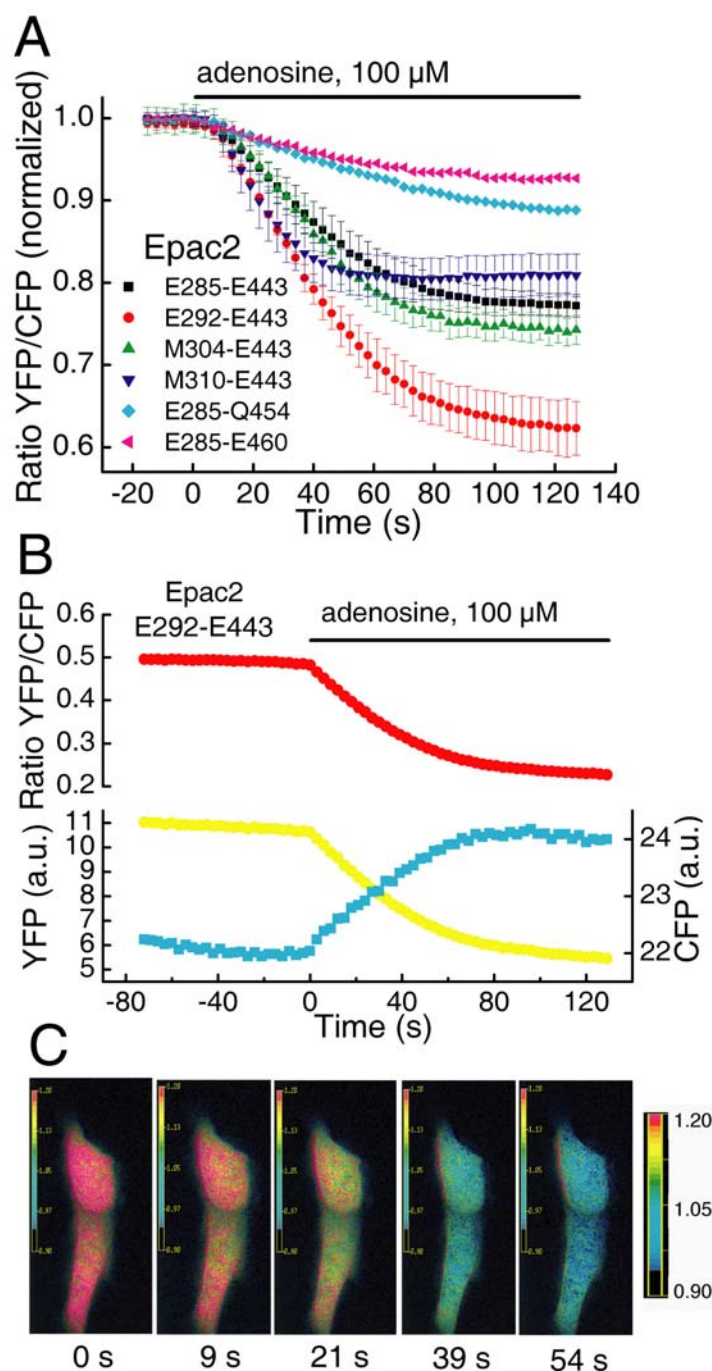
*Fig. 9. Optimization of the Epac2-based cAMP sensor by varying the positions of fluorophore insertion. **A.** Measurements of cAMP in transiently transfected CHOA2B cells upon full A_{2B}-receptor activation using different Epac2-constructs. Ratio traces are presented from 4 experiments ± S.D. **B.** Original traces of YFP and CFP fluorescence from a representative (n=4) cAMP measurement using the E292-E443 construct. A decrease in FRET upon activation is demonstrated. Conditions are as in A. **C.** On-line cell ratio images of the E292-E443 Epac2-sensor in CHOA2B cells at different times after agonist application (100 µM adenosine). Decrease in cAMP is represented here as a change of false colours from warm to cold ones over time.*

By having created a series of fluorescent biosensors based on a single cAMP-binding domain of Epac2 it was experimentally proven that a ligand-dependent conformational change exists and might play a role in the protein activation as predicted by previous studies (see 1.5). This biological mechanism could be used for monitoring cAMP *in vitro* and in live cells with high temporal and spatial resolution, improving traditional biochemical and previously developed FRET-approaches. The next question was, if this mechanism is the case for cyclic nucleotide-binding domains (CNBD) of other proteins and whether it might be possible to create biosensors on the basis of their structure.

3.1.2 Sensors based on binding domains of Epac1, protein kinase A and cyclic nucleotide-gated channels

Among the cAMP-binding protein family, there is another isoform of Epac described, which is called Epac1 and contains only one high affinity cAMP binding site[30,160,161]. However, the crystal structure of this protein has not been solved. To create a FRET-biosensor based on Epac1, the sequence homologous to that of Epac2-camps (E157-E316 in Epac1) was fused between YFP and CFP (Fig. 10). This construct produced an extensive change in FRET as tested in CHOA2B cells (comparable with Epac2-sensors) and was termed **Epac1-camps**.

64

Each regulatory subunit of PKA contains two cAMP-binding domains, one of which (the B domain) is supposed to have a higher affinity and to be occupied first in the presence of cAMP, whereas the A-domain has a lower affinity for cAMP, but interacts with the catalytic subunit and regulates its release after binding the second cAMP molecule (see 1.5). Sandwiching the two domains together between fluorophores did not yield any detectable change in FRET. However, fusion of CFP and YFP at different positions to the B-domain produced three functional sensors (V255-A416, M264-A416, M264-A403). The best one bears the sequence M264-A403 of the PKA and was termed **PKA-camps** (Fig. 10). The third cAMP binding protein that could serve as a backbone for a biosensor is HCN2 channel, which contains a single CNBD of a known structure. To create a new fluorescent cAMP-probe based on HCN2 the GFP-variants were inserted on different α-helices covering the CNBD. This led to three constructs with various amplitude of the signal, the best of which contained the sequence A467-K638 and was called **HCN2-camps** (Fig. 10).

Next, the properties of the four **camps** based on different CNBDs were compared in live cells and *in vitro*. In the next series of experiments another G_s-coupled receptor, namely β_1-adrenergic receptor, was used to elevate intracellular cAMP levels. In transiently transfected HEKβ_1-cells stimulated with isoproterenol the sensors demonstrated differences in the amplitude of the FRET-signal (Fig. 11A). The ratio changes for all sensors in these cells were slightly smaller than in CHOA2B, but the relative change in ratio was
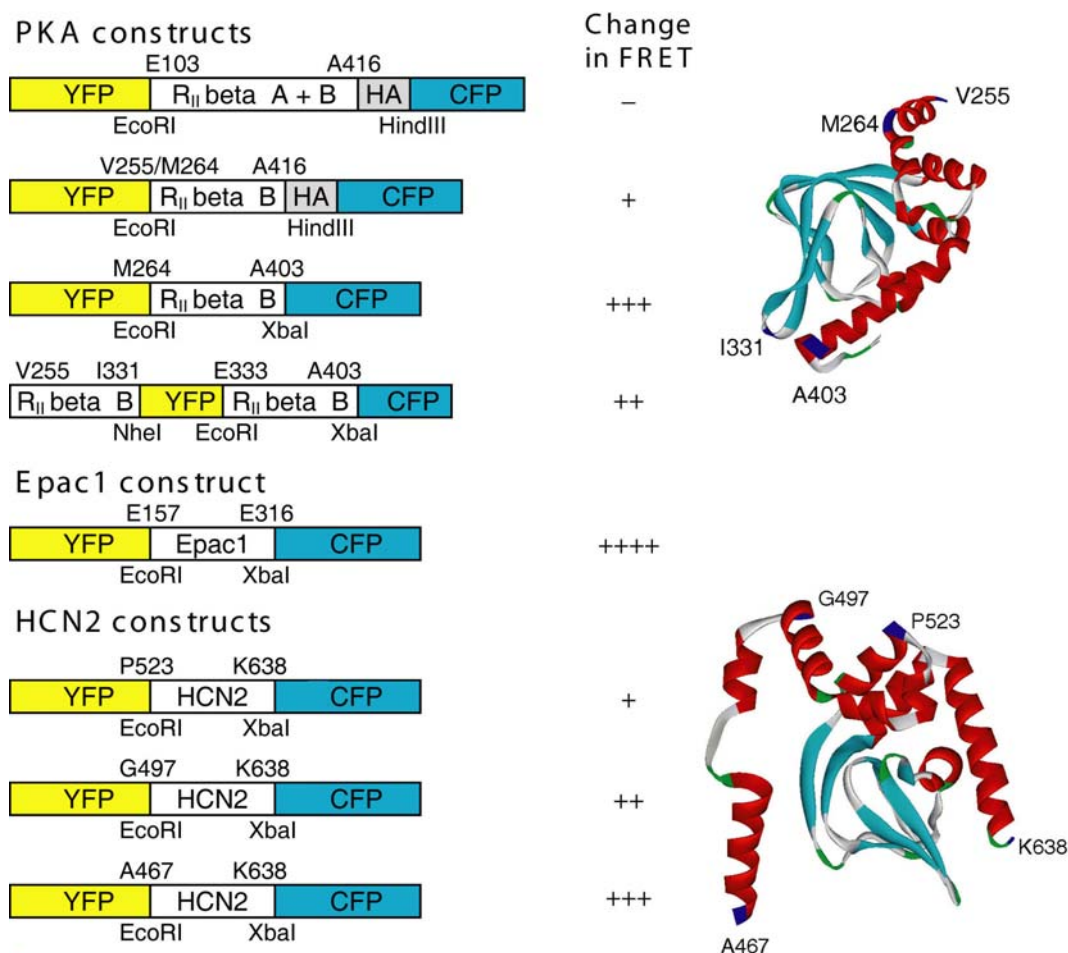
Fig. 10. Creating cAMP biosensors based on PKA, Epac1 and HCN2. Schematic representation of the constructs (left), relative amplitude of the signal (middle) and corresponding crystals structures of PKA and HCN2 with positions of fluorophore insertion labelled (right) are shown. All experiments were performed as described in Fig. 7

comparable, favouring Epac1-camps as a sensor which exhibits the largest magnitude of the signal (Fig. 11A). This indicator was tested in cell imaging experiments and demonstrated a high spatial resolution, allowing visualizing cAMP changes in different regions of the cell (Fig. 11B). Interestingly, different probes not only revealed various amplitudes of the signal, but also differences in the duration of the so-called plateau achieved within some tens of seconds after the addition of the agonist and indicating the saturation of a sensor. This fact

could be due to differences of the binding affinities of cAMP to the four sensors.

Therefore, additional *in vitro* experiments were performed to measure an

effective cAMP concentration producing a 50% change in the FRET-signal

(EC_{50}). To do this the camps were transiently expressed in TsA201 cells,

cytosol was prepared by lysis and centrifugation, and different concentrations of
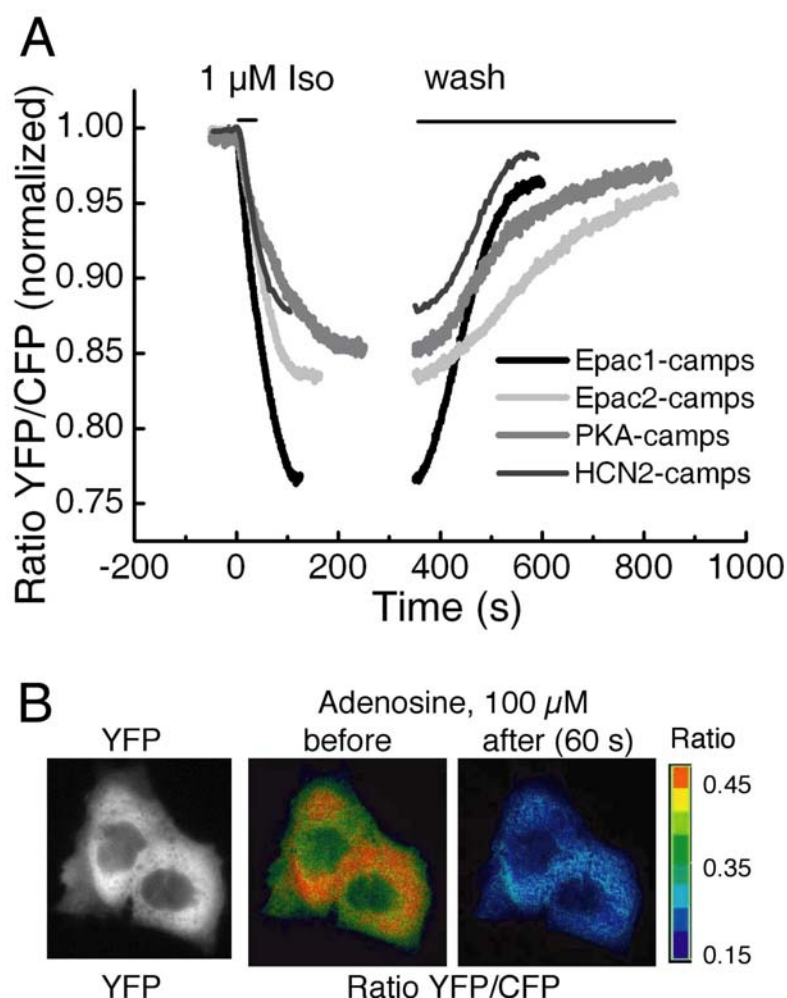
cAMP were added to the cytosol in a fluorometer cuvette.

*Fig. 11. Comparing biosensors based on four different CNBDs in their ability to report changes in cAMP in live cells. **A.** FRET changes in HEKβ1-cells transiently expressing the indicators were measured fluorometrically upon addition and withdrawal of 1 µM isoproterenol (Iso). The traces are dissected to better compare the kinetics of the sensors. **B.** Cell imaging experiments performed using Epac1-camps as described in Fig. 9C.*

Indeed, the different sensors exhibited different affinities for cAMP (Fig. 12), which is in line with the data on differences in affinities of the CNBDs of Epac1 and 2 [161]. HCN2-camps demonstrated the lowest affinity for cAMP, which might explain the obvious absence of the plateau in live cell experiments (not shown). On contrary, the longest plateau was observed with Epac2-camps, which has the highest affinity (Fig. 12). In this case the intracellular cAMP concentrations exceeded the upper measuring limit of the indicator. This might be improved by using the sensors with lower affinities for cAMP (e.g. HCN2-camps).
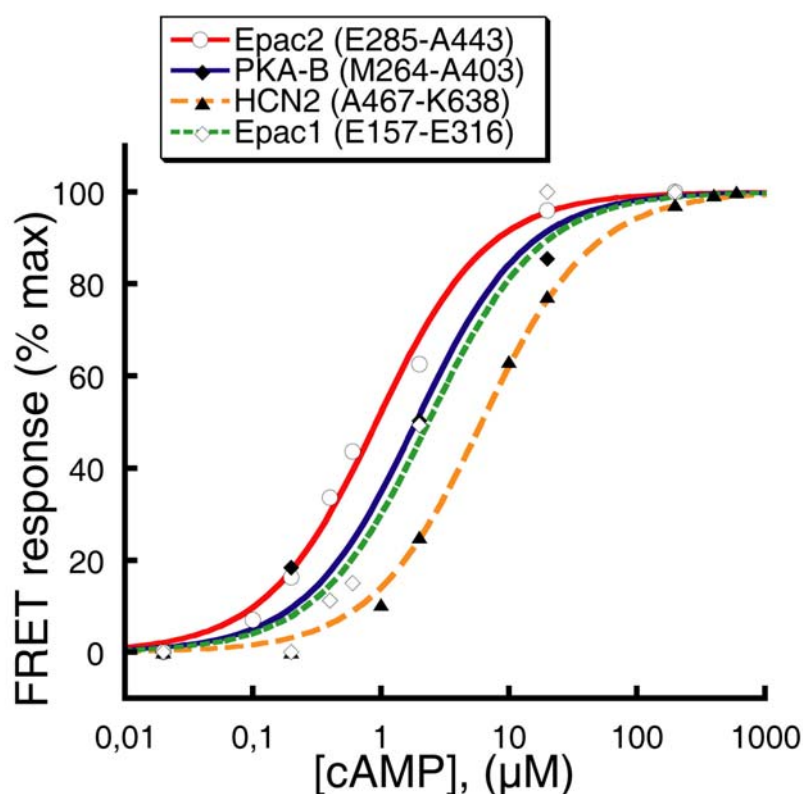
Fig. 12. Comparing the binding properties of the cAMP-sensors based on four different CNBDs. Measurements were performed with the cytosol of transiently transfected TsA201 cells. The representative concentration-response curves are presented (n=3). The EC_{50} values were as follows: Epac2-camps - 0.92 ± 0.07 µM, PKA-camps – 1.88 ± 0.37 µM, Epac1-camps – 2.35 ± 0.42 µM, HCN2-camps – 6.00 ± 0.52 µM. Data are expressed in means ± S.D.

In the same system, the selectivity of Epac2-camps towards other nucleotides, which are present in cells, was tested, demonstrating that cGMP, ATP and AMP were recognized only weakly (Table 1).

Table 1. Affinities of Epac2-camps for different nucleotides measured as in Fig. 12 (n=3, means ± S.D.)

Nucleotide	Affinity for Epac2-camps (EC_{50})
cAMP	0.92 ± 0.07 μM
cGMP	10.6 ± 0.4 μM
ATP	2.5 ± 0.4 mM
AMP	>10 mM

In summary, the cAMP-sensors that were generated using the binding domain of different proteins as a backbone demonstrate different affinities for cAMP, and together also allow to measure the concentration of this second messenger in a broad physiological range from ~ 100 nM to ~ 30 μM. Depending on the intracellular cAMP concentrations in a given type of cells, different camps or their combinations might be applied to cover the dynamic range of the signalling.

A special case of a CNBD is the **A binding site of PKA**. It has a dual role in the activation of the holotetrameric complex serving as a binding partner for both cAMP and the catalytic subunit, mediating the release of the latter when cAMP is bound in both B and A sites (see 1.5). The interface of regulatory-catalytic subunits interaction has a complicated architecture involving over 10 key amino acid residues of contact in the helical and phosphate-binding domains. The most crucial helical interface is located on the helix A (Fig. 5) [24]. Fusion of the A-domain sequences of the PKA to CFP and YFP resulted in a generation of a single functional sensor (Fig. 13A). Only the fusion protein containing the helix A (Q139-M264, Fig. 13B) was functional and revealed an interplay between cAMP and the catalytic subunit on the binding site A of the PKA. Fluorescent spectra of this protein demonstrated an initial FRET between the fluorophores that slightly decreased upon addition of cAMP. When the purified catalytic subunit was added to the cuvette this initial FRET-signal was significantly elevated and again was greatly reduced upon addition of cAMP (Fig. 13C). This behaviour of the A-domain sensor demonstrated binding of the catalytic subunit with a change of conformation and the reversal of this structural rearrangement upon binding of cAMP, which serves as an allosteric competitor of the catalytic subunit. Thus, it was possible to generate a fluorescent sensor, which reports the binding of catalytic subunit to the A-domain of the PKA and its concurrent displacement by cAMP. Such an indicator supports the scenario of PKA-

complex activation proposed based on its crystal structure and allows to further

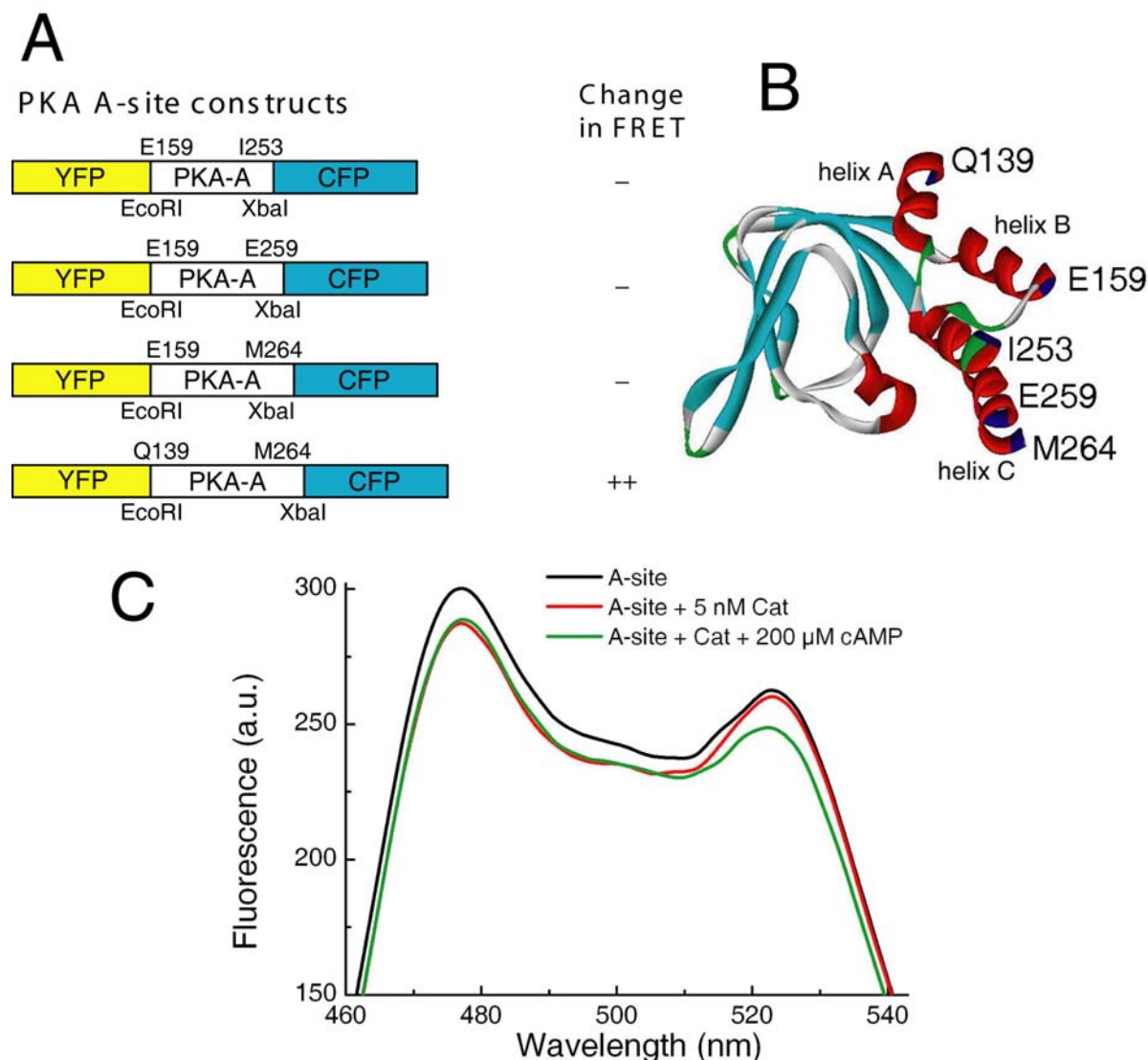study the molecular dynamics of PKA.

Fig. 13. Generating a FRET-sensor based on a single A binding site of PKA. **A.** Structure of the constructs and relative change in FRET upon addition of cAMP to the protein expressed in TsA201 cells as measured with cytosolic preparations *in vitro*. **B.** Crystal structure of the A-domain of PKA with the positions of fluorophore insertion labelled. **C.** Fluorescent spectra taken as described in Fig. 7A without the ligand and catalytic subunit (black), after addition of 5 nM of catalytic subunit (red) and after addition of cAMP to the complex of the sensor with the catalytic subunit (green).

In summary, a series of FRET-based biosensors for cAMP was created, which now allow measuring this second messenger *in vitro* and in live cells with high temporal and spatial resolution. All known cAMP binding domains were used as a backbone for fluorescent sensors and demonstrated a decrease in FRET upon binding of the ligand. Therefore, this study proved the previously suggested conformational change, which was proposed on the basis of X-ray crystal structure analysis as a ubiquitous mechanism of cAMP binding domain activation. This conformational change could be used to measure dynamic changes of cAMP by means of FRET.

3.2 Applications of cAMP sensors

After having produced a variety of novel fluorescent probes for cAMP, it was decided to apply them to investigate physiologically relevant aspects of cAMP signaling. First, spatio-temporal dynamics of cAMP diffusion were studied in different cell types. Secondly, real-time monitoring of PDE2 activity in aldosterone-producing cells was performed. Further on, the sensors were applied for screening of the cAMP-activating anti-β_1-receptor antibodies in heart failure patients. Finally, using the family of fluorescent indicators chemical mechanisms of cAMP-binding domain activation in terms of conformational change were studied.

3.2.1 Spatio-temporal dynamics of cAMP signaling

It has been argued over decades, whether cAMP acts in cells as a freely diffusing second messenger or whether such signals are more localized, for example via activation of local pools of PDE activity[162]. In line with this hypothesis, PKA-dependent β_2-adrenergic mediated stimulation of L-type calcium channels in primary hippocampal neurons has been suggested to occur in spatially restricted signaling complexes[163]. In this part of the study it was decided to investigate the intracellular distribution of cAMP signals in different cells using the novel Epac-camps as a biosensor.

To assess the spatio-temporal aspects of cAMP signaling primary hippocampal neurons were transfected with Epac1-camps. The Epac1-camps expressing cells were then stimulated with the β-adrenergic agonist isoproterenol (50 nM) delivered locally with a patch pipette under constant perfusion in the opposite direction in order to prevent agonist diffusion on the cell surface. This local stimulation resulted in a rapidly spreading change in the FRET-signal, reflecting a rise in cAMP propagating from the site of stimulation through the whole neuron on the scale of a few hundred milliseconds (Fig. 14A). Rapidly spreading cAMP-signals were also observed with Epac1-camps in other cells, including mouse peritoneal macrophages stimulated locally with isoproterenol (Fig. 14D). In CHOA2B cells as well as in PC12 cells with endogenous
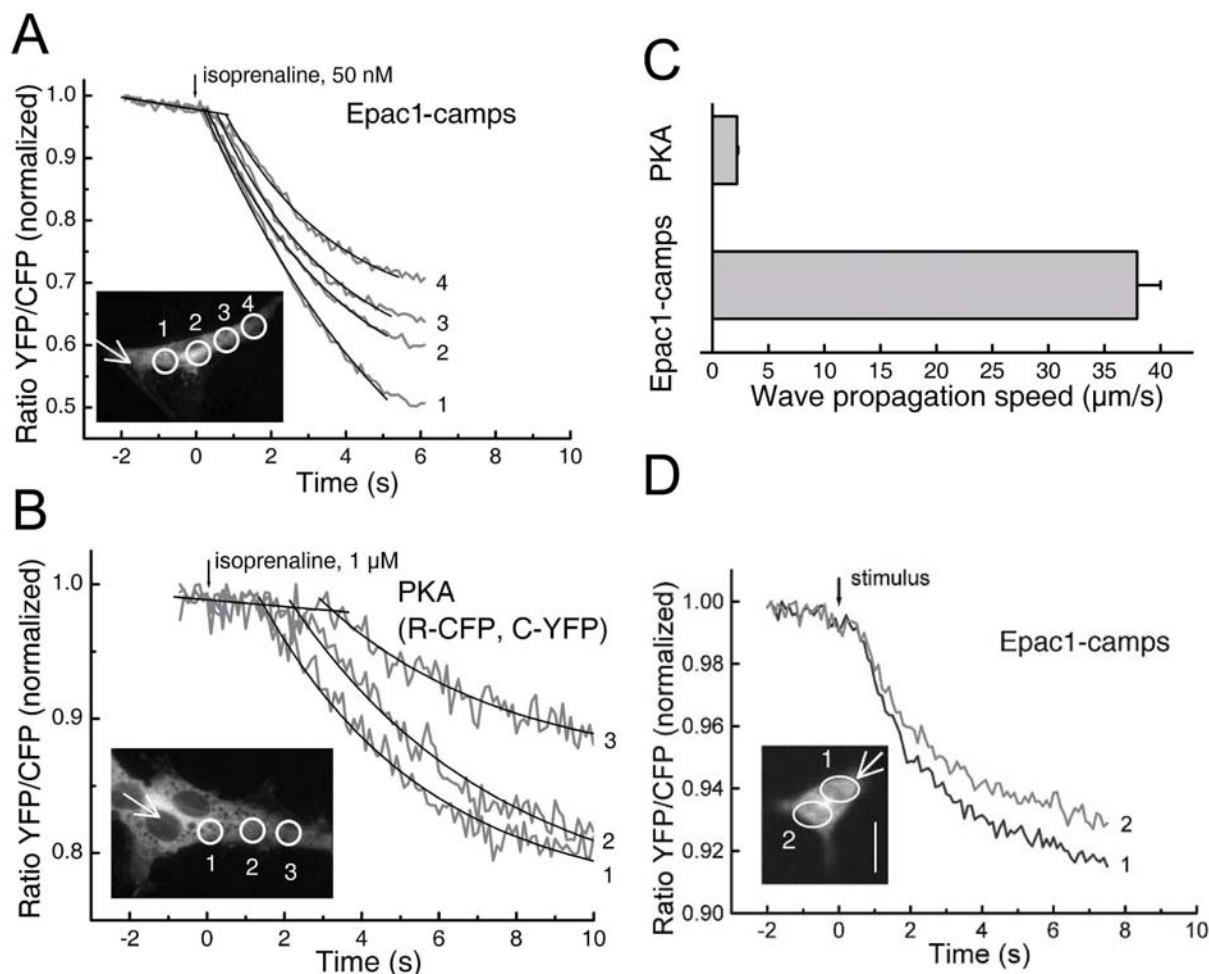
*Fig. 14. cAMP gradients in murine primary hippocampal neurons and peritoneal macrophages. **A.** Neurons transiently transfected with Epac1-camps were stimulated by gently touching with a patch pipette filled with 50 nM isoproterenol (arrow in inset) under a constant perfusion to avoid agonist diffusion along the membrane. FRET-responses were measured in different regions of the cell away from the site of stimulation. Representative experiment (n=5). Scale bar, 10 μm. **B.** Gradients in neurons transfected with the tetrameric PKA-indicator and stimulated with 1 μM isoproterenol (n=5) demonstrate lower amplitude and speed of cAMP propagation. Scale bar, 10 μm. **C.** Calculated cAMP-gradient propagation speed measured in hippocampal neurons with Epac1-camps in A (37.9 ± 2.2 μm/s, diffusion constant 478.2 ± 23.0 μm^2/s) and PKA-system in B (2.1 ± 0.1 μm/s).**D.** cAMP gradients in murine peritoneal macrophages. The cells were transfected with Epac1-camps and stimulated with 10 μM isoproterenol delivered locally by a patch pipette (stimulus, white arrow). FRET-responses are demonstrated for two different regions of the cell. Representative experiment (n=4). Scale bar, 5 μm.*

adenosine A$_{2A}$-receptors[164] similar spatial patterns of cAMP-signaling were observed in response to adenosine. Another cell type tested were HEK293 cells stably expressing parathyroid hormone receptors, where the local delivery of the ligand led to a cAMP-gradient freely propagating through the whole cell.

Measuring these rapidly propagating FRET-changes in many cells made it possible to calculate the speed of the cAMP gradient in neurons. To do so, the FRET-signals in different regions of the cell (Fig. 14A) were fitted to a first-order exponential function, and the intersection of the fit with the baseline was defined as the time of activation.

To study the difference between cAMP levels measured with Epac1-camps and the previously described tetrameric PKA-indicator, the latters was also studied in the same primary neuronal cells. In this case, the speed of cAMP-propagation (even at 1 µM isoproterenol, Fig. 14B) was ≈20-fold slower than that recorded with Epac1-camps (Fig. 14C). In addition, the PKA-sensor allowed recording in only a third of the transfected neurons compared to a ≈100% responsiveness with Epac1-camps and furthermore the PKA-sensor had a smaller signal amplitude than Epac1-camps.

The speed of cAMP-gradients measured with Epac1-camps after local stimulation with 50 nM isoproterenol was calculated at almost 40 µm/s, from which a diffusion coefficient at 487 ± 23 µm^2/s was derived. This is much faster than previously described for cells stimulated with neurotransmitters and measured using PKA subunits labeled with rodamine and fluorescein[144]. The

kinetics of cAMP propagation measured with Epac1-camps corresponds well with those estimated for cAMP using patch-clamp recording of cyclic nucleotide-gated channels (270 $\mu m^2/s$)[165] and with the diffusion coefficients calculated for cGMP (500 $\mu m^2/s$)[166] and free microinjected cAMP (780 $\mu m^2/s$)[143]. cAMP signals recorded with Epac1-camps were uniformly distributed throughout hippocampal neurons, whereas PKA mediated signals such as β-adrenergic stimulation of L-type calcium channels were reported to be locally restricted, presumably due to formation of signaling complexes including receptors, G proteins adenylyl cyclases, PKA, effectors and phosphatases[163].

3.2.2 Real-time monitoring of phosphodiesterase activity of live cells

In different kinds of primary cells (neurons and macrophages) as well as in intact cells expressing various G_s-coupled receptors such as A_{2B}-adenosine, PTH, $β_2$-adrenergic receptors no localized cAMP signals were observed, suggesting that cAMP behaves in those cells as a freely diffusing second messenger, propagating through the cells with very high speed. The so-called compartmentalization of the signaling or the access of cAMP to its intracellular targets appears to be regulated by certain isoforms of PDE through cAMP-hydrolysis[102]. Little is known, however, about the kinetic properties of these enzymes in live cells and about the mechanisms responsible for the PDE-dependent compartmentalization. For this reason, in the next part of the study

the PDE activity was directly measured in live cells using the developed cAMP-sensors to better understand the role of PDEs in regulating cAMP-signaling.

To monitor PDE activity in real-time, the novel cAMP biosensor was used in a physiological system. It seemed most interesting to analyze such a PDE that can be selectively activated by a specific stimulus and represents a predominant isoform in the cells of interest in order to avoid a possible interplay with other PDEs. Among the numerous PDEs, PDE2 has been characterized as a cGMP-stimulated isoform hydrolyzing cAMP (see 1.1). In adrenal *zona glomerulosa* (ZG) cells PDE2 serves as a cGMP-stimulated effector of ANP to decrease cAMP-stimulated aldosterone secretion (Fig. 15). In the present study PDE2 activity was measured in bovine adrenal ZG cells, where PDE2 is not only a predominant isozyme providing almost 100 % of PDE activity[47], but also the unique cGMP-binding protein, because in contrast to rat ZG cells GK and cGMP-gated ion channels are not expressed in this cell type[156].

To test whether an Epac-based fluorescent indicator could be used to monitor PDE activity in these cells it was first investigated, how fast bound cAMP dissociates from the sensor. In case of slow dissociation this step might become time-limiting for the system, making correct measurements of PDE2 action impossible. After saturating purified Epac2-camps with 20 μM cAMP (with a fast on-rate of 2.0 ± 0.2 s), a high amount of purified catalytically active PDE (10 μM) was added to the cuvette to degrade unbound ligand.
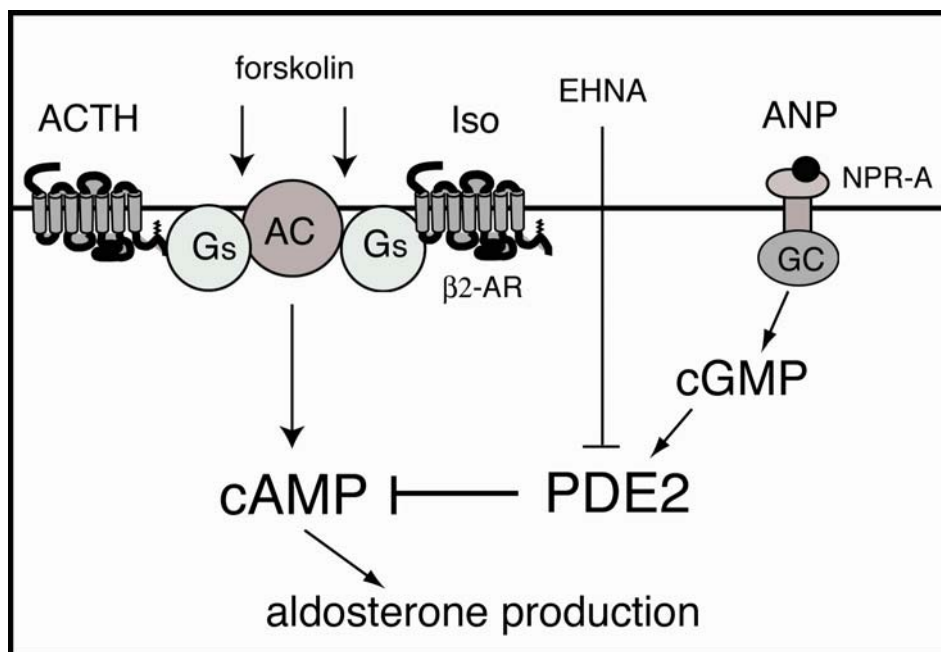
Fig. 15. Experimental system for monitoring PDE2 activity. Signalling pathway in bovine adrenal ZG cells, which regulates aldosterone production. cAMP is produced by adenylyl cyclases (AC), which are activated by G_s-protein coupled receptors, e.g. ACTH- or β-adrenergic receptors, or directly by forskolin. cGMP-stimulated PDE2 blocks aldosterone production by degrading cAMP after activation of ANP receptors, which contain a guanylyl cyclase domain (GC). EHNA - erythro-9-(2-hydroxy-3-nonyl)-adenine – is a selective inhibitor of PDE2.

cAMP depletion led to an immediate dissociation of the sensor-bound ligand fraction with an apparent half-life of 2.9 ± 0.3 s (Fig. 16). At a catalytic activity of the PDE-preparation used of 0.3 mol of cAMP/s/mol of PDE, degradation of cAMP in the cuvette can be estimated to occur with a half-life of ~3 s. Since cAMP depletion in this experiment is limited by the speed of PDE-mediated cAMP-hydrolysis, the real kinetics of cAMP dissociation from the sensor are difficult to estimate, but must be much faster than the speed of increase of the

FRET signal. This indicates that Epac2-camps could be used to monitor PDE2 activity provided that the latter process occurs with a half-life above 2 s.
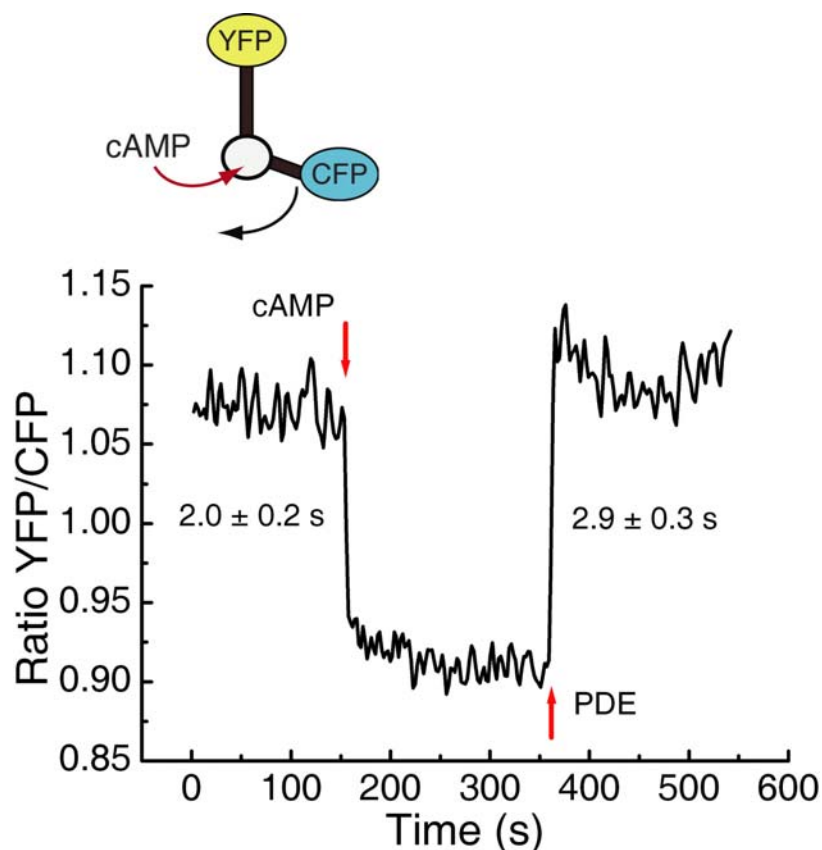

Fig. 16. Measuring dissociation of cAMP from Epac2-camps. 40 nM solution of purified protein (600 µl) was saturated with 20 µM cAMP and the bovine heart PDE at 10 µM final concentration was added to the cuvette leading to a rapid dissociation of the bound ligand. Representative experiment (n=4).

To monitor PDE2 activity in primary adrenal ZG cells, they were transfected with Epac2-camps using adenovirus, because these cells are not transfectable by other known techniques (Fig. 17B). After 2-3 days in culture single-cell microscopic measurements were performed. cAMP degradation by PDE was monitored as an increase of the FRET signal. Stimulation of adenylyl cyclase

by addition of 10 μM forskolin resulted in a substantial increase of intracellular cAMP (monitored as a decrease in FRET-ratio) from basal sub-micromolar levels up to a plateau (Fig. 17A), suggesting saturation of the sensor ($\approx$ 20 μM). Next, PDE2 was activated in the cells by stimulation with ANP. A very rapid increase in the FRET-signal was observed, demonstrating a fast degradation of cAMP by PDE2. After a few seconds delay, PDE2 apparently became active and hydrolyzed the majority of intracellular cAMP with a half-live ($t_{0.5}$) of 15.5 ± 0.9 s (Fig. 17A). This time is at least 5 times higher than the speed of cAMP dissociation from purified Epac2-camps *in vitro* (Fig. 16), suggesting that PDE2 activity can be accurately monitored as a time-limiting process. Using this protocol a concentration-response dependence of the ANP-effect on PDE2 activity was measured with a half-maximal response at 0.43 ± 0.02 pM ANP (Fig. 17C). Levels of intracellular cAMP measured in real-time with this system correlated well with the data of conventional biochemical experiments on aldosterone production and phosphorylation of VASP, a substrate of PKA and GK (Fig. 17D). In addition to the generally accepted concept that aldosterone production in adrenal cortex cells is critically dependent on cAMP levels, which are regulated by ANP-activated PDE2, it could thus be demonstrated that PDE2 activity kinetically overcomes the forskolin-induced cAMP production, providing a mechanism to hydrolyze extensive amounts of the second messenger and thereby put aldosterone secretion under the control of the ANP-NO-cGMP axis.
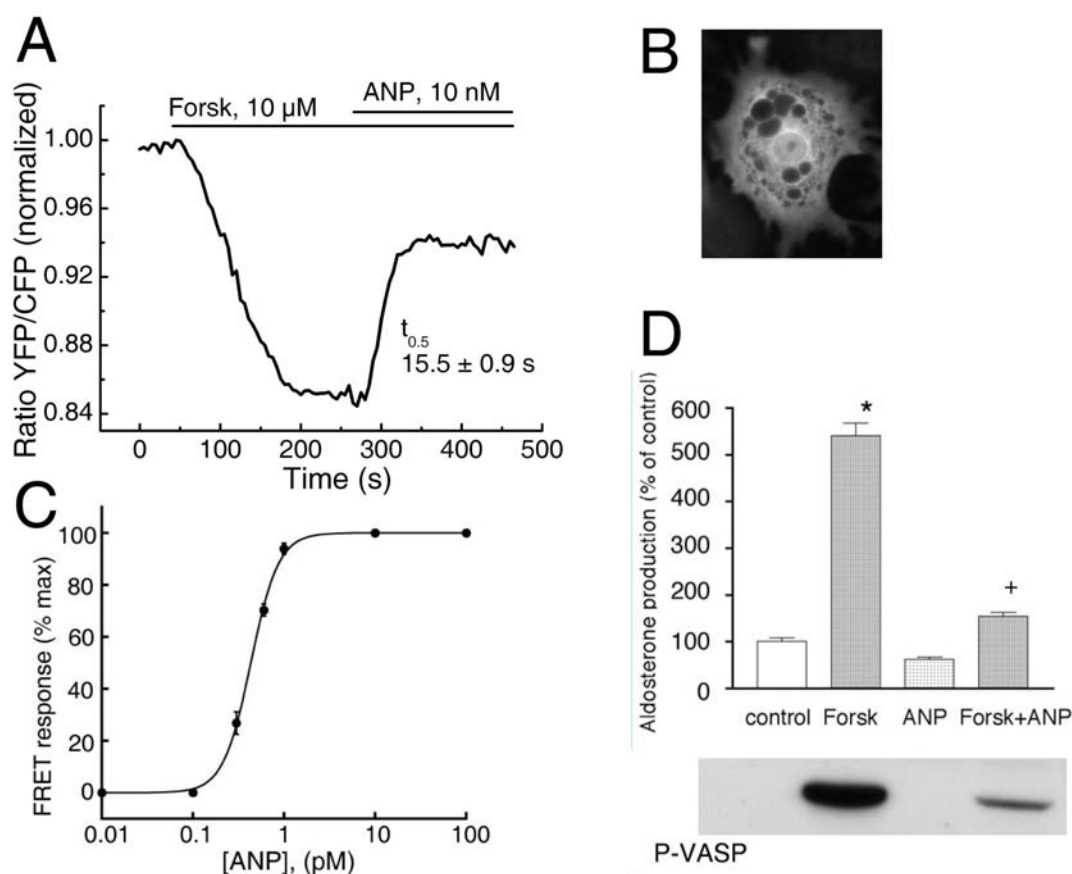
Fig. 17. ANP inhibits forskolin-induced cAMP accumulation and aldosterone production in bovine adrenal zona glomerulosa cells. **A.** Measuring cAMP in aldosterone-producing cells demonstrates a rapid action of PDE2. cAMP, which is produced in cells by stimulation with forskolin (Forsk), was rapidly ($t_{0.5}$ 15.5 ± 0.9 s) degraded upon addition of ANP, presumably via cGMP-mediated activation of PDE2. Intracellular cAMP was monitored microscopically as a FRET-ratio YFP/CFP in single cells, infected with Epac2-camps adenovirus (YFP image in **B**) and superfused with different compounds. A decrease in the ratio represents an increase in cAMP. Representative experiment (n=5). **C.** Concentration-response dependence of the ANP effect on PDE2 activity as measured with a FRET-based system as in A. Data of 5 experiments are presented ± S.E. EC_{50} value is 0.43 ± 0.02 pM, Hill slope – 2.9±0.4. **D.** ANP inhibits aldosterone production and PKA activity. Bovine ZG cells were stimulated with 5 µM forskolin, 10 nM ANP, or a combination of forskolin with ANP. After 1 h of incubation, the culture medium was collected for aldosterone RIA and cells were harvested for Western blot analysis of the phosphorylated PKA-substrate P-VASP. Results are mean ± S.E. of three different experiments. *, Significant differences ($p < 0.05$) compared to control values. +, significant differences ($p < 0.05$) compared to forskolin stimulated values.

Next, the activity of PDE2 was investigated under different conditions including stimulation of the cells via a physiologically relevant GPCR. To further characterize PDE2 activity in ZG cells, we used its specific inhibitor EHNA, which at micromolar concentrations allows to selectively block the enzyme, inhibiting other PDEs at more than 100 µM only partially[167]. When applying EHNA to the cells under basal conditions, little effect on cAMP could be observed even at 100 µM (Fig. 18A), indicating that basal PDE2 activity in unstimulated ZG cells is very low. In contrast, applying a saturating concentration of ANP activated PDE2, which led to a decrease in cAMP, even though this effect was not as prominent as after forskolin stimulation (Fig. 18A), corresponding well with the functional data on aldosterone production (Fig. 16D). ACTH as a natural ligand capable of stimulating aldosterone secretion induced a slow cAMP-accumulation, which could be fully and rapidly blocked ($t_{0.5}$ 13.0 ± 3.2 s) by ANP (Fig. 18B). This effect was inhibited by the specific PDE2-inhibitor EHNA, applied in addition to ACTH and ANP. Interestingly, the ACTH effect on cAMP production in this case was much stronger. Similar effects have been previously observed for specific PDE3 and PDE4 inhibitors and adrenergic stimulation in cardiac myocytes[100]. Upon removal of the inhibitor, ANP-induced PDE2 activity was immediately restored and brought cAMP in cells down to the basal level. The $t_{0.5}$ for this restoration of PDE2 activity was 18.3 ± 1.9 s, which is comparable with the speed of ANP-effects in presence of forskolin (Fig. 17A).
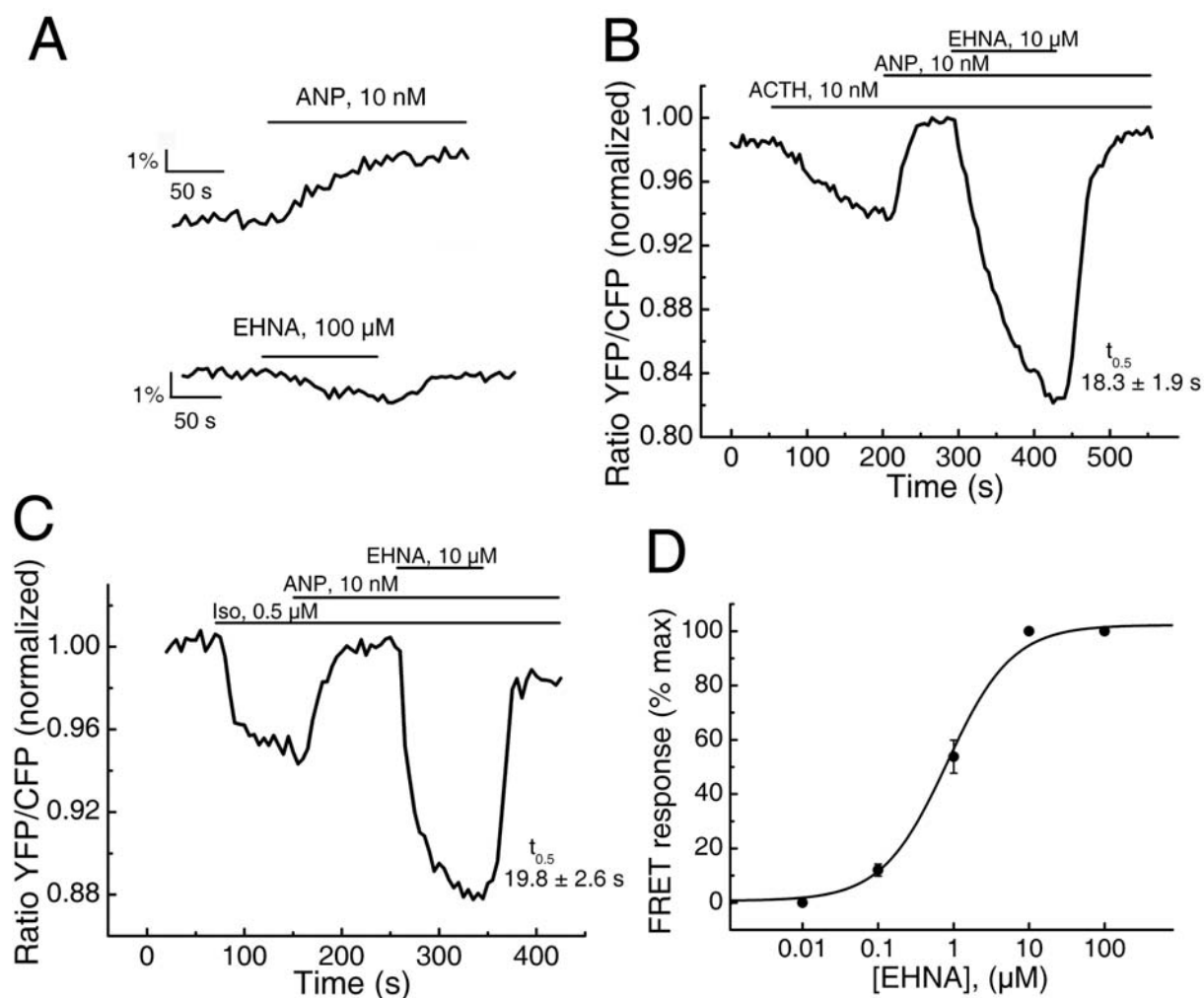
*Fig. 18. Real-time monitoring of PDE2 activity under basal and agonist-stimulated conditions. **A.** Low basal PDE2 activity in ZG cells is demonstrated by the fact that EHNA, a specific PDE2 inhibitor, even at 100 µM caused only minor changes in intracellular cAMP. ANP (10 nM) alone exhibited a small stimulatory effect on intracellular cAMP. % change in ratio YFP/CFP is demonstrated. Representative experiments (n=4). **B.** ACTH-induced (10 nM) cAMP-accumulation is rapidly terminated by ANP-stimulated (10 nM) PDE2 action, which was fully blocked by EHNA (10 µM). Representative experiment (n=6). **C.** Isoproterenol-mediated activation of endogenous adrenergic receptors in ZG cells leads to cAMP accumulation. Rapid PDE2 activation kinetically overcomes cAMP production. Representative experiment (n=9). **D.** Concentration-response dependence of the EHNA effect on PDE2 activity demonstrated in C. Data of 3 experiments ± S.E. EC_{50} value is 0.82 ± 0.16 µM, Hill slope 1.17.*

PDE2 activity was 18.3 ± 1.9 s, which is comparable with the speed of ANP-effects in presence of forskolin (Fig. 17A).

EHNA has been demonstrated to reverse the inhibitory effect of cGMP-dependent PDE2 on cAMP-stimulated calcium current in frog ventricular cardiomyocytes after isoproterenol treatment[168]. Therefore ANP and EHNA effects on β-adrenergic receptor-mediated cAMP production in ZG cells were studied. The β-adrenergic receptor agonist isoproterenol induced a cAMP signal that was again blocked by ANP-stimulated PDE2 (Fig. 18C). EHNA, comparable with the ACTH experiments, fully blocked PDE2 activity and together with isoproterenol further increased cAMP, exhibiting a half-maximal effect at ≈1 μM (Fig. 18D), which corresponds well with the previously measured constants[157,159]. Again, PDE2 recovery demonstrated rapid kinetics with a $t_{0.5}$ of 19.8 ± 2.6 s (Fig. 18C).

In summary, using the bovine adrenal cells as a model system, the monitoring of PDE activity in live cells was achieved. Taking advantage of the high expression of PDE2 in ZG cells and specifically stimulating it with ANP, which is responsible for physiological regulation of aldosterone production, it was possible to analyze real-time kinetics of cAMP hydrolysis by PDE2. An extremely fast action of PDE2 was observed, which allows to kinetically overcome forskolin-, ACTH- or β-adrenergic receptor-mediated cAMP-accumulation, in order to fully block their effects on aldosterone production. Epac2-camps in this measuring system is capable of measuring PDE2 activity

due to a much faster ligand dissociation from the sensor (Fig. 16), compared to the speed of PDE2-mediated, time-limiting cAMP hydrolysis (Fig. 17A, Fig. 18B,C). In contrast to classical biochemical studies where the activity of PDE is estimated on a scale of minutes, the real-time live cell experiments reveal that the endogenous PDE2 only needs 15-20 s to decrease intracellular cAMP from high micromolar (saturation of the sensor at $\approx$ 20 µM) to sub-micromolar (the lower detection limit of Epac2-camps at $\approx$ 100 nM) concentrations (Fig. 16A, 17B,C). Such a high catalytic activity and rapid action of PDEs could be crucial for their physiological function to rapidly antagonize cAMP formation in cells and shut down its signaling. Extremely rapid PDE2-mediated cAMP degradation observed in the present experiments could also be important for compartmentalization of the cAMP signaling, which might be resulting from the much higher speed of PDE-catalyzed cAMP hydrolysis compared to the speed of cAMP production in living cells.

3.2.3 Detection of anti-β_1-receptor autoantibodies in cardiac myopathy patients

Over the past two decades evidence has accumulated that functionally active autoantibodies targeting the human β_1-adrenergic receptor (β_1-AR) may play an important role in the development and clinical course of progressive cardiac dilatation and failure[169]. In this context, it became recently possible to

demonstrate that rats immunized against the presumably antigenic second extra-cellular β_1-receptor loop (100% sequence-identity between human and rat)[170] developed both, stimulating anti-β_1-receptor antibodies (anti-β_1-AR) and progressive dilated cardiomyopathy (DCM).[171] Subsequent isogenic transfer of anti-β_1-AR from immunized to healthy rats (in order to mimic autoantibodies) also transferred the disease and hence provided direct evidence for a cause-and-effect relationship between stimulating anti-β_1-AR antibodies and DCM in human-analogous animal model. To date, conventional methods do not allow to functionally detect anti-β_1-AR with high sensitivity and temporal resolution. In the present study FRET was used to establish a novel technique to measure β_1-AR-induced cAMP signals in live cells.

To determine the anti-β_1-AR antibodies *via* receptor-induced signal propagation β_1-AR-expressing cells (HEKβ_1-cells) were transfected with Epac1-camps Before testing IgG from DCM-patients (and healthy control subjects) IgG isolated from previously characterized anti-β_1-AR-positive rats with dilated immune-cardiomyopathy and isogenic control rats were used to establish the FRET-detection system[171]. None of the IgG from isogenic control rats affected cAMP levels in β_1-AR expressing cells, whereas activating rat anti-β_1-AR produced clear-cut signals and induced a rapid, more than 70%-loss in FRET, indicating an effective receptor activation. The onset of the response was delayed by some 100-150 s, which might indicate binding events (Fig. 19).
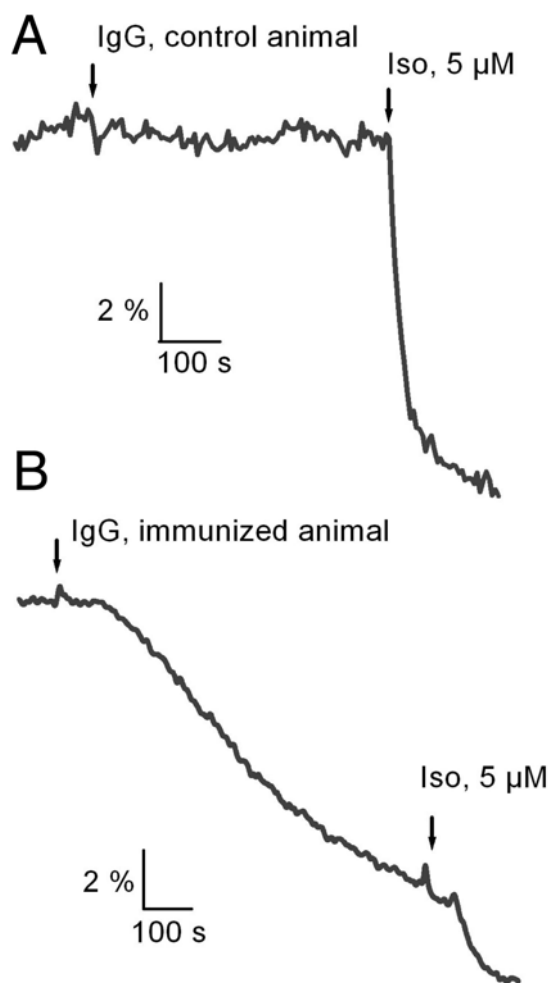
Fig. 19. Effects of rat IgG preparations on intracellular cAMP.

IgG fractions from rats immunized against the 2nd extracellular loop of the human β_1-AR (**B**) were tested on HEKβ_1-cells transfected with Epac1-camps compared to unimmunized animals to verify the reliability of the approach (**A**). FRET ratio traces are presented (% indicates a relative change in YFP/CFP intensity ratio, Iso-isoproterenol). IgG concentration used in the assay was 0.13 µg/µl. The measuring buffer C in all anti- β_1-AR experiments was supplemented with 50 nM ICI 118.551 to block endogenous β_2-ARs. Representative experiments (n=6).

These experiments with the animal sera suggested that the measuring system might be capable of detecting the presence of specific anti-β_1-AR also in heart failure patients.

Next, IgG-fractions isolated from n=55 previously antibody-typed DCM-patients and n=20 healthy control subjects[172] were re-analyzed by FRET. None of the IgG from healthy controls affected Epac-FRET (Fig. 20A), whereas IgG from all previously anti-β_1-AR-positive judged DCM-patients induced a rapid loss of FRET, indicating receptor activation (Fig. 20A). In addition to all anti-β_1-AR-positive DCM subjects, IgG from 30 of 37 previously anti-β_1-AR-negative judged by immunofluorescence DCM-patients induced a modest but

significant increase in cAMP (Fig. 20A). The strength of the cAMP-signal in this group of sera was significantly lower than in the case of previously positive-judged samples (p<0.01, Fig. 20B).

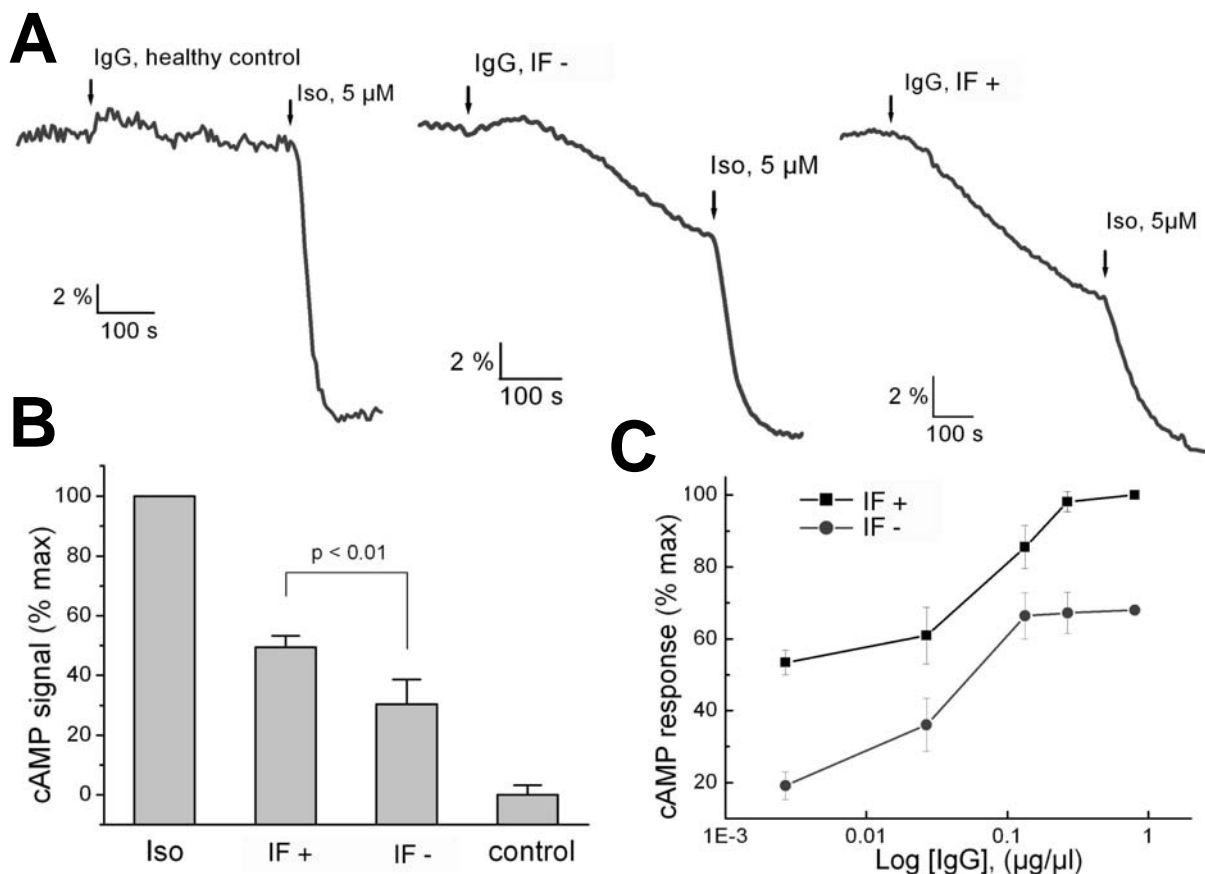*Fig. 20. Epac1-camps is able to detect anti-β_1-AR antibodies in DCM patients. **A**. None of the n=20 healthy control serums induces a visible cAMP-FRET response in live cells (left). Representative experiment (n=20). IgG from all patients with DCM judged by immunofluorescence anti-β_1-AR-positive (IF+) elicit substantial cAMP-response (49.5 ± 3.8 % of maximal Iso-signal, right). Representative experiment (n=18). IgG from 81% of anti-β_1-AR-negative patients (IF-) demonstrate a robust, but significantly smaller increase in cAMP (30.3 ± 8.4 %, middle). Representative experiment (n=30). Quantifications are shown in **B**. Data is expressed in mean ± S.D. **C**. Concentration-response dependencies of the IgG preparations from IF+ and IF- patients demonstrate differences in maximal response. % of maximal cAMP-response is presented ± S.D. Representative experiments (n=4).*

Analysis of the concentration-response dependencies for IgG from these two groups demonstrated that the low-activating IgGs even at higher concentrations did not increase cAMP levels as much as did the antibodies from the previously identified anti-β_1-AR-positive patients (Fig. 20C), excluding the possibility of just lower titers and rather suggesting different mechanism of action at the receptor (e.g. activation of different epitopes on the receptor).

The therapeutic strategies aimed at counteracting the action of anti-β_1-AR by using receptor antagonists proved beneficial in DCM patients.[172] Therefore the action of some clinically relevant drugs on autoantibody-induced cAMP signals was analyzed in the FRET-based system. Indeed, both β_1-selective (bisoprolol, metoprolol) and unselective (alprenolol, carvedilol) beta-blockers largely suppressed the cAMP production (Fig. 21A,B). However, they produced only a partial effect resulting in maximally 60-80% cAMP-suppression (Fig. 21C). Despite being used in saturating concentrations (Fig. 21D) bisoprolol like all other drugs tested was not capable of fully reversing the cAMP-elevating effect of the antibodies. A possible explanation for this could be different mechanisms by which antibodies and antagonists act on the receptors. Antibodies induce receptor activation by binding at the extracellular loops[169,173], distant to the ligand binding site. Therefore, further therapeutic strategies are needed to minimize autoantibody-induced cAMP-signalling in the heart.
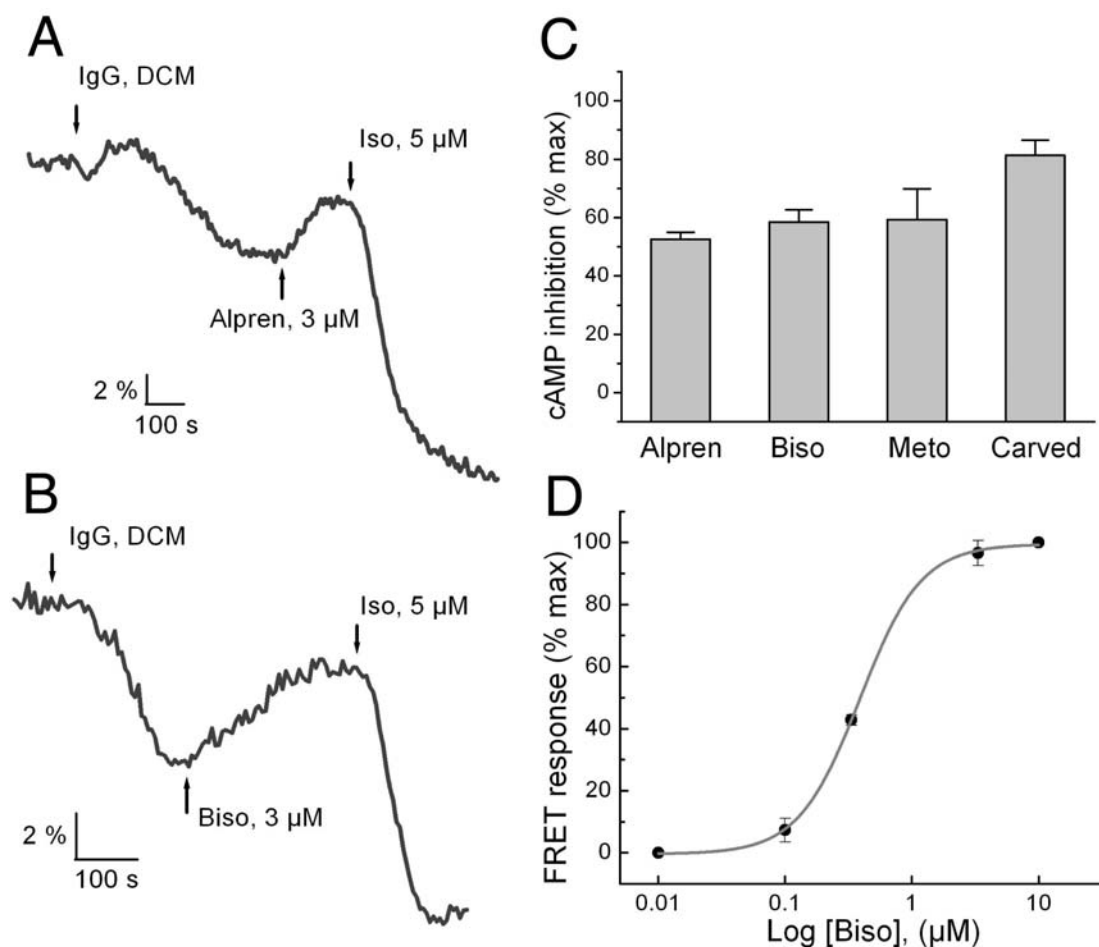
Fig. 21. Beta blockers do not allow to fully reverse the cAMP-signal in β_1-autoantibody stimulated live cells. Neither unselective β-blockers alprenolol (Alpren) (**A**) and carvedilol (Carved), nor selective β_1-AR drugs bisoprolol (Biso) (**B**) and metoprolol (Meto) are able in saturating concentrations (3 µM) to suppress more than 80% of the IgG-response. Data (means ± S.D) are presented in **C** as calculated from 4 independent experiments. **D**. Concentration-response dependence for the blocking action of bisoprolol measured as in B. % of maximal effect is presented ± S.D (n=4).

In summary, the novel technique based on measurements of the β_1-AR-antibody-induced cAMP signal using FRET allowed not only to achieve a high specificity (substantial cAMP-response in heart failure patients and absence of visible signal in healthy controls), but also to greatly improve detection of

functional autoantibodies in the group of DCM-patients, that were not detected by previously available techniques. These patients might have the anti-β_1-AR against other epitopes than the 2nd extracellular loop of the receptor and were previously judged anti-β_1-AR-negative[140]. The new method detects increases in cAMP *via* the receptor activation by anti-β_1-AR from ~80 % of all DCM-patients, supporting the hypothesis of β_1-autoantibodies as an important mechanism in the development of DCM and heart failure[169,174]. This prevalence correlates well with the functional data obtained on isolated neonatal cardiomyocytes, where the antibodies from humans with DCM prolonged action potential duration and enhanced contractility[175].
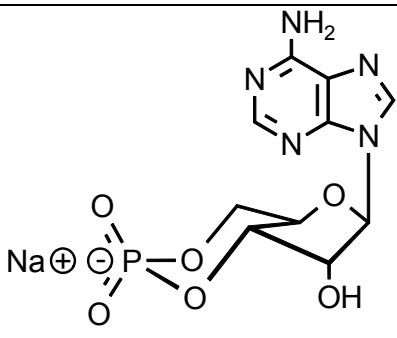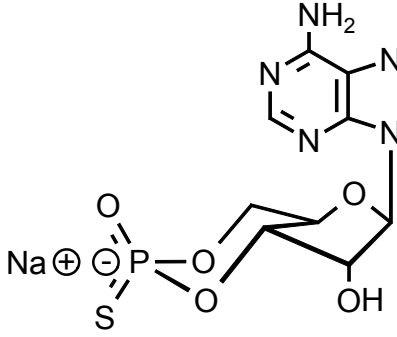
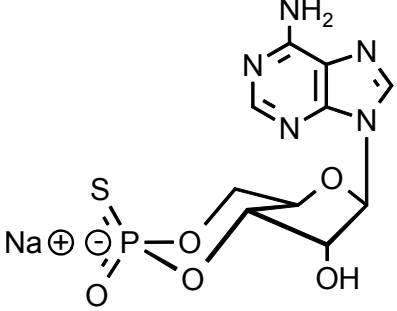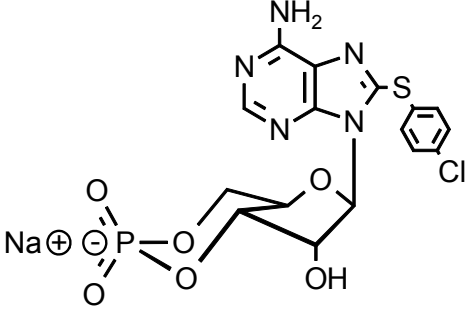### 3.2.3 Chemical mapping of the cAMP-binding domains in terms of the conformational change
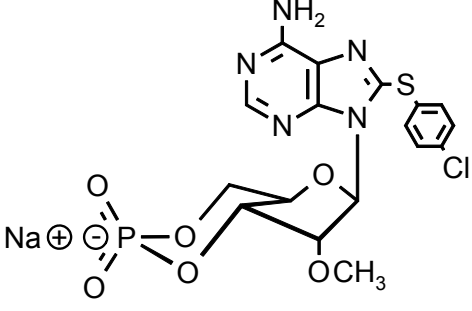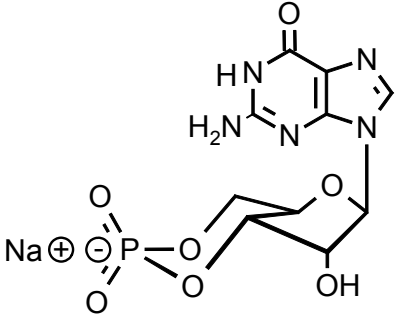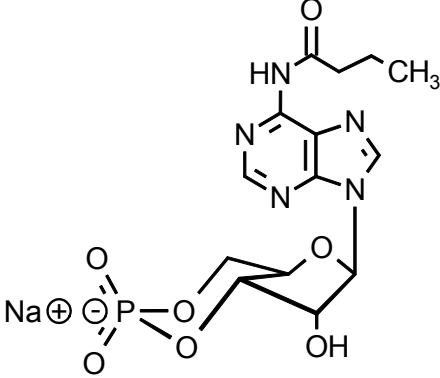
Development of the family of cAMP biosensors allowed to measure different aspects of the signaling by this second messenger. Different cAMP binding domains demonstrated similar activation properties, exhibiting a uniform conformational change upon binding of the ligand. Measurements by means of FRET suggest an increase in distance between helices A/B and C (hinge), covering the phosphate-binding cassette. This structural rearrangement was suggested to play a central role in cAMP-induced activation of Epac, PKA and HCN-channels (see 1.5). This part of the project was aimed at understanding
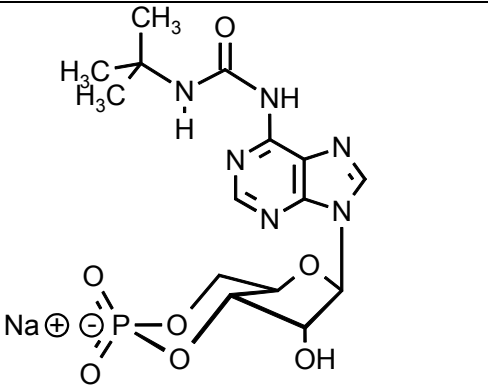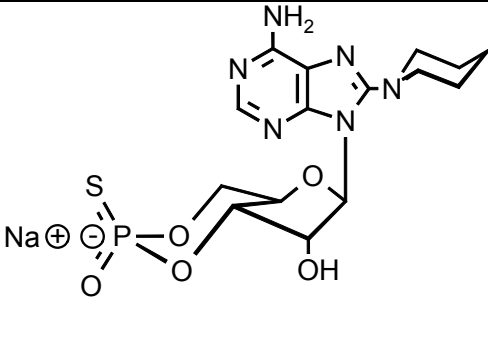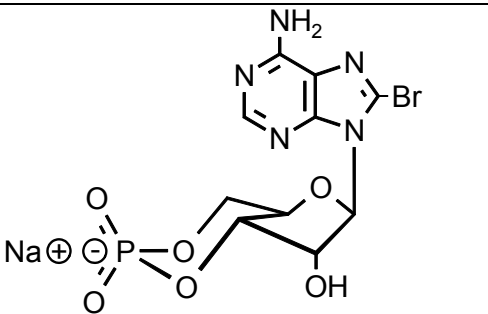
molecular mechanisms underlying the conformational change in different CNBD by using chemical compounds, which represented systematic changes of the lead structure of cAMP, allowing preferential binding to and activating of particular proteins. These substances are widely used in biochemical assays to selectively activate particular signaling cascades, but the detailed mechanisms of their action remain elusive. Here ten different cAMP derivatives were tested in terms of induction of the conformational change of different binding domains. The structure and known properties of the compounds are listed in Table 2.

Table 2. Chemical structure and biological profile of cAMP-derivatives used in the current study. All compounds were from the BIOLOG Life Science Institute, home page (www.biolog.de).

Systematic name	Chemical structure	Biological properties
cAMP		Activates PKA, Epac and HCN-channels. See 1.1
Adenosine-3',5'-monophosphothionate Rp-isomer (Rp-cAMPS)		Competitive inhibitor of PKA, partial agonist for Epac1 [176]

Adenosine-3',5'-monophosphothionate Sp-isomer (Sp-cAMPS)		Activates PKA, is not hydrolyzed by PDEs[177]
8-(4-Chlorophenylthio)-cAMP (8-pCPT-cAMP)		Stimulates both PKA and GK[178], inhibits PDE5[179]
8-(4-Chlorophenylthio)-2'-*O*-methyl-cAMP (8-pCPT-2'-O-Me-cAMP)		Epac-selective compound, does not activate PKA [34]
cGMP		Activates GKs, cGMP-regulated PDEs and cGMP-gated channels (see 1.1.)
N$_6$-Monobutyryl-cAMP (6-MB-cAMP)		Selective activator of A-site of PKA I [180]

*N*6-Mono-butylcarbamoyl-cAMP (6-MBC-cAMP)		Specific activator of PKA type II with a strong preference for the A-site[180]
8-Piperidinoadenosine-3',5'-cyclic monophosphorothioate, Sp-isomer (Sp-8-PIP-cAMPS)		Site-selective activator of PKAII B-site[181]
8-Bromo-cAMP (8-Br-cAMP)		Activator of PKA and Epac[176,180]

To study the conformational changes induced by the compounds they were analyzed *in vitro* using the previously described sensor proteins purified from *E.coli*. The FRET-signals were detected directly after addition of compounds at different concentrations in a 96-well plate by using a high throughput MITRAS reader in order to obtain concentration-response dependencies for each substance. First, the ability of compounds to activate **Epac1-camps** was studied (Fig. 22, Table 3).

Fig. 22. Mapping of the Epac1 cAMP binding site using different compounds. A representative curve for each substance is shown (n=3). EC_{50}-values are shown in Table 3.

Interestingly, all compounds induced a conformational change to some extent in the binding domain of Epac1 but had different affinities. Two substances exhibited a partial effect. These were Rp-cAMPS and Sp-8-PIP-cAMP. The first substance is known as an inhibitor of PKA. The change of cyclic oxygen to sulfur with an additional change of overall configuration to Rp-isomer disfavors binding and activation of the CNBD. Previously, the action of Rp-cAMPS on Epac1 was analyzed by gel filtration experiments and revealed a lower affinity

than for cAMP, compatible with the present data. Rp-cAMPS was also

demonstrated as a partial agonist in terms of Epac1 activation in intact cells[176].

Another, previously unidentified, partial agonist of Epac1 is Sp-8-PIP-cAMP

(selective ligand for the B-site of PKA), which may have these properties due to

the presence of the piperidine substitution in the 8-position of adenine. It is

described that the purine ring of the cAMP molecule interacts with the binding

domain of PKA, Epac and HCN by a series of hydrophobic interactions, which

might be disturbed by introduction of polar substituents[182]. However,

introduction of 4-chlorophenylthio substituent in the same position did not lead

to partiality of activation, but significantly increased the affinities, almost 100-

fold for 8-pCPT-cAMP and 10-fold for the Epac selective substance 8-pCPT-2'-

O-Me-cAMP. A previous study[176] has demonstrated various other substances to

be full agonists for Epac; this was confirmed in the present work. All other

substances studied were full agonists for Epac1-camps, although having

different affinities. For example, cGMP had a lower affinity than cAMP or the

sulphur-derivatives such as Sp-cAMPS were several times less affine.

Surprisingly, 6-MB-cAMP, which was described not to activate Epac1, induced

(like another 6-derivative 6-MBC-cAMP) a change of conformation in Epac1-

camps. The overall affinities exhibited by different substances on the Epac1

binding domain were comparable with those estimated by an alternative method

used for only Epac1 and PKA-sites before[176], demonstrating that the current

method applicable to study structure-effect relationships for CNBD. Thus, it

was, next, sought to analyze the behavior of previously non-characterized Epac2 and HCN2 domains.
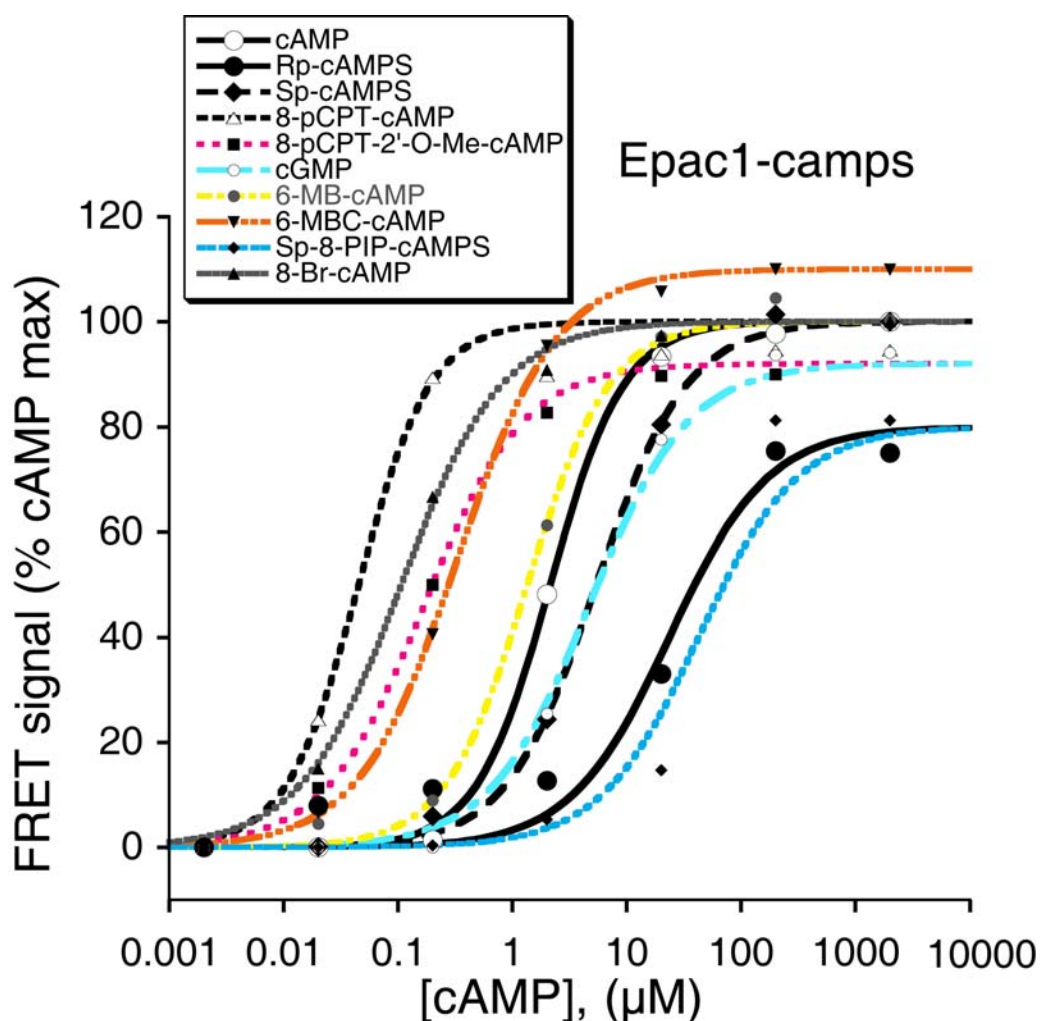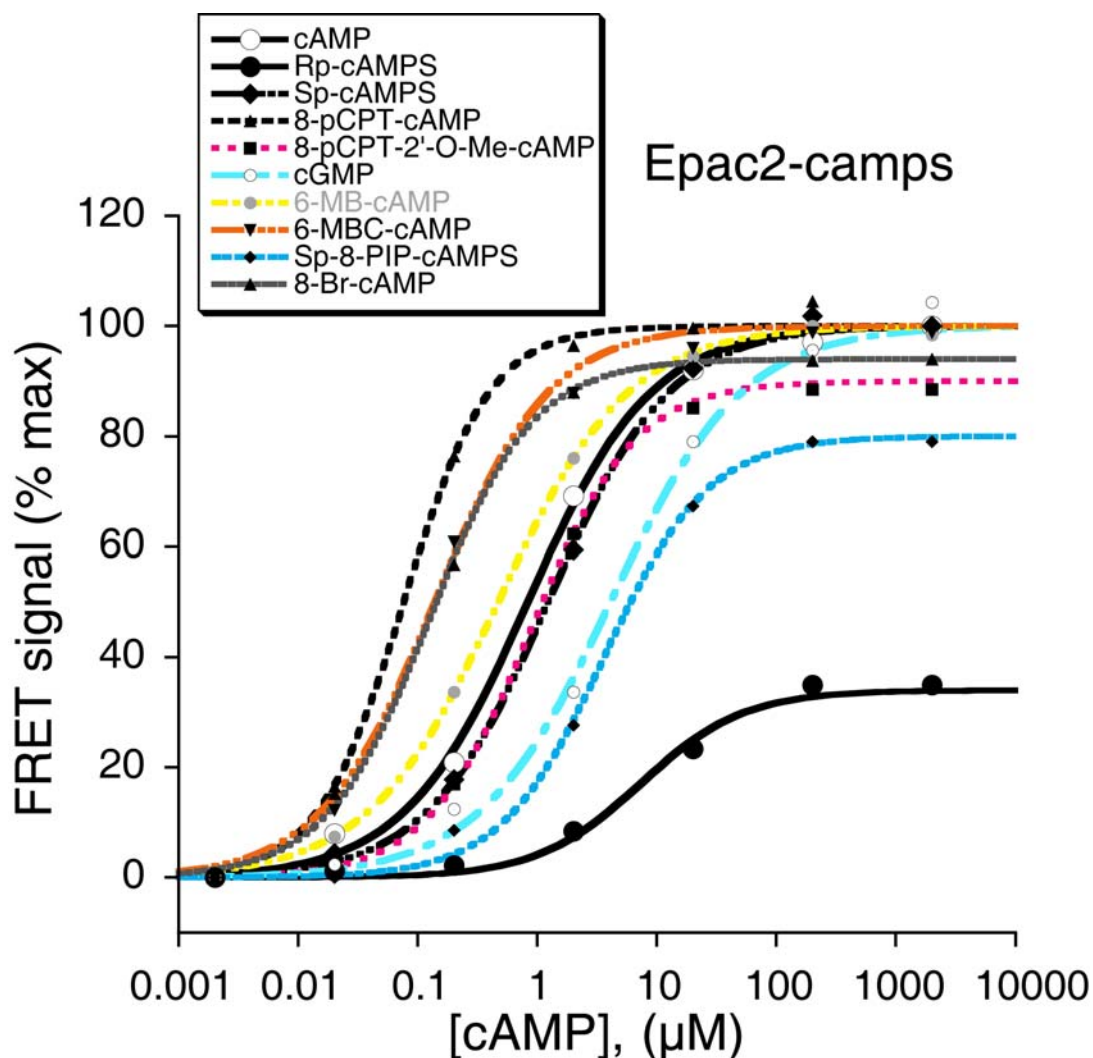

Fig. 23. Mapping of the Epac2 cAMP binding site B using different compounds. A representative curve for each substance is presented (n=3). EC_{50}-values are shown in Table 3.

Fig. 23 demonstrates concentration-response dependencies of the substances to induce a conformational change in **Epac2-camps.** Here all compounds behave almost similar to the Epac1 situation with slightly different affinities. Rp-cAMPS and Sp-8-PIP-cAMPS still act as partial agonist. However, the effect of

Rp-cAMPS is significantly lower than on Epac1-camps. The Epac-selective activator 8-pCPT-2'-*O*-Me-cAMP also demonstrates a 10-fold lower affinity for Epac2 compared to Epac1 (Fig. 22). In general, the binding domains of Epac isoforms appear rather similar in their behavior towards different compounds.

Next, it was sought to study a CNBD from another class of cAMP-regulated proteins. The most intriguing situation is observed when analyzing the conformational changes in **HCN2-camps** (Fig. 24, Table 3). Here, only cAMP remains a full agonist. cGMP and 6-MB-cAMP are only partial agonists stimulating the sensors rather weakly (~ 20 %). Sp-8-PIP-cAMPS is likewise a partial agonist as in the case of the Epac isoforms. Surprisingly, 8-Br-cAMP can also not completely activate the HCN2 CNBD, exhibiting only ~ 80% of the maximal signal. The sulphur substituents do not exhibit any measurable binding to the domain. Strikingly, 8-pCPT derivatives and 6-MBC-cAMP exhibit a increase in FRET upon activation, resulting in a signal in the other direction than antagonists (Fig. 24). The Epac-selective substance 8-pCPT-2-O'-Me-cAMP does not activate, but rather inhibits the conformational switch in HCN2-camps. Unlike Epac CNBDs, the binding site of HCN2-channel represents a structurally different domain. Only cAMP could fully activate HCN2-camps. This suggests the importance of all chemical components of cAMP, which interact with the binding site of the channel and induce a change of conformation. Further investigations are necessary to investigate the functional consequences of action of 8-pCPT-cAMP and 6-MBC-cAMP compounds, which might be proved to be

functional inhibitors of the channel, which plays a role in the physiological regulation of cardiac pacemaker activity[22]
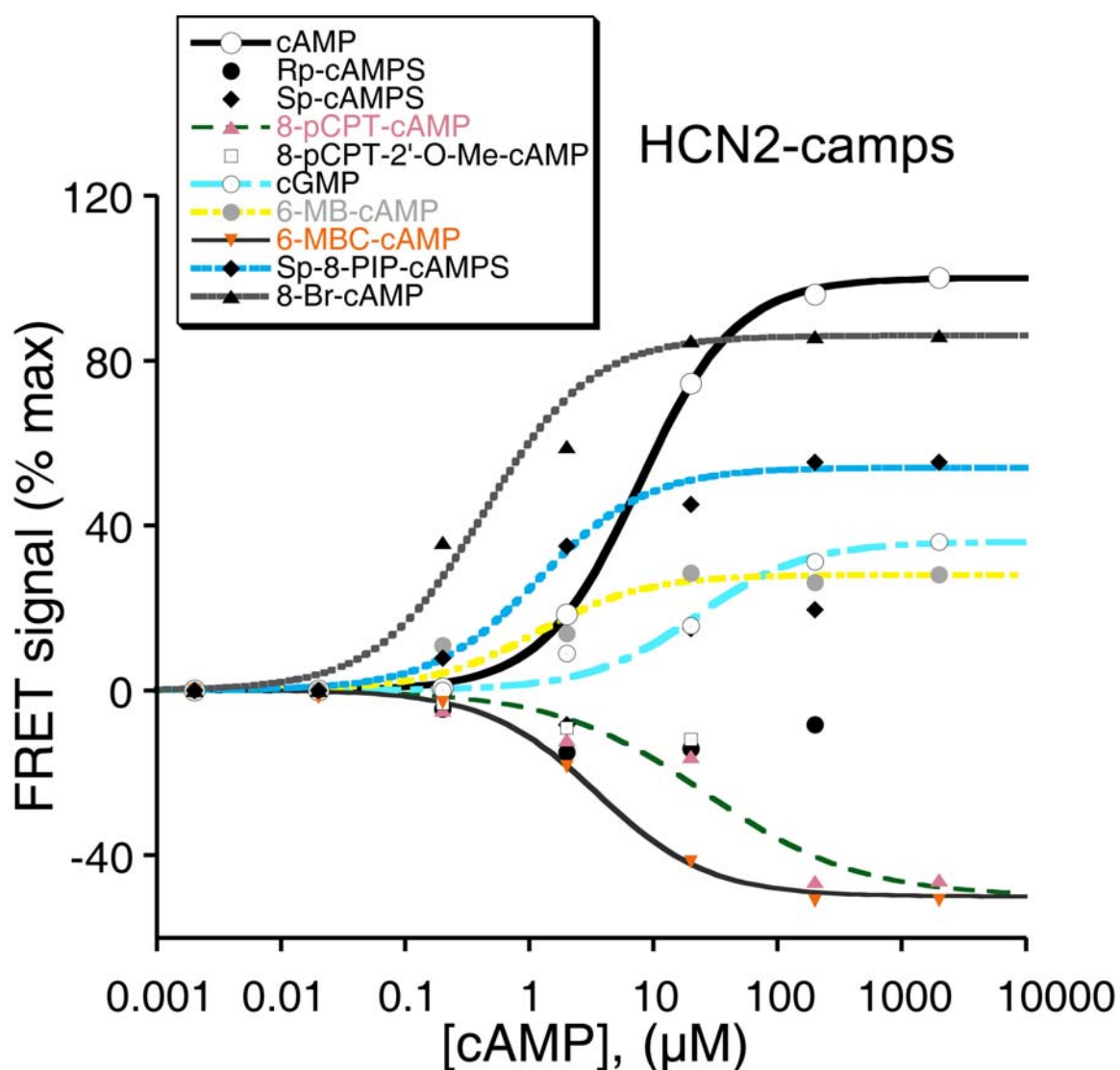
Fig. 24. Mapping of HCN2-camps using different compounds. Representative curves or solely data points for each substance are presented (n=3). EC$_{50}$-values are shown in Table 3.

The unusual behavior of the HCN2 binding domain in terms of the nucleotide-induced conformational change could be explained based on the crystal structure of this protein[22], which significantly differs from the domains of PKA and Epac2 in terms of the chemical mechanisms of interaction with the cAMP molecule.

Fig. 25 schematically describes the major interactions between cAMP and phosphate-binding cassettes of PKA site B, Epac2 and HCN2. Interestingly, HCN2 domain has, compared to other cAMP binding sites, numerous residues hydrophobically interacting with the purine ring. Probably, this is a reason for a
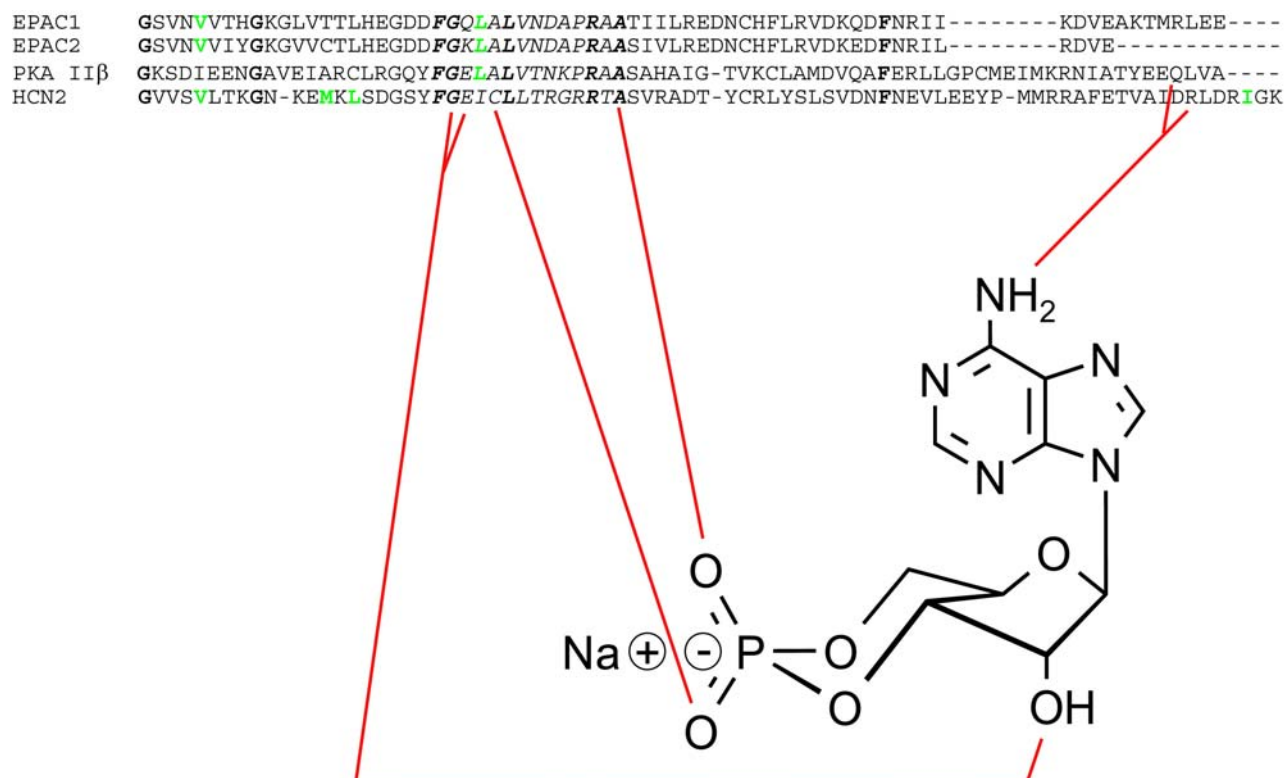
Fig. 25. Amino acid sequence alignment of phosphate binding cassettes of Epac2, PKA site B and HCN2 channel and the major chemical interactions with cAMP molecule. The highly conserved residues are in bold. The amino acids responsible for the hydrophobic interaction with the purine ring are shown in green. Compared to other proteins, HCN2 has numerous residues responsible for hydrophobic interactions with the adenine ring. Hydroxyl bonds are presented as red lines[22,182].

major disturbance of the conformational change in the HCN2 domain for all compounds having substitutions in the adenine residue.

Table 3. EC$_{50}$-values measured for different sensor proteins and cAMP analogues (in µM, means ± S.D., n=3). * - the substance exhibit an opposite effect on the conformational change in HCN2-camps.

Substance	EC$_{50}$-values for different proteins		
	Epac1-camps	Epac2-camps	HCN2-camps
cAMP	2.53±0.34	1.0±0.2	9.1±2.1
Rp-cAMPS	48.0±5.3	22.5±7.3	-
Sp-cAMPS	4.8±0.5	1.3±0.2	-
8-pCPT-cAMP	0.04±0.01	0.09±0.02	26.7±11.7*
8-pCPT-2'-O-Me-cAMP	0.36±0.11	1.5±0.4	-
cGMP	6.7±1.4	6.3±2.1	10.3±1.8
6-MB-cAMP	1.2±0.1	0.63±0.14	1.9±0.8
6-MBC-cAMP	0.33±0.13	0.11±0.04	9.5±0.3*
Sp-8-PIP-cAMPS	55.2±6.3	7.5±2.0	3.0±1.6
8-Br-cAMP	0.13±0.02	0.15±0.05	0.9±0.5

In summary, the following conclusions can be drawn based on the comparative study of the conformational change induced by different compounds:

1. Numerous cAMP derivatives that had been thought selectively activate PKA are capable of inducing a conformational change also in Epac1, Epac2 and HCN2.

2. Sp-8-PIP-cAMPS, a site-selective PKA activator with a preference for the B-site is a partial agonist for the binding domains of Epac2 and HCN2.

3. Rp-cAMPS, an inhibitor of PKA, is a partial agonist for both Epac isoforms and has no major effect on HCN2.

4. A-site selective PKA-agonists, 6-MB-cAMP and 6-MBC-cAMP, are also full agonists for Epac1 and Epac2. 6-MB-cAMP is a partial agonist and 6-MBC-cAMP is an inhibitor for HCN2.

5. Epac selective substance 8-pCPT-2'-0-Me-cAMP does not activate HCN2.

The described properties of different derivatives should be taken into account when doing biochemical experiments using them to specifically activate distinct signalling cascades.

3.3   Development of cGMP biosensors

The single-domain cAMP sensors proved to be very sensitive and efficient in various biological applications. They have allowed to overcome the major drawbacks of an older system based on the entire kinase as a backbone for a sensor. The same problems of low sensitivity, large unstable architecture and unphysiologically slow kinetics are the case for GK-based sensors for cGMP (see 1.4). Here, it was sought to improve real-time fluorescent measurements of cGMP signaling by developing similar single-domain biosensors, in order to increase the sensitivity and to achieve a physiological level of performance.

3.3.1 GK-based cGMP sensors

Like in case of cAMP-binding proteins, GK has emerged to be not a unique binding partner of cGMP, which also binds to and activates PDEs and cGMP-gated channels. All three effector proteins have one or two regulatory domains to bind cGMP (see 1.1). Although the activation mechanisms of these domains are poorly understood and no conformational change has been described so far, based on the similarities in structure to cAMP-domains it could be assumed that cGMP-binding sites of GK and regulatory GAF-domains of PDEs might have similar mechanisms of activation. Therefore, it was tested whether the generation of similar single-domain biosensors is possible with the high and low affinity domains of GKI (Fig. 26A). Indeed, fusing YFP and CFP to the low affinity B domain resulted in constructs exhibiting a dynamic change in FRET, a minor increase in a E242-A350 or a larger decrease in a L231-A350 construct (Fig. 26B,C). Although affinities of these sensors for cGMP were comparable with cAMP-indicators and the full-length GK-probes (~ 1μM and ~ 5μM, respectively), they demonstrated an extremely slow speed of activation after stimulating transiently transfected cells expressing these sensors with high concentrations of an NO-donor (see Fig. 28B).

Fusing YFP and CFP to a single high affinity A domain of GKI (Fig. 26A) resulted in a sensor that demonstrated a decrease in FRET upon activation,
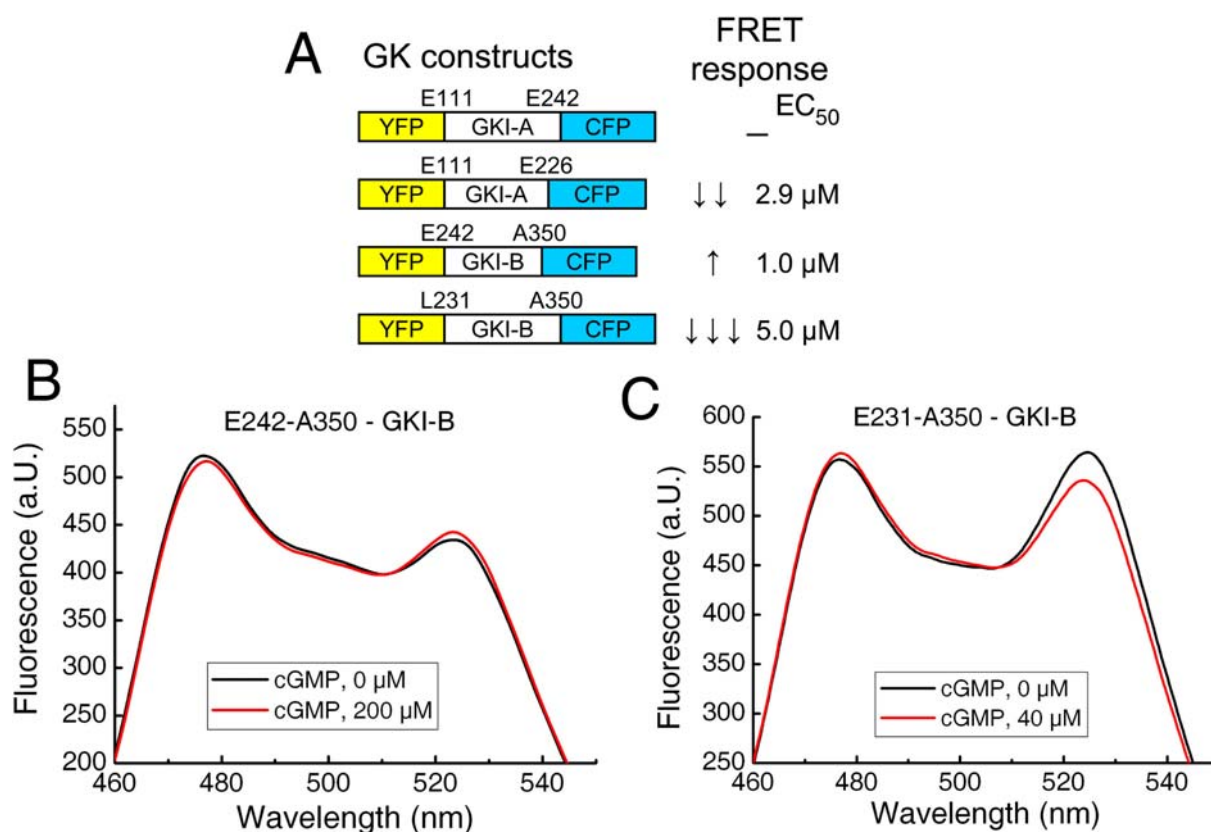
Fig. 26. Single-domain sensors based on GKI. **A.** Schematic representation of the constructs based on high affinity A and low affinity B domains of GKI. A relative change in FRET and EC$_{50}$ values for cGMP are presented. **B** and **C**. Fluorescent spectra of the sensor proteins based on the domain B of GKI taken as described in Fig. 7A from TsA201-cell lysates expressing two different constructs. Minor increase vs. decrease in FRET is shown. Representative spectra (n=4).

which was also very slow in live cells (see Fig. 28B). Such slow kinetics of the activation could argue for a poor performance of these GKI-based sensors or for a general "slow nature" of this binding site. Unfortunately, the crystal structure of GK has not been solved, so that it seems difficult to make any predictions on or to further optimize the structure of the sensor. Thus, another cGMP effector was, next, chosen as a backbone, namely PDE2, for which the structure is available[98].

3.3.2 Regulatory GAF-B domain of PDE2 as backbone for a cGMP-sensor

In PDE2 cGMP-binding to the regulatory GAF-B domain induces the catalytic activity. The structural architecture of this domain resembles that of the previously discussed cAMP-binding domains. The fluorophores were inserted on the α-helices covering the phosphate-binding cassette (Fig. 27A,B). This led to a functional sensor protein exhibiting a large increase in FRET upon binding cGMP (Fig. 27B). Importantly, the speed of the FRET-signals was high and comparable with single-domain cAMP-sensors (see Fig. 28B), allowing the use of the PDE2-based indicator to measure cGMP with high temporal resolution. To study the selectivity of the sensor, its binding affinities were compared for cGMP and cAMP, obtaining 0.9±0.1 and 115±17 µM, respectively, which corresponds to a >120:1 preference for cGMP (Fig. 27C). The novel PDE2 sensor exhibited slightly higher affinity and lower selectivity than the previously published *cygnets* sensors based on the GKI[146]. However, the speed of activation of GAF-B domain was faster compared to the single domains of GKI.

To further investigate the ability of the sensor to report fast changes of cGMP in live cells, we stimulated such cells with atrial natriuretic peptide and the NO-donor Na-nitroprusside (SNP). The PDE2-sensor was localized uniformly in the

cytosol of the cells and produced a rapid, reversible increase in FRET upon addition of ANP (Fig. 28A).
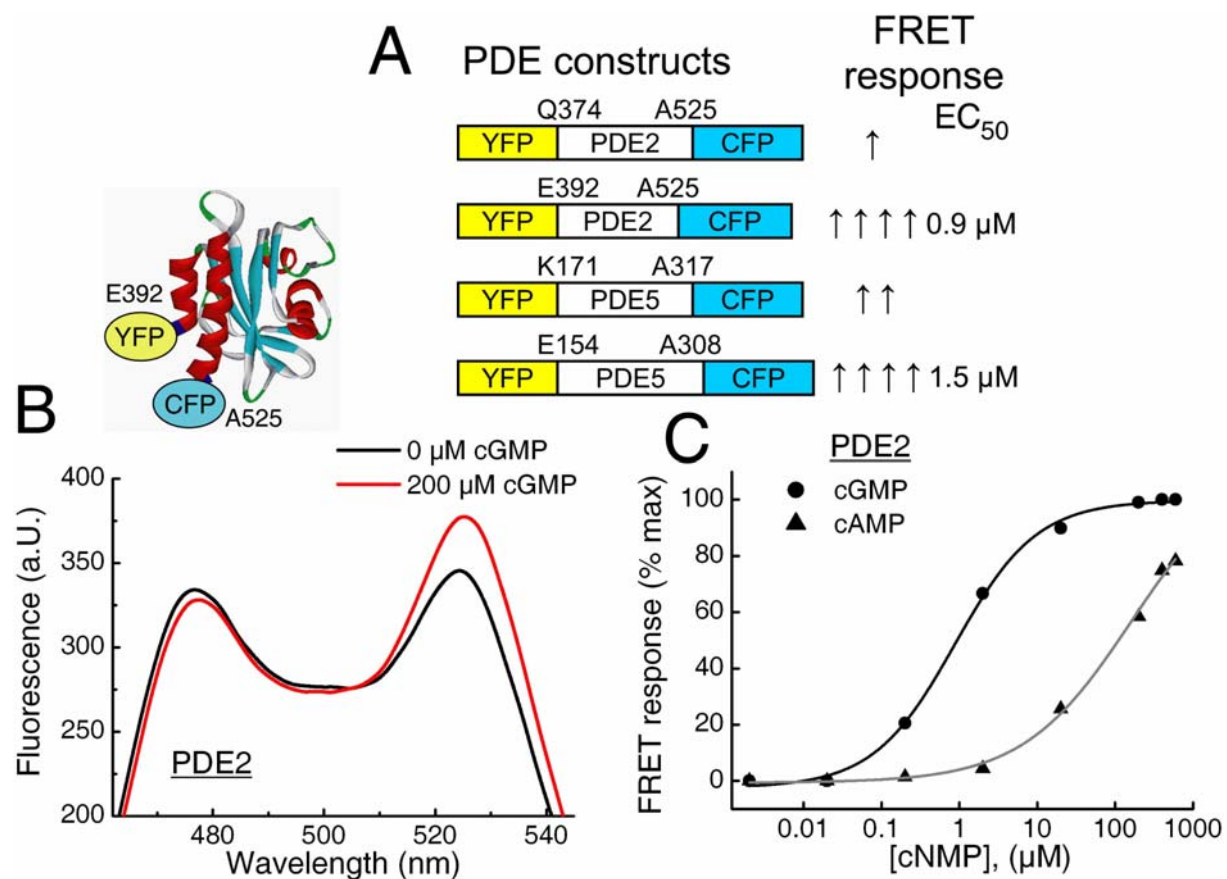
Fig. 27. Development of cGMP sensors based on a single binding domain of phosphodiesterase. A. Structure of the constructs for PDE-based sensors, which were designed in a way similar to single-domain camps (see 3.1). *B.* Schematic view and fluorescent spectra of PDE2-based sensor measured as described in Fig. 7A. *C.* Representative saturation curves of PDE2 sensor for cGMP and cAMP (n=3) measured as in Fig. 12. EC_{50}-values are stated in text.

The increase in FRET was observed already within a few seconds after simulation, and was present in virtually every cell transfected with the PDE2-sensor, demonstrating high robustness and temporal resolution of the single-
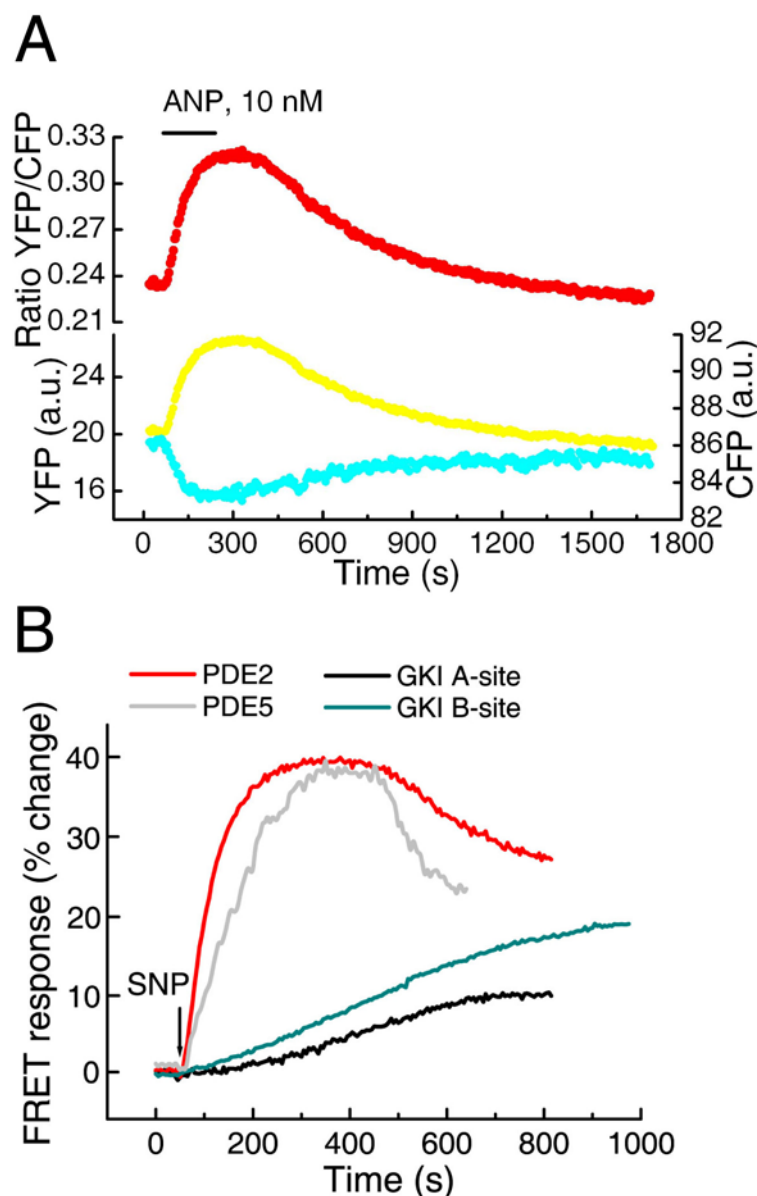
*Fig. 28. Measurements of cGMP in live cells using PDE2 sensor. **A.** Sample YFP, CFP intensity and ratio traces of HEK293 cells transiently transfected with the ANP receptor NPRA and the PDE2-sensor after ANP stimulation with subsequent withdrawal of the agonist (n=5). A reversible increase of FRET is observed. **B.** Comparing kinetics of cGMP-signals after stimulation of endogenous soluble GC in HEK293 cells with 50 µM SNP as reported by PDE2, PDE5 (see 3.3.3 below), GKI A-site (E111-E226) and B-site (L231-A350) sensors. Unphysiologically slow signals from GKI sensors are seen. Representative traces from at least 5 experiments.*

domain PDE2-based sensor. In contrast, the GK-based probes showed a much

inferior performance that became especially visible by comparing the speed of

signals from PDE2 and GKI-based indicators after NO-donor stimulation (Fig. 28B). A construct based on the high affinity A domain of GKI had a delay of 98.5 ± 24.9 s (n=13) (Fig. 28B), typical also for *cygnets*[146]. Moreover, this protein had a diffuse cytosolic localization only in a minor percentage of the cells. The sensor based on the low affinity B domain of GKI produced not a delayed but also a very slow signal (Fig. 28B). Therefore, the sensors based on the GKI seemed unsuitable for reliable measurements of intracellular cGMP. Their kinetic properties were significantly surpassed by creating a sensor based on a single GAF-B domain of PDE2.

3.3.3 Improving the selectivity of cGMP measurements. Sensor based on the GAF-A domain of PDE5

PDE2 is a dual-specific phosphodiesterase, which can be activated by higher cAMP concentrations (see 1.1 and Fig. 27C). To test whether the PDE2-sensor is switched on by cAMP in HEK293 cells, they were stimulated with saturating amounts of the β-adrenergic agonist isoproterenol, increasing cAMP concentrations in this cell type to higher μM values. Under these conditions, a minor signal was observed (Fig. 29A, top), demonstrating that the selectivity of the PDE2-sensor is not high enough and might lead to contamination of cGMP-FRET by cAMP in some applications.
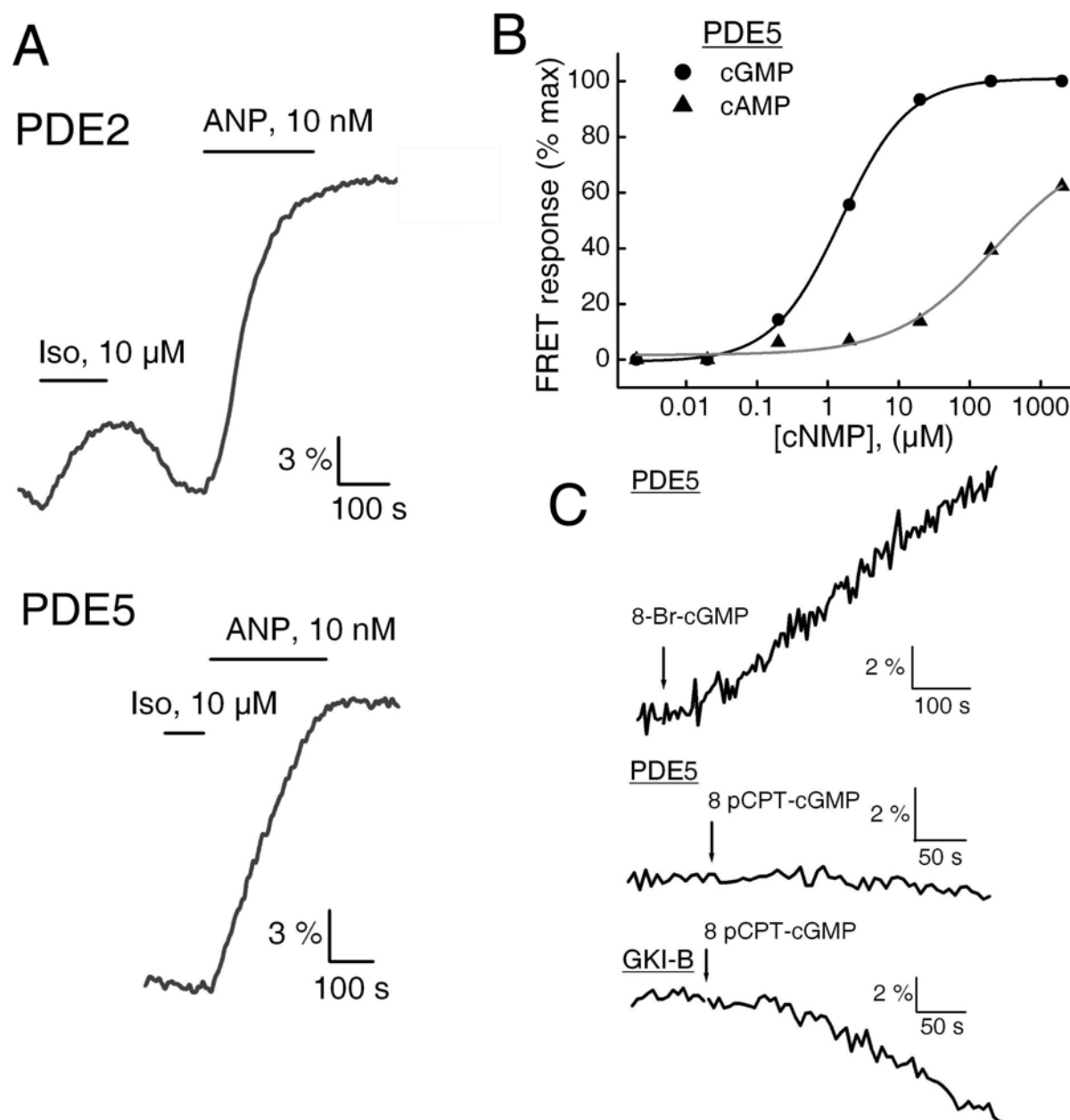
*Fig. 29. PDE5-based sensor demonstrates high selectivity for cGMP. **A.** Measurements with PDE2 (E392-A525)- and PDE5 (E154-A308)-based sensors upon full stimulation of cGMP- and cAMP-production in cells as described in Fig. 28A. PDE2-sensor shows a small signal to isoproterenol (Iso), whereas the PDE5-based sensor gives no apparent response to Iso (representative from n=4 cells). **B.** High selectivity of the PDE5-sensor was confirmed also by concentration-response curves measured in lysates of transiently transfected TsA201 cells as in Fig. 12. EC_{50}-values were 1.5±0.2 µM for cGMP and 630±100 µM for cAMP (n=3). **C.** Characterization of chemical selectivity of PDE5- and GK-B (L231-A350)-sensors using 8-Br-cGMP and 8-pCPT-cGMP (both 100 µM) in HEK293 cells transiently transfected with PDE5- or GKI (L231-A350)-constructs. Representative traces (n=5).*

To increase the selectivity for cGMP, the GAF-A binding domain of PDE5A1 was used, which is described as a cGMP-specific phosphodiesterase with a high selectivity for cGMP [99]. The position of fluorophore attachment was optimized based on the PDE2-sensor design and using the model structure of PDE5 GAF-A domain[183]. Several constructions were produced to obtain a sensor with an amplitude of the FRET signal similar to PDE2-probe (Fig. 27A). The PDE5-sensor demonstrated no apparent signal after cAMP pathway stimulation and almost similar kinetic properties as the PDE2-indicator (Fig. 29A, bottom). Indeed, the selectivity for cGMP was greatly improved as measured *in vitro*, exceeding 400:1 preference for cGMP, whereas cAMP in micromolar concentrations was not able to fully stimulate the sensor (Fig. 29B).

The next series of experiments aimed at a characterization of chemical selectivity of PDE- and GK-based sensors using cGMP analogs. 8-Br-cGMP, which is known as an agonist for GKI and PDEs[184], was also able to activate the PDE5-sensor (Fig. 29C) and PDE2 sensor (not shown). However, 8-pCPT-cGMP, which was described not to activate PDEs[184], did not produce any signal of the PDE5-sensor. In contrast, a single-domain GKI-sensor was activated by this analog (Fig. 29C), demonstrating that the sensors based on single cGMP-binding domains retain the biochemical properties of the unmodified binding sites and can differentiate between derivatives stimulating distinct cGMP-dependent signaling pathways.

In summary, novel cGMP sensors based on single GAF domains of PDE2 and 5 were created to achieve highly sensitive dynamic cGMP measurements with higher temporal resolution than have been described previously for kinase-based *cygnets*. Comparable to cAMP sensors, single-domain cGMP probes greatly improved cyclic nucleotide measurements in live cells, opening up new possibilities for physiological studies.

3.4 Applications of cGMP sensors

3.4.1 Spatio-temporal dynamics of cGMP production by soluble and membrane-bound guanylyl cyclases

Membrane-bound GC as an intracellular domain of the ANP receptor NPRA and soluble NO-activated GC represent two distinct types of enzymes, which exhibit different properties (see 1.1). For example, in cardiac myocytes different effects of CNP and SNP on contractility were observed that led to the hypothesis that NRPA-receptor signals are compartmentalized[185]. To analyze the spatio-temporal aspects of these two different signalling cascades, the kinetics of ANP and the NO-donor SNP signals were compared in HEK293 cells.

Interestingly, the speed of cGMP production after ANP stimulation was higher than after the addition of the NO-donor (Fig. 30). This behaviour of different GC types could be explained by the site of their intracellular localization. Membrane-bound GC is readily activated by ANP, which binds to the extracellular domain of the NPRA-receptor and through a conformational change activates the GC activity in the intracellular domain (see 1.1). Soluble GC, however, is activated by NO which applied extracellulary must first diffuse through the plasma membrane and into the cytosol of the cell to induce cGMP synthesis.
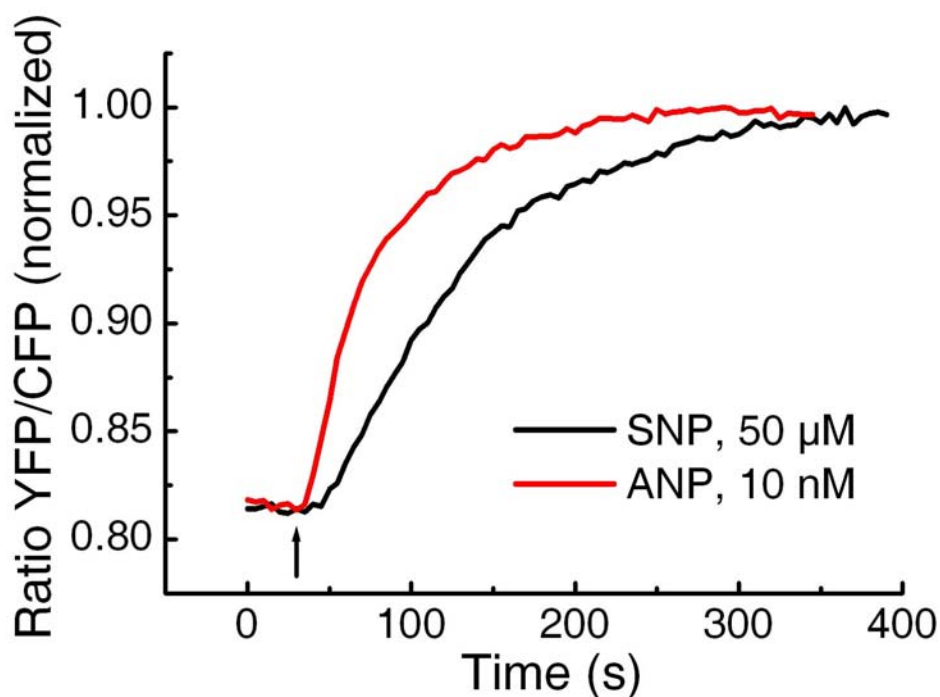
Fig. 30. Comparing kinetics of cGMP signals after stimulation of different GC types. HEK293 cells were transiently transfected with PDE2-sensor and NPRA receptor. Addition of ANP leads to a rapid increase of intracellular cGMP, whereas activation of endogenous soluble GC with SNP results in a slower cGMP accumulation in cells. Representative experiments from n=6 cells for each condition.

The differences in kinetics of cGMP production by different types of GC might be important for the functional compartmentation of cGMP action, providing higher concentrations of rapidly synthesized cGMP at the plasma membrane. In the HEK293 cells studied here, microscopic imaging showed no visible restriction of cGMP diffusion (not shown). After both ANP and SNP stimulation the whole cell altered its FRET, suggesting that the entire cytosol was filled with cGMP without apparent restricted domains. In general, similar diffusion patterns were monitored as for free cAMP-diffusion. To further analyze possibilities of compartmentation, more physiologically relevant cell types were used.

3.4.2 Characterization of cGMP signaling in mesangial cells

Having demonstrated high performance of the PDE5-sensor in HEK293 cells it was, next, studied how the sensor reports cGMP-dynamics in a physiologically relevant system. Mesangial cells of kidney glomerula represent a specialized type of smooth muscle cells, which regulates blood vessel tension in response to angiotensin as a vasoconstrictor and to ANP, NO, and cAMP-stimulating hormones, which induce vasodilatation[158]. Primary rat mesangial cells were isolated and transfected with PDE5-sensor without any additional manipulation to maintain physiological conditions for cGMP-production. Both ANP and SNP induced a rapid increase in FRET which is measurable already within 5 seconds

after stimulation (Fig. 31A), demonstrating high sensitivity and temporal resolution of the sensor.

Interestingly, in mesangial cells the FRET signals measured by PDE5-sensor were even bigger than in HEK293 cells (compare Figs. 28,29,31A), reaching up to 45 % ratio change after ANP and 55 % after SNP stimulation. The FRET-signals were fully reversible and did not demonstrate a long plateau at saturating concentrations of ANP and SNP (Fig. 31A), suggesting that the sensor has a large dynamic range to measure cGMP at physiologically relevant concentrations.

In contrast to HEK293 cells transfected with NPRA receptor (Fig. 30), SNP-induced cGMP signals in mesangial cells were faster than ANP signals (Fig. 31A), which might be due to a lower expression of endogenous ANP-receptors on these cells compared to the higher amounts of soluble GC. Full stimulation of cAMP production by isoproterenol produced a very small increase in FRET, which was negligible compared to cGMP-induced changes in PDE5-sensor ratio. It suggests a very high cAMP production induced by Iso in these cells which results in a minor activation of the PDE5-sensor (Fig. 31A).

Rapid functional effects of cGMP (and of cAMP, for comparison) in mesangial cells were also confirmed by analysis of the phosphorylation of the GK- and PKA-substrate protein, vasodilator-stimulated phosphoprotein (VASP). Isoproterenol (via PKA) and SNP or ANP (via GK) all cause phosphorylation of VASP as evidenced by a shift in electrophoretic mobility and by detection with
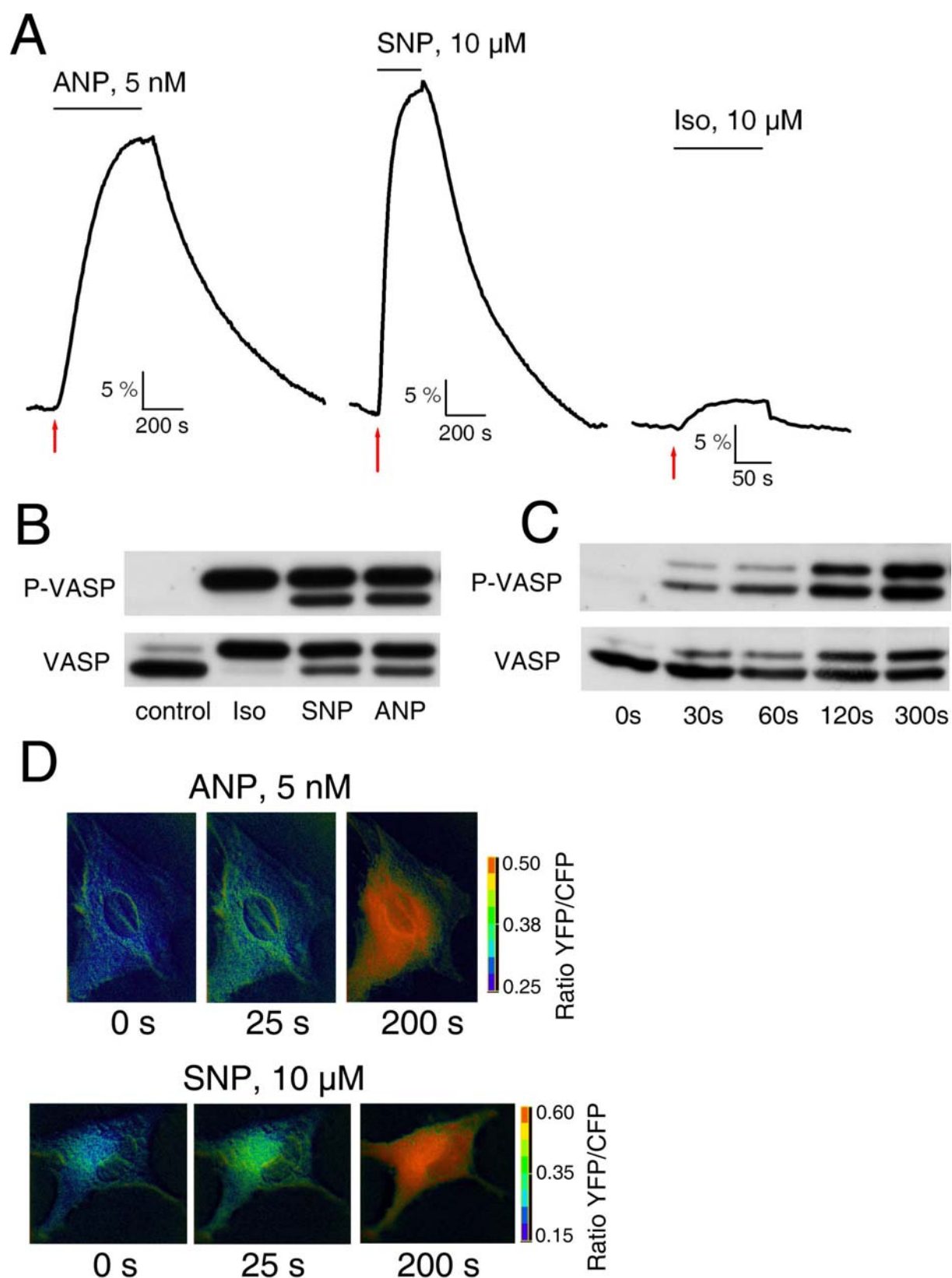
Fig. 31. Measuring cGMP-dynamics in primary rat mesangial cells. ***A.*** Monitoring reversible increases in cGMP after ANP and NO-donor stimulation in rat mesangial cells transiently transfected with the PDE5 (E154-A308)-sensor. Representative experiments (n=5) for each compound are shown. FRET-dynamics are presented as

a YFP/CFP ratio change in percent. Red arrow indicates the time-point of agonist application. *B.* Western blot analysis of GK substrate phosphorylation after incubating mesangial cells for 5 minutes with 10 µM Iso, 10 µM SNP or 5 nM ANP. The lower band of P-VASP represents the cGMP-mediated phosphorylation by GK, the upper band the PKA-induced phosphorylation. *C.* Time-dependent VASP-phosphorylation analyzed by Western blot after stimulation of mesangial cells with 50 µM SNP. Apparently already after 30 s GK phosphorylates its substrate. *D.* Cell imaging of intracellular cGMP in mesangial cells stimulated by ANP or SNP and visualized in real time by increases in FRET (YFP/CFP ratio) of the PDE5 sensor. Representative ratiometric images at different times after stimulation are presented (n=5).

phosphorylation-sensitive antibodies (Fig. 31B). Interestingly, GK-dependent VASP phosphorylation is visible already within 30 s after stimulation of cGMP production with SNP (Fig. 31C). Maximal phosphorylation was achieved after 2 minutes, demonstrating a correlation of phosphorylation kinetics (Fig. 31C) with cGMP-levels as measured with the PDE5-sensor (Fig. 31A).

Finally, imaging experiments in live mesangial cells were done for spatially and temporally resolved monitoring of cGMP-production (Fig. 31D). Already 25 s after application of ANP or SNP a visible change in cGMP was observed. In contrast, previously developed indicators did not allow to image cGMP elevations in a closely related cells type up to 200 s after activation[146]. The large increase of cGMP of mesangial cells reported by the PDE5-sensor was uniformly distributed in the cytosol without any evidence for compartmentation (Fig 31D).

In summary, using primary mesangial cells stimulated with ANP and SNP as a physiological model, it was demonstrated that the PDE5-sensor has high

sensitivity and a large dynamic range. It reports rapid changes in intracellular cGMP and demonstrates high amplitude (up to 55% dynamic change) of the FRET-signal, which allows to use the sensor for live cell imaging in order to study cGMP signalling with high spatial and temporal resolution.

4 Discussion

The present study aimed at developing effective methods for physiologically relevant imaging of cyclic nucleotide signaling in live cells. Classical biochemical techniques have unraveled the major elements and mechanisms of the intracellular signaling involving cAMP and cGMP. However, it remained unclear how the second messengers exert their effects in a living system, such as single cells of an organism, in terms of spatial and temporal regulation. The major question of the second messenger paradigm is how only two types of cyclic nucleotides can achieve high specificity and coordinated regulation of hundreds of proteins and intracellular functions. A hypothesis proposed in recent years suggests the compartmentation of signaling, which results in localized effects of cyclic nucleotides not equally distributed in cells via restriction of their diffusion by phosphodiesterase activity. The most commonly accepted explanation for local signaling events is that cyclic nucleotides can not freely diffuse on long distances from activated receptors, which are surrounded by PDEs that restrict cAMP- or cGMP-diffusion[124,186-188]. The detailed mechanisms of compartmentation, however, remain largely elusive. In the present work, new highly sensitive biosensors were developed to image cAMP- and cGMP-signaling in live cells and were applied to different physiologically relevant questions, including the characterization of phosphodiesterase activity as an

enzyme responsible for compartmentation. Another issue of the work was to delineate the mechanisms of interaction of cAMP and cGMP cascades at the level of phosphodiesterases. Moreover, using the sensors based on native binding domains of cAMP- and cGMP-regulated proteins, chemical and structural mechanisms of CNBD activation and specificity were addressed. Finally, clinically relevant methods of cAMP-detection were developed to screen for receptor autoantibodies as a cause of heart failure.

4.1   Family of single-domain biosensors for cyclic nucleotides

FRET-imaging has become a revolutionary approach to monitor biochemical signaling events in living systems. Based on GFP and its mutants various biosensors have been developed that allowed to visualize protein-protein interactions and conformational changes, thereby measuring receptor activation, G-protein dissociation, protein phosphorylation, intracellular dynamics of seconds messengers etc. The first biosensors for cAMP and cGMP were developed based on large molecules of protein kinases fused to GFP-mutants to monitor FRET, which was supposed to reflect changes in second messenger concentrations[123,142,146]. However, such sensors had limited performance and potential, which were the result of biochemical properties of these kinases.

PKA is a tetrameric holoenzyme comprised of regulatory and catalytic subunits which dissociate after binding of cAMP. The ligand binds to four different sites of the complex with different affinities, triggering a complex mechanism of enzyme activation occurring through a series of conformational changes that lead to release of catalytic subunits[23,24,153]. This particular later event, the dissociation of the complex, is monitored by using older fluorescent cAMP biosensors. The complex nature of this process results in an apparent delay of cyclic nucleotides signals. Moreover, the catalytic activity of the enzyme is directly involved in regulation of cAMP-levels via phosphorylation and, thereby, activation of PDE4. This is detrimental for reliable measurements. Furthermore, the whole PKA complex has an interaction interface with anchoring proteins, that target it to cell membranes and prevent unrestricted cAMP measurements in the cytosol. To overcome these various disadvantages a new approach was developed in this study, which for the first time was based on a single CNBD as a backbone for a fluorescent sensor to measure cAMP. The novel sensors took advantage of the prediction that cAMP induces a conformational change in the binding domain[152]. Based on the crystal structure of Epac2 a new sensor, Epac2-camps, was developed, which rapidly reported dynamic changes in intracellular cAMP upon receptor activation. The sensor had only one single cAMP-binding site, was deplete of catalytic and interacting domains and contained both fluorophores on one protein molecule allowing for easily detectable intramolecular FRET, which dynamically changed, in response

to cAMP-concentrations. The very first *in vitro* and live cell experiments demonstrated how much faster the cAMP-signals were detected by Epac2-camps compared to a previously published PKA-sensor. These data showed the poor performance of the kinase-based indicator, which due to sequential cooperative ligand binding and catalytic activity is not able to rapidly report changing cAMP-concentrations in cells. Single-domain Epac2-camps opened up new ways for cAMP-imaging. Based on the same principle, similar cAMP sensors were, next, developed using all cAMP-binding domains described up to date. From the Epac1-domain the Epac1-camps sensor was generated, which demonstrated the largest amplitude of the signal. A single binding domain of the HCN2-channel became part of HCN2-camps, which exhibited lower affinity for cAMP, allowing to extend the dynamic range of the sensors towards higher cAMP-concentrations. PKA domains B and A served as backbones for PKA-camps and the A-domain sensor, respectively. The latter was able to visualize not only cAMP-binding but also the interaction with the catalytic subunit. Later on, the crystal structure of this domain in complex with the catalytic subunit was solved and indeed proved a conformational change in the A domain as a mechanism of catalytic subunit release[24].

The developed single-chain cAMP-sensors proved useful in several applications. First, the spatio-temporal dynamics of cAMP were analyzed in different cell types (simple HEK293 cells, expressing various receptors, and hippocampal neurons) after stimulating cAMP-synthesis via different GPCRs. cAMP freely

diffused in the cytosol from the patch of activated receptors through the whole cell within a few hundred milliseconds without visible barriers. It was possible to calculate the speed of this diffusion and its coefficient, indicating a free unrestricted diffusion of cAMP (see 3.2.1). To better understand how compartmentation could be provided under this free cAMP diffusion, the activity of the major compartmentalizing enzymes, PDEs, was directly monitored in live adrenal cells on the basis of cAMP-hydrolysis. Interestingly, the kinetics of PDE2 action in these cells was enormously fast. Not only did PDE2 rapidly hydrolyze cAMP, but the speed of cAMP-degradation is even faster than the speed of cAMP synthesis in the continuing presence of forskolin, ACTH or adrenergic receptor agonist (see 3.2.2). Such properties of PDE characterize this enzyme as a very fast regulator of cAMP-concentrations in cells. Its high activity makes it capable of compartmentalizing cAMP-signaling. Why, then is there no evidence of cAMP-compartmentation in our cells? Constitutively active PDEs were described to be localized together with cAMP-targets such as PKA through interaction with AKAPs[145]. This colocalization of cAMP-targets with PDEs might just locally restrict the access of cAMP to PKA, Epac or channels, preventing their activation. In this case one would see free cAMP gradients propagating in the whole cell, which do not activate particular proteins in microdomains with a high PDE activity which are too small to be localized by light microscopy. This scenario might be the reason for the apparent unrestricted cAMP diffusion observed with Epac1-camps (see 3.2.1).

Only those sensors, which are themselves targeted to particular subcellular locations in close proximity with PDEs (PKA sensor or olfactory cyclic-nucleotide-gated channels used to measure cAMP), would then report compartmentation[124,186,188-190] because they are located inside such microdomains, protected from cAMP by PDEs, which create a kind of shelter zones or barriers for cyclic nucleotides coming from the outside where they diffuse freely. Such barriers would not allow the targets to be activated, even thought the second messenger is present around in the cytosol. This hypothesis might also explain a visible absence of barriers for cGMP (see 3.4.2). Another possibility would be that the cells used in the present study have no cAMP-compartments, which might be the case for highly specialized types of cells such as cardiomyocytes.

To image cGMP, novel sensors were developed based on single regulatory GAF domains of PDE2 and 5 (see 3.3). Similar to cAMP-sensors, single cGMP-binding domains yielded sensors which were, for the first time, able to report dynamic changes of cGMP on the physiologically relevant timescale. An older approach using a kinase-based indicator[146] was temporally limited: it produced extensive delays in its responses, whereas in reality during this time several cellular proteins such as GK (Fig. 30C), PDEs or channels are already activated. By creating single-domain probes in the present study it was demonstrated that the binding sites of GK fused to CFP and YFP, however, exhibit very slow kinetics and, therefore, could not be used to report rapidly changing cGMP-

concentrations. GAF-domains, on the contrary, produced sensors capable of measuring cGMP with high temporal resolution. Due to its physiological properties[98] the binding domain of PDE2 was not selective enough for cGMP, which led to a minor contamination of the FRET-signal in the presence of high concentrations of cAMP. To produce sensors of even higher selectivity, a single GAF-A domain of cGMP-specific PDE5 was, next, successfully used to create a highly selective cGMP sensor.

Having new cGMP imaging tools developed it was then attempted to characterize cGMP-compartmentation. Similar to the cAMP system, no visible restrictions for cGMP diffusion were observed after stimulation of both membrane-bound and soluble GC. In simple HEK293 cells as well as in more physiologically relevant mesangial cells, cGMP freely diffused in the cytosol and did not demonstrate any visible compartmentation, supporting the idea that compartmentation of the signaling by both cyclic nucleotide might be organized rather at the level of second messenger access to the effectors, than by restriction of their whole-cell diffusion. Another possibility could be the absence of the microdomains in this particular cell type.

The single-domain cyclic nucleotide sensors designed, developed and applied in the present study have allowed to overcome the major disadvantages typical for old generation of kinase-based indicators for cAMP and cGMP, which prevented them to be widely applied for live cell imaging (see 1.4):

1. The novel biosensors are single relatively small proteins which consist of a CNBD flanked with two GFP mutants. Thus, they can by easily transfected into mammalian cells and exhibit good expression levels. They can also be expressed in and purified from bacteria in fully functional state. The latter aspects might be important for large scale and low-expenditure purifications in order to measure cAMP or cGMP for drug development purposes (further discused in 4.3).

2. The single-domain biosensors lack the catalytic activity characteristic for PKA and GK, thereby excluding the possibility of interfering with biochemical processes in cells such as activation of negative "feed-back" mechanisms or phosphorylation of other proteins.

3. Biosensors developed in the present study (in contrast to PKA and GK) lack interacting domains which might anchor them to different subcellular locations, allowing to measure uniformly cytosolic cyclic nucleotide signals.

4. Single CNBD as a backbone for a sensor allows, for the first time, to measure true kinetics of cAMP and cGMP, maximally corresponding to physiological fluctuations of the second messengers in cells. This is achieved due to depletion of CNBD cooperativity and sequential binding of cAMP or cGMP to multiple sites in PKA and GK.

The development of single-domain biosensors for cyclic nucleotides became possible as a result of our understanding of the mechanisms of CNBD-activation, where the central role is played by the ligand-induced conformational change.

4.2 Conformational change as a ubiquitous activation mechanism of cAMP- and cGMP-regulated proteins

At the beginning of the cAMP-sensor development there were only a few indirect and rather intuitive evidences available that suggested a conformational change as a mechanism for CNBD-activation (see 1.5). It was mainly the work done by Holger Rehmann and Alfred Wittinghofer which presented at that time the first apo-structure of a CNBD of Epac2 [152]. Comparing this structure with the crystallographic data for binding domains of PKA in the presence of cAMP[25] the authors made a prediction that during CNBD activation a major conformational rearrangement should take place in the C-terminal helical part of the domain leading to release of the autoinhibited catalytic site of the protein[152]. A similar mechanism has been postulated for activation of GK by cGMP even though its crystal structure is unavailable[69].

Based on this proposed mechanism we started to construct cAMP-biosensors, which should monitor the conformational change in the high-affinity binding domain of Epac2 and thereby report changing cAMP-concentrations by means of FRET. In this study, FRET could be considered not only as a tool for molecular imaging and development of biosensors (see 1.2), but also as a method that allows to monitor conformational changes in protein molecules. Epac2-camps exhibited a conformational change dependent on cAMP-

concentrations, thereby proving the hypothesis of a conformational rearrangement as a mechanism of activation.

The next question that the study tried to address was whether the conformational change observed for Epac2 could be the case for other cAMP-binding proteins, representing a kind of ubiquitous mechanism of activation. Indeed, the development of Epac1-camps, HCN2-camps and the sensors based on single A and B domains of PKA confirmed a uniform universal mechanism of cAMP-induced sensor activation, which supports a common principle of regulation.

However, the fine mechanisms of the activation of different domains were distinct and dictated by their individual structure. This could be appreciated in chemical mapping experiments where different cAMP-derivatives were used to characterize conformational changes in CNBDs of Epac1, Epac2 and HCN2 (see 3.2.3). These experiments provided two important observations. First, the chemical selectivity of Epac1-camps determined by FRET was nearly identical to the native CNBD measured previously using biochemical techniques[176], nicely illustrating that positioning of GFP mutants on the CNBD did not alter the selectivity of the domain and did not disfavor its physiological binding and activation properties, allowing further domains (of Epac2 and HCN2) to be characterized in a similar way. Secondly, different substances behaved differently on the domains of Epacs and HCN2, again demonstrating distinct structure-dependent mechanisms of cAMP-binding. Several substances were identified that activated the HCN2-domain only partially or even induced a

conformational change opposite to that driven by cAMP. Further investigations might be needed to study how these compounds might affect the activity of the whole channel.

After the single-domain cAMP-sensors were developed and described[191], excellent crystallographic investigations performed in the group of Susan Taylor were presented, where the crystal structure of the same CNBD of PKA was solved in the absence and presence of the ligand, now unequivocally confirming the ligand-induced conformational change as a mechanism of PKA-activation. The first study demonstrated this mechanism for the B domain of PKA regulatory subunit[153]. The second investigation deal with the mechanism of activation of the A domain of PKA in the context of catalytic subunit release (see 1.5) [24]. Crystallographic data presented in this publication were in full agreement with the functional behavior of the sensor based on the A-site of PKA with respect to cAMP-binding and catalytic subunit release (see 3.1.2), indicating the similar scenario of cAMP-induced PKA complex activation (see 1.4).

Much less is known for cGMP-binding domains and their activation. Except for the crystal structure of cGMP-bound GAF-domains of PDE2 solved in Joseph Beavo's laboratory[98] and some other studies indirectly demonstrating conformational rearrangements in GK (discussed in 1.5) there was no further evidences which might characterize molecular mechanism of cGMP-domain activation. In the present work, several biosensors were developed based on a

conformational change of single binding domains of GK, PDE2 and PDE5 (see 3.3.). By creating these sensors, it was, for the first time, demonstrated that a cGMP-induced conformational change is present and might play a role in the activation of regulatory GAF domains of PDE2 and 5. Therefore, a cyclic nucleotide-induced conformational change seems to represent a central mechanism of CNBD activation for both cAMP and cGMP binding domains.

4.3 Clinically relevant applications of the cAMP and cGMP sensors

How can the sensors developed in this study be applied for purposes of contemporary pharmacy and medicine? As was mentioned in part 1.1, cAMP and cGMP as second messengers play pivotal roles in numerous physiological and pathological processes. cAMP-synthesis in cells is regulated by GPCRs, which represent the target of about one third of currently used drugs. The cGMP-system becomes constantly more attractive for therapeutic intervention, for example because hormones like ANP stimulate cGMP-synthesis which is beneficial for heart failure. Here, some possibilities will be considered how the single-domain cAMP- and cGMP-sensors could be applied for disease diagnostics and drug discovery.

One intriguing example of a disease where cAMP produced by adrenergic receptors plays a causative role in pathogenesis is autoimmune dilated

cardiomyopathy. This disease is often characterized by the production of activating antibodies against β_1-AR, which induce elevated cAMP production in cardiac myocytes leading to enhanced contractility and over extensive periods of time to development of heart failure. In the present study a diagnostic system has been established that allows to measure autoantibodies against β_1-AR in preparations from blood serum of DCM patients (see 3.2.3). A highly sensitive cAMP-sensor Epac1-camps transiently transfected in cells expressing β_1-AR served as an indicator for antibodies stimulating the receptor. The new system allows for reliable functional measurements and identification of autoantibodies in their ability to increase cAMP-levels in live cells. Compared to classical techniques such as ELISA or cAMP-RIA, the FRET-based approach demonstrates much higher sensitivity and reliability. It allows to detect antibodies in much greater number (up to 80 %) of patients with clinical symptoms of DCM. The cAMP-signals induced by autoantibodies could be largely blocked by β_1-AR antagonists, although not fully. Thus, the system is capable of analyzing efficacy of different therapeutic approaches for this disease and might be used in the near future for screening of new strategies and compounds to antagonize the detrimental effects of antibodies.

In principle, the biosensors developed here for cAMP and cGMP might be applied for screening of any potential therapeutically interesting compound that affects mechanisms of cAMP- and cGMP-synthesis and degradation. Beta-blockers are not the only examples of medicines which regulate cAMP-synthesis

via modulation of GPCR activity. Several further receptors are coupled to regulation of cAMP synthesis via G_s or G_i proteins such as serotonin and adenosine receptors used as targets for anti-inflammatory and anti-allergic drug or α-adrenergic receptors conveying blood pressure lowering effects of clonidine or modulation of blood vessel tone by oxymetazoline. For the development of new therapeutics acting at GPCRs, which are linked to cAMP-production, it is important to have reliable high-throughput systems for cAMP-measurements. Classical methods such as RIA are time-consuming and relatively expensive. They include the use of radioactivity and do not allow to measure cAMP with high temporal resolution. Fluorescent biosensors developed in this study, on the other hand, are capable of highly sensitive cAMP measurements with low cost, high sensitivity, temporal and spatial resolution. The goal of the near future would be to establish the technique in a high-throughput format on a microtiter plate, which perfectly works with purified sensor proteins but has not been developed so far for cell-based assays. This would allow to perform a fast screening of compounds which affect cAMP and to diagnostically test for anti-β_1-AR autoantibodies in large collectives of patients.

Strategies aimed at regulation of cGMP concentrations in cells have been gaining increased interest over the last years[192]. Natriuretic peptide hormones are used in medicine to increase cGMP in cardiac myocytes in order to counteract detrimental pathological mechanisms of heart failure and remodelling after cardiac infarction[193]. In addition to their cardioprotective properties natriuretic

peptides could also be applied as vasoprotective drugs[194]. The action of peptide hormones or other therapeutically promising compounds on cGMP-production in live cells could be monitored used the cGMP-biosensors developed in the present study (see 3.3).

Another interesting aspect of therapy is the use of drugs that regulate cAMP- and cGMP-hydrolysis by inhibiting different PDE isoforms. The most therapeutically relevant ones are PDE4 and PDE5. PDE4 inhibitors have been developed and are being successfully applied for the treatment of bronchial asthma, inflammatory and allergic diseases[195] or as antidepressants[196]. However, two very effective PDE4 inhibitors, rolipram and roflumilast, have been recently withdrawn from the marked due to their side effects. Now, novel PDE4 inhibitors should be developed, which dictates a need for sensitive screening techniques. In the present study, the activity of PDE2 was, for the first time, monitored in real time using a physiologically relevant cell system including its modulation by a selective inhibitor[197] (see 3.2.2). Epac-based cAMP-biosensors used to report PDE-induced cAMP-hydrolysis could be applied for screening of compounds acting at other PDE isoforms such as PDE4, thereby providing a measuring system for PDE4 inhibitors.

cGMP-dependent PDEs such as PDE5 represent another important target of therapeutics, for example sildenafil currently used to treat erectile dysfunction. The activity of PDE5 inhibitors might be also measured in real time in live cells using PDE-based cGMP-sensors developed in this study (see 3.3 and 3.4).

In summary, novel single-domain fluorescent biosensors for cAMP and cGMP could be effectively applied for the diagnostics of DCM-antibodies as well as for drug development, including high-throughput screening of therapeutically promising compounds that regulate cAMP- and cGMP-production (agonists and antagonists of GPCR and GCs) and hydrolysis (PDE inhibitors).

References

1.   Beavo, J. A. & Brunton, L. L. Cyclic nucleotide research -- still expanding after half a century. *Nat Rev Mol Cell Biol* **3**, 710-8 (2002).
2.   Sutherland, E. W., Jr. & Wosilait, W. D. Inactivation and activation of liver phosphorylase. *Nature* **175**, 169-70 (1955).
3.   Sutherland, E. W. & Wosilait, W. D. The relationship of epinephrine and glucagon to liver phosphorylase. I. Liver phosphorylase; preparation and properties. *J Biol Chem* **218**, 459-68 (1956).
4.   Ross, E. M. & Gilman, A. G. Reconstitution of catecholamine-sensitive adenylate cyclase activity: interactions of solubilized components with receptor-replete membranes. *Proc Natl Acad Sci U S A* **74**, 3715-9 (1977).
5.   Ross, E. M., Howlett, A. C. & Gilman, A. G. Identification and partial characterization of some components of hormone-stimulated adenylate cyclase. *Prog Clin Biol Res* **31**, 735-49 (1979).
6.   Ross, E. M. et al. Hormone-sensitive adenylate cyclase: resolution and reconstitution of some components necessary for regulation of the enzyme. *Adv Cyclic Nucleotide Res* **9**, 53-68 (1978).
7.   Ross, E. M. & Gilman, A. G. Resolution of some components of adenylate cyclase necessary for catalytic activity. *J Biol Chem* **252**, 6966-9 (1977).
8.   Pfeuffer, T. & Helmreich, E. J. Activation of pigeon erythrocyte membrane adenylate cyclase by guanylnucleotide analogues and separation of a nucleotide binding protein. *J Biol Chem* **250**, 867-76 (1975).
9.   Helmreich, E. J., Zenner, H. P. & Pfeuffer, T. Signal transfer from hormone receptor to adenylate cyclase. *Curr Top Cell Regul* **10**, 41-87 (1976).
10.   Pierce, K. L., Premont, R. T. & Lefkowitz, R. J. Seven-transmembrane receptors. *Nat Rev Mol Cell Biol* **3**, 639-50 (2002).
11.   Hepler, J. R. RGS protein and G protein interactions: a little help from their friends. *Mol Pharmacol* **64**, 547-9 (2003).
12.   Hollinger, S. & Hepler, J. R. Cellular regulation of RGS proteins: modulators and integrators of G protein signaling. *Pharmacol Rev* **54**, 527-59 (2002).
13.   Cooper, D. M. Regulation and organization of adenylyl cyclases and cAMP. *Biochem J* **375**, 517-29 (2003).
14.   Lamb, T. D. & Pugh, E. N., Jr. G-protein cascades: gain and kinetics. *Trends Neurosci* **15**, 291-8 (1992).
15.   Lee, K. A. Transcriptional regulation by cAMP. *Curr Opin Cell Biol* **3**, 953-9 (1991).
16.   Prasad, K. N. et al. Defects in cAMP-pathway may initiate carcinogenesis in dividing nerve cells: a review. *Apoptosis* **8**, 579-86 (2003).
17.   McLeod, S. J., Shum, A. J., Lee, R. L., Takei, F. & Gold, M. R. The Rap GTPases regulate integrin-mediated adhesion, cell spreading, actin polymerization, and Pyk2 tyrosine phosphorylation in B lymphocytes. *J Biol Chem* **279**, 12009-19 (2004).
18.   Ozaki, N. et al. cAMP-GEFII is a direct target of cAMP in regulated exocytosis. *Nat Cell Biol* **2**, 805-11 (2000).
19.   Holz, G. G. Epac: A new cAMP-binding protein in support of glucagon-like peptide-1 receptor-mediated signal transduction in the pancreatic beta-cell. *Diabetes* **53**, 5-13 (2004).
20.   Torgersen, K. M., Vang, T., Abrahamsen, H., Yaqub, S. & Tasken, K. Molecular mechanisms for protein kinase A-mediated modulation of immune function. *Cell Signal* **14**, 1-9 (2002).

21. Morozov, A. et al. Rap1 couples cAMP signaling to a distinct pool of p42/44MAPK regulating excitability, synaptic plasticity, learning, and memory. *Neuron* **39**, 309-25 (2003).

22. Zagotta, W. N. et al. Structural basis for modulation and agonist specificity of HCN pacemaker channels. *Nature* **425**, 200-5 (2003).

23. Taylor, S. S., Buechler, J. A. & Yonemoto, W. cAMP-dependent protein kinase: framework for a diverse family of regulatory enzymes. *Annu Rev Biochem* **59**, 971-1005 (1990).

24. Kim, C., Xuong, N. H. & Taylor, S. S. Crystal structure of a complex between the catalytic and regulatory (RIalpha) subunits of PKA. *Science* **307**, 690-6 (2005).

25. Diller, T. C., Madhusudan, Xuong, N. H. & Taylor, S. S. Molecular basis for regulatory subunit diversity in cAMP-dependent protein kinase: crystal structure of the type II beta regulatory subunit. *Structure (Camb)* **9**, 73-82 (2001).

26. Kopperud, R., Krakstad, C., Selheim, F. & Doskeland, S. O. cAMP effector mechanisms. Novel twists for an 'old' signaling system. *FEBS Lett* **546**, 121-6 (2003).

27. Kamp, T. J. & Hell, J. W. Regulation of cardiac L-type calcium channels by protein kinase A and protein kinase C. *Circ Res* **87**, 1095-102 (2000).

28. Yamaoka, K. & Kameyama, M. Regulation of L-type Ca2+ channels in the heart: overview of recent advances. *Mol Cell Biochem* **253**, 3-13 (2003).

29. Kawasaki, H. et al. A family of cAMP-binding proteins that directly activate Rap1. *Science* **282**, 2275-9 (1998).

30. de Rooij, J. et al. Epac is a Rap1 guanine-nucleotide-exchange factor directly activated by cyclic AMP. *Nature* **396**, 474-7 (1998).

31. Kawasaki, H. et al. A Rap guanine nucleotide exchange factor enriched highly in the basal ganglia. *Proc Natl Acad Sci U S A* **95**, 13278-83 (1998).

32. Ueno, H. et al. Characterization of the gene EPAC2: structure, chromosomal localization, tissue expression, and identification of the liver-specific isoform. *Genomics* **78**, 91-8 (2001).

33. Bos, J. L. Epac: a new cAMP target and new avenues in cAMP research. *Nat Rev Mol Cell Biol* **4**, 733-8 (2003).

34. Enserink, J. M. et al. A novel Epac-specific cAMP analogue demonstrates independent regulation of Rap1 and ERK. *Nat Cell Biol* **4**, 901-6 (2002).

35. Rangarajan, S. et al. Cyclic AMP induces integrin-mediated cell adhesion through Epac and Rap1 upon stimulation of the beta 2-adrenergic receptor. *J Cell Biol* **160**, 487-93 (2003).

36. Bos, J. L. et al. The role of Rap1 in integrin-mediated cell adhesion. *Biochem Soc Trans* **31**, 83-6 (2003).

37. Kang, G. et al. Epac-selective cAMP analog 8-pCPT-2'-O-Me-cAMP as a stimulus for Ca2+-induced Ca2+ release and exocytosis in pancreatic beta-cells. *J Biol Chem* **278**, 8279-85 (2003).

38. Holz, G. New insights concerning the glucose-dependent insulin secretagogue action of glucagon-like peptide-1 in pancreatic beta-cells. *Horm Metab Res* **36**, 787-94 (2004).

39. Robinson, R. B. & Siegelbaum, S. A. Hyperpolarization-activated cation currents: from molecules to physiological function. *Annu Rev Physiol* **65**, 453-80 (2003).

40. Biel, M., Schneider, A. & Wahl, C. Cardiac HCN channels: structure, function, and modulation. *Trends Cardiovasc Med* **12**, 206-12 (2002).

41. DiFrancesco, D. & Tortora, P. Direct activation of cardiac pacemaker channels by intracellular cyclic AMP. *Nature* **351**, 145-7 (1991).

42. Dremier, S., Kopperud, R., Doskeland, S. O., Dumont, J. E. & Maenhaut, C. Search for new cyclic AMP-binding proteins. *FEBS Lett* **546**, 103-7 (2003).

43. Kuhn, M. Structure, regulation, and function of mammalian membrane guanylyl cyclase receptors, with a focus on guanylyl cyclase-A. *Circ Res* **93**, 700-9 (2003).
44. Potter, L. R. & Hunter, T. Guanylyl cyclase-linked natriuretic peptide receptors: structure and regulation. *J Biol Chem* **276**, 6057-60 (2001).
45. Kuhn, M. Molecular physiology of natriuretic peptide signalling. *Basic Res Cardiol* **99**, 76-82 (2004).
46. He, X., Chow, D., Martick, M. M. & Garcia, K. C. Allosteric activation of a spring-loaded natriuretic peptide receptor dimer by hormone. *Science* **293**, 1657-62 (2001).
47. MacFarland, R. T., Zelus, B. D. & Beavo, J. A. High concentrations of a cGMP-stimulated phosphodiesterase mediate ANP-induced decreases in cAMP and steroidogenesis in adrenal glomerulosa cells. *J Biol Chem* **266**, 136-42 (1991).
48. Spat, A. & Hunyady, L. Control of aldosterone secretion: a model for convergence in cellular signaling pathways. *Physiol Rev* **84**, 489-539 (2004).
49. Pyriochou, A. & Papapetropoulos, A. Soluble guanylyl cyclase: more secrets revealed. *Cell Signal* **17**, 407-13 (2005).
50. Collier, J. & Vallance, P. Second messenger role for NO widens to nervous and immune systems. *Trends Pharmacol Sci* **10**, 427-31 (1989).
51. Kamisaki, Y. et al. Soluble guanylate cyclase from rat lung exists as a heterodimer. *J Biol Chem* **261**, 7236-41 (1986).
52. Harteneck, C., Koesling, D., Soling, A., Schultz, G. & Bohme, E. Expression of soluble guanylyl cyclase. Catalytic activity requires two enzyme subunits. *FEBS Lett* **272**, 221-3 (1990).
53. Buechler, W. A., Nakane, M. & Murad, F. Expression of soluble guanylate cyclase activity requires both enzyme subunits. *Biochem Biophys Res Commun* **174**, 351-7 (1991).
54. Chinkers, M. et al. A membrane form of guanylate cyclase is an atrial natriuretic peptide receptor. *Nature* **338**, 78-83 (1989).
55. Krupinski, J. et al. Adenylyl cyclase amino acid sequence: possible channel- or transporter-like structure. *Science* **244**, 1558-64 (1989).
56. Thorpe, D. S. & Morkin, E. The carboxyl region contains the catalytic domain of the membrane form of guanylate cyclase. *J Biol Chem* **265**, 14717-20 (1990).
57. Lincoln, T. M., Cornwell, T. L., Komalavilas, P. & Boerth, N. Cyclic GMP-dependent protein kinase in nitric oxide signaling. *Methods Enzymol* **269**, 149-66 (1996).
58. Juilfs, D. M., Soderling, S., Burns, F. & Beavo, J. A. Cyclic GMP as substrate and regulator of cyclic nucleotide phosphodiesterases (PDEs). *Rev Physiol Biochem Pharmacol* **135**, 67-104 (1999).
59. Pfeifer, A. et al. Structure and function of cGMP-dependent protein kinases. *Rev Physiol Biochem Pharmacol* **135**, 105-49 (1999).
60. Lincoln, T. M., Komalavilas, P., Boerth, N. J., MacMillan-Crow, L. A. & Cornwell, T. L. cGMP signaling through cAMP- and cGMP-dependent protein kinases. *Adv Pharmacol* **34**, 305-22 (1995).
61. Arshavsky, V. Y., Lamb, T. D. & Pugh, E. N., Jr. G proteins and phototransduction. *Annu Rev Physiol* **64**, 153-87 (2002).
62. Leskov, I. B. et al. The gain of rod phototransduction: reconciliation of biochemical and electrophysiological measurements. *Neuron* **27**, 525-37 (2000).
63. Pugh, E. N., Jr. & Lamb, T. D. Amplification and kinetics of the activation steps in phototransduction. *Biochim Biophys Acta* **1141**, 111-49 (1993).
64. Eigenthaler, M., Lohmann, S. M., Walter, U. & Pilz, R. B. Signal transduction by cGMP-dependent protein kinases and their emerging roles in the regulation of cell adhesion and gene expression. *Rev Physiol Biochem Pharmacol* **135**, 173-209 (1999).

65. Biel, M., Zong, X., Ludwig, A., Sautter, A. & Hofmann, F. Structure and function of cyclic nucleotide-gated channels. *Rev Physiol Biochem Pharmacol* **135**, 151-71 (1999).

66. Biel, M., Sautter, A., Ludwig, A., Hofmann, F. & Zong, X. Cyclic nucleotide-gated channels--mediators of NO:cGMP-regulated processes. *Naunyn Schmiedebergs Arch Pharmacol* **358**, 140-4 (1998).

67. Tamura, N. et al. cDNA cloning and gene expression of human type Ialpha cGMP-dependent protein kinase. *Hypertension* **27**, 552-7 (1996).

68. Orstavik, S. et al. Molecular cloning, cDNA structure, and chromosomal localization of the human type II cGMP-dependent protein kinase. *Biochem Biophys Res Commun* **220**, 759-65 (1996).

69. Lohmann, S. M., Vaandrager, A. B., Smolenski, A., Walter, U. & De Jonge, H. R. Distinct and specific functions of cGMP-dependent protein kinases. *Trends Biochem Sci* **22**, 307-12 (1997).

70. Uhler, M. D. Cloning and expression of a novel cyclic GMP-dependent protein kinase from mouse brain. *J Biol Chem* **268**, 13586-91 (1993).

71. Jarchau, T. et al. Cloning, expression, and in situ localization of rat intestinal cGMP-dependent protein kinase II. *Proc Natl Acad Sci U S A* **91**, 9426-30 (1994).

72. Pfeifer, A. et al. Intestinal secretory defects and dwarfism in mice lacking cGMP-dependent protein kinase II. *Science* **274**, 2082-6 (1996).

73. Raeymaekers, L., Eggermont, J. A., Wuytack, F. & Casteels, R. Effects of cyclic nucleotide dependent protein kinases on the endoplasmic reticulum Ca2+ pump of bovine pulmonary artery. *Cell Calcium* **11**, 261-8 (1990).

74. Komalavilas, P. & Lincoln, T. M. Phosphorylation of the inositol 1,4,5-trisphosphate receptor. Cyclic GMP-dependent protein kinase mediates cAMP and cGMP dependent phosphorylation in the intact rat aorta. *J Biol Chem* **271**, 21933-8 (1996).

75. Pryzwansky, K. B., Wyatt, T. A. & Lincoln, T. M. Cyclic guanosine monophosphate-dependent protein kinase is targeted to intermediate filaments and phosphorylates vimentin in A23187-stimulated human neutrophils. *Blood* **85**, 222-30 (1995).

76. Aszodi, A. et al. The vasodilator-stimulated phosphoprotein (VASP) is involved in cGMP- and cAMP-mediated inhibition of agonist-induced platelet aggregation, but is dispensable for smooth muscle function. *Embo J* **18**, 37-48 (1999).

77. Endo, S. et al. Molecular identification of human G-substrate, a possible downstream component of the cGMP-dependent protein kinase cascade in cerebellar Purkinje cells. *Proc Natl Acad Sci U S A* **96**, 2467-72 (1999).

78. Wang, G. R., Zhu, Y., Halushka, P. V., Lincoln, T. M. & Mendelsohn, M. E. Mechanism of platelet inhibition by nitric oxide: in vivo phosphorylation of thromboxane receptor by cyclic GMP-dependent protein kinase. *Proc Natl Acad Sci U S A* **95**, 4888-93 (1998).

79. Jahn, H., Nastainczyk, W., Rohrkasten, A., Schneider, T. & Hofmann, F. Site-specific phosphorylation of the purified receptor for calcium-channel blockers by cAMP- and cGMP-dependent protein kinases, protein kinase C, calmodulin-dependent protein kinase II and casein kinase II. *Eur J Biochem* **178**, 535-42 (1988).

80. Fukao, M. et al. Cyclic GMP-dependent protein kinase activates cloned BKCa channels expressed in mammalian cells by direct phosphorylation at serine 1072. *J Biol Chem* **274**, 10927-35 (1999).

81. Murthy, K. S. & Makhlouf, G. M. Identification of the G protein-activating domain of the natriuretic peptide clearance receptor (NPR-C). *J Biol Chem* **274**, 17587-92 (1999).

82. Rodriguez-Pascual, F., Ferrero, R., Miras-Portugal, M. T. & Torres, M. Phosphorylation of tyrosine hydroxylase by cGMP-dependent protein kinase in intact bovine chromaffin cells. *Arch Biochem Biophys* **366**, 207-14 (1999).

83. Surks, H. K. et al. Regulation of myosin phosphatase by a specific interaction with cGMP- dependent protein kinase Ialpha. *Science* **286**, 1583-7 (1999).

84. Lincoln, T. M., Dey, N. B., Boerth, N. J., Cornwell, T. L. & Soff, G. A. Nitric oxide--cyclic GMP pathway regulates vascular smooth muscle cell phenotypic modulation: implications in vascular diseases. *Acta Physiol Scand* **164**, 507-15 (1998).

85. Qian, Y. et al. cGMP-dependent protein kinase in dorsal root ganglion: relationship with nitric oxide synthase and nociceptive neurons. *J Neurosci* **16**, 3130-8 (1996).

86. Gray, D. B. et al. A nitric oxide/cyclic GMP-dependent protein kinase pathway alters transmitter release and inhibition by somatostatin at a site downstream of calcium entry. *J Neurochem* **72**, 1981-90 (1999).

87. Yawo, H. Involvement of cGMP-dependent protein kinase in adrenergic potentiation of transmitter release from the calyx-type presynaptic terminal. *J Neurosci* **19**, 5293-300 (1999).

88. Gudi, T. et al. Regulation of gene expression by cGMP-dependent protein kinase. Transactivation of the c-fos promoter. *J Biol Chem* **271**, 4597-600 (1996).

89. Gudi, T., Lohmann, S. M. & Pilz, R. B. Regulation of gene expression by cyclic GMP-dependent protein kinase requires nuclear translocation of the kinase: identification of a nuclear localization signal. *Mol Cell Biol* **17**, 5244-54 (1997).

90. Vaandrager, A. B., Bot, A. G. & De Jonge, H. R. Guanosine 3',5'-cyclic monophosphate-dependent protein kinase II mediates heat-stable enterotoxin-provoked chloride secretion in rat intestine. *Gastroenterology* **112**, 437-43 (1997).

91. Gambaryan, S. et al. Endogenous or overexpressed cGMP-dependent protein kinases inhibit cAMP-dependent renin release from rat isolated perfused kidney, microdissected glomeruli, and isolated juxtaglomerular cells. *Proc Natl Acad Sci U S A* **95**, 9003-8 (1998).

92. Gambaryan, S. et al. Expression of type II cGMP-dependent protein kinase in rat kidney is regulated by dehydration and correlated with renin gene expression. *J Clin Invest* **98**, 662-70 (1996).

93. Wagner, C., Pfeifer, A., Ruth, P., Hofmann, F. & Kurtz, A. Role of cGMP-kinase II in the control of renin secretion and renin expression. *J Clin Invest* **102**, 1576-82 (1998).

94. Conti, M. & Jin, S. L. The molecular biology of cyclic nucleotide phosphodiesterases. *Prog Nucleic Acid Res Mol Biol* **63**, 1-38 (1999).

95. Mehats, C., Andersen, C. B., Filopanti, M., Jin, S. L. & Conti, M. Cyclic nucleotide phosphodiesterases and their role in endocrine cell signaling. *Trends Endocrinol Metab* **13**, 29-35 (2002).

96. Corbin, J. D. & Francis, S. H. Cyclic GMP phosphodiesterase-5: target of sildenafil. *J Biol Chem* **274**, 13729-32 (1999).

97. McAllister-Lucas, L. M. et al. The structure of a bovine lung cGMP-binding, cGMP-specific phosphodiesterase deduced from a cDNA clone. *J Biol Chem* **268**, 22863-73 (1993).

98. Martinez, S. E. et al. The two GAF domains in phosphodiesterase 2A have distinct roles in dimerization and in cGMP binding. *Proc Natl Acad Sci U S A* **99**, 13260-5 (2002).

99. Zoraghi, R., Bessay, E. P., Corbin, J. D. & Francis, S. H. Structural and Functional Features in Human PDE5A1 Regulatory Domain That Provide for Allosteric cGMP Binding, Dimerization, and Regulation. *J Biol Chem* **280**, 12051-63 (2005).

100. Mongillo, M. et al. Fluorescence resonance energy transfer-based analysis of cAMP dynamics in live neonatal rat cardiac myocytes reveals distinct functions of compartmentalized phosphodiesterases. *Circ Res* **95**, 67-75 (2004).

101. Vaandrager, A. B. et al. Differential role of cyclic GMP-dependent protein kinase II in ion transport in murine small intestine and colon. *Gastroenterology* **118**, 108-14 (2000).

102. Conti, M. et al. Cyclic AMP-specific PDE4 phosphodiesterases as critical components of cyclic AMP signaling. *J Biol Chem* **278**, 5493-6 (2003).

103. Tsien, R. Y. The green fluorescent protein. *Annu Rev Biochem* **67**, 509-44 (1998).

104. Tsien, R. Y., Bacskai, B. J. & Adams, S. R. FRET for studying intracellular signalling. *Trends Cell Biol* **3**, 242-5 (1993).

105. Zhang, J., Campbell, R. E., Ting, A. Y. & Tsien, R. Y. Creating new fluorescent probes for cell biology. *Nat Rev Mol Cell Biol* **3**, 906-18 (2002).

106. Shaner, N. C. et al. Improved monomeric red, orange and yellow fluorescent proteins derived from Discosoma sp. red fluorescent protein. *Nat Biotechnol* **22**, 1567-72 (2004).

107. Wang, L., Jackson, W. C., Steinbach, P. A. & Tsien, R. Y. Evolution of new nonantibody proteins via iterative somatic hypermutation. *Proc Natl Acad Sci U S A* **101**, 16745-9 (2004).

108. Miyawaki, A. Fluorescence imaging of physiological activity in complex systems using GFP-based probes. *Curr Opin Neurobiol* **13**, 591-6 (2003).

109. Miyawaki, A. Visualization of the spatial and temporal dynamics of intracellular signaling. *Dev Cell* **4**, 295-305 (2003).

110. Zaccolo, M. Use of chimeric fluorescent proteins and fluorescence resonance energy transfer to monitor cellular responses. *Circ Res* **94**, 866-73 (2004).

111. Karasawa, S., Araki, T., Nagai, T., Mizuno, H. & Miyawaki, A. Cyan-emitting and orange-emitting fluorescent proteins as a donor/acceptor pair for fluorescence resonance energy transfer. *Biochem J* **381**, 307-12 (2004).

112. Matz, M. V. et al. Fluorescent proteins from nonbioluminescent Anthozoa species. *Nat Biotechnol* **17**, 969-73 (1999).

113. Pollok, B. A. & Heim, R. Using GFP in FRET-based applications. *Trends Cell Biol* **9**, 57-60 (1999).

114. Miyawaki, A. et al. Fluorescent indicators for Ca2+ based on green fluorescent proteins and calmodulin. *Nature* **388**, 882-7 (1997).

115. Truong, K. et al. FRET-based in vivo Ca2+ imaging by a new calmodulin-GFP fusion molecule. *Nat Struct Biol* **8**, 1069-73 (2001).

116. van der Wal, J., Habets, R., Varnai, P., Balla, T. & Jalink, K. Monitoring agonist-induced phospholipase C activation in live cells by fluorescence resonance energy transfer. *J Biol Chem* **276**, 15337-44 (2001).

117. Cicchetti, G., Biernacki, M., Farquharson, J. & Allen, P. G. A ratiometric expressible FRET sensor for phosphoinositides displays a signal change in highly dynamic membrane structures in fibroblasts. *Biochemistry* **43**, 1939-49 (2004).

118. Zhang, J., Ma, Y., Taylor, S. S. & Tsien, R. Y. Genetically encoded reporters of protein kinase A activity reveal impact of substrate tethering. *Proc Natl Acad Sci U S A* **98**, 14997-5002 (2001).

119. Ting, A. Y., Kain, K. H., Klemke, R. L. & Tsien, R. Y. Genetically encoded fluorescent reporters of protein tyrosine kinase activities in living cells. *Proc Natl Acad Sci U S A* **98**, 15003-8 (2001).

120. Sato, M., Ozawa, T., Inukai, K., Asano, T. & Umezawa, Y. Fluorescent indicators for imaging protein phosphorylation in single living cells. *Nat Biotechnol* **20**, 287-94 (2002).

121. Janetopoulos, C., Jin, T. & Devreotes, P. Receptor-mediated activation of heterotrimeric G-proteins in living cells. *Science* **291**, 2408-11 (2001).

122. Bunemann, M., Frank, M. & Lohse, M. J. Gi protein activation in intact cells involves subunit rearrangement rather than dissociation. *Proc Natl Acad Sci U S A* **100**, 16077-82 (2003).

123. Zaccolo, M. et al. A genetically encoded, fluorescent indicator for cyclic AMP in living cells. *Nat Cell Biol* **2**, 25-9 (2000).

124. Zaccolo, M. & Pozzan, T. Discrete microdomains with high concentration of cAMP in stimulated rat neonatal cardiac myocytes. *Science* **295**, 1711-5 (2002).

125. Elangovan, M. et al. Characterization of one- and two-photon excitation fluorescence resonance energy transfer microscopy. *Methods* **29**, 58-73 (2003).

126. Xia, Z. & Liu, Y. Reliable and global measurement of fluorescence resonance energy transfer using fluorescence microscopes. *Biophys J* **81**, 2395-402 (2001).

127. Creemers, T. M., Lock, A. J., Subramaniam, V., Jovin, T. M. & Volker, S. Photophysics and optical switching in green fluorescent protein mutants. *Proc Natl Acad Sci U S A* **97**, 2974-8 (2000).

128. Karpova, T. S. et al. Fluorescence resonance energy transfer from cyan to yellow fluorescent protein detected by acceptor photobleaching using confocal microscopy and a single laser. *J Microsc* **209**, 56-70 (2003).

129. Gadella, T. W., Jr. & Jovin, T. M. Oligomerization of epidermal growth factor receptors on A431 cells studied by time-resolved fluorescence imaging microscopy. A stereochemical model for tyrosine kinase receptor activation. *J Cell Biol* **129**, 1543-58 (1995).

130. Bastiaens, P. I. & Squire, A. Fluorescence lifetime imaging microscopy: spatial resolution of biochemical processes in the cell. *Trends Cell Biol* **9**, 48-52 (1999).

131. Elangovan, M., Day, R. N. & Periasamy, A. Nanosecond fluorescence resonance energy transfer-fluorescence lifetime imaging microscopy to localize the protein interactions in a single living cell. *J Microsc* **205**, 3-14 (2002).

132. Weiss, S. Measuring conformational dynamics of biomolecules by single molecule fluorescence spectroscopy. *Nat Struct Biol* **7**, 724-9 (2000).

133. Weiss, S. Fluorescence spectroscopy of single biomolecules. *Science* **283**, 1676-83 (1999).

134. Vilardaga, J. P., Bunemann, M., Krasel, C., Castro, M. & Lohse, M. J. Measurement of the millisecond activation switch of G protein-coupled receptors in living cells. *Nat Biotechnol* **21**, 807-12 (2003).

135. Hoffmann, C. et al. A FlAsH-based FRET approach to determine G protein-coupled receptor activation in living cells. *Nat Methods* **2**, 171-176 (2005).

136. Adams, S. R. et al. New biarsenical ligands and tetracysteine motifs for protein labeling in vitro and in vivo: synthesis and biological applications. *J Am Chem Soc* **124**, 6063-76 (2002).

137. Griffin, B. A., Adams, S. R., Jones, J. & Tsien, R. Y. Fluorescent labeling of recombinant proteins in living cells with FlAsH. *Methods Enzymol* **327**, 565-78 (2000).

138. Rudolf, R., Mongillo, M., Rizzuto, R. & Pozzan, T. Looking forward to seeing calcium. *Nat Rev Mol Cell Biol* **4**, 579-86 (2003).

139. Nagai, T., Yamada, S., Tominaga, T., Ichikawa, M. & Miyawaki, A. Expanded dynamic range of fluorescent indicators for Ca(2+) by circularly permuted yellow fluorescent proteins. *Proc Natl Acad Sci U S A* **101**, 10554-9 (2004).

140. Rudolf, R., Mongillo, M., Magalhaes, P. J. & Pozzan, T. In vivo monitoring of Ca(2+) uptake into mitochondria of mouse skeletal muscle during contraction. *J Cell Biol* **166**, 527-36 (2004).

141. Tanimura, A., Nezu, A., Morita, T., Turner, R. J. & Tojyo, Y. Fluorescent biosensor for quantitative real-time measurements of inositol 1,4,5-trisphosphate in single living cells. *J Biol Chem* **279**, 38095-8 (2004).

142. Adams, S. R., Harootunian, A. T., Buechler, Y. J., Taylor, S. S. & Tsien, R. Y. Fluorescence ratio imaging of cyclic AMP in single cells. *Nature* **349**, 694-7 (1991).

143. Bacskai, B. J. et al. Spatially resolved dynamics of cAMP and protein kinase A subunits in Aplysia sensory neurons. *Science* **260**, 222-6 (1993).

144. Hempel, C. M., Vincent, P., Adams, S. R., Tsien, R. Y. & Selverston, A. I. Spatio-temporal dynamics of cyclic AMP signals in an intact neural circuitm. *Nature* **384**, 166-9 (1996).

145. Scott, J. D. A-kinase-anchoring proteins and cytoskeletal signalling events. *Biochem Soc Trans* **31**, 87-9 (2003).

146. Honda, A. et al. Spatiotemporal dynamics of guanosine 3',5'-cyclic monophosphate revealed by a genetically encoded, fluorescent indicator. *Proc Natl Acad Sci U S A* **98**, 2437-42 (2001).

147. Sato, M., Hida, N., Ozawa, T. & Umezawa, Y. Fluorescent indicators for cyclic GMP based on cyclic GMP-dependent protein kinase Ialpha and green fluorescent proteins. *Anal Chem* **72**, 5918-24 (2000).

148. Ponsioen, B. et al. Detecting cAMP-induced Epac activation by fluorescence resonance energy transfer: Epac as a novel cAMP indicator. *EMBO Rep* **5**, 1176-80 (2004).

149. Zhao, J. et al. Progressive cyclic nucleotide-induced conformational changes in the cGMP-dependent protein kinase studied by small angle X-ray scattering in solution. *J Biol Chem* **272**, 31929-36 (1997).

150. Martinez, S. E., Beavo, J. A. & Hol, W. G. GAF Domains: Two-Billion-Year-Old Molecular Switches that Bind Cyclic Nucleotides. *Mol Interv* **2**, 317-23 (2002).

151. Martinez, S. E. et al. Crystal structure of the tandem GAF domains from a cyanobacterial adenylyl cyclase: Modes of ligand binding and dimerization. *Proc Natl Acad Sci U S A* **102**, 3082-7 (2005).

152. Rehmann, H. et al. Structure and regulation of the cAMP-binding domains of Epac2. *Nat Struct Biol* **10**, 26-32 (2003).

153. Wu, J., Brown, S., Xuong, N. H. & Taylor, S. S. RIalpha subunit of PKA: a cAMP-free structure reveals a hydrophobic capping mechanism for docking cAMP into site B. *Structure (Camb)* **12**, 1057-65 (2004).

154. Odaka, C., Mizuochi, T., Yang, J. & Ding, A. Murine macrophages produce secretory leukocyte protease inhibitor during clearance of apoptotic cells: implications for resolution of the inflammatory response. *J Immunol* **171**, 1507-14 (2003).

155. Dityatev, A., Dityateva, G. & Schachner, M. Synaptic strength as a function of post-versus presynaptic expression of the neural cell adhesion molecule NCAM. *Neuron* **26**, 207-17 (2000).

156. Gambaryan, S. et al. cGMP-dependent protein kinase type II regulates basal level of aldosterone production by zona glomerulosa cells without increasing expression of the steroidogenic acute regulatory protein gene. *J Biol Chem* **278**, 29640-8 (2003).

157. Gallo-Payet, N., Cote, M., Chorvatova, A., Guillon, G. & Payet, M. D. Cyclic AMP-independent effects of ACTH on glomerulosa cells of the rat adrenal cortex. *J Steroid Biochem Mol Biol* **69**, 335-42 (1999).

158. Burkhardt, M. et al. KT5823 inhibits cGMP-dependent protein kinase activity in vitro but not in intact human platelets and rat mesangial cells. *J Biol Chem* **275**, 33536-41 (2000).

159. Smolenski, A. et al. Functional analysis of cGMP-dependent protein kinases I and II as mediators of NO/cGMP effects. *Naunyn Schmiedebergs Arch Pharmacol* **358**, 134-9 (1998).

160. Rehmann, H., Rueppel, A., Bos, J. L. & Wittinghofer, A. Communication between the regulatory and the catalytic region of the cAMP-responsive guanine nucleotide exchange factor Epac. *J Biol Chem* **278**, 23508-14 (2003).

161. Rehmann, H., Schwede, F., Doskeland, S. O., Wittinghofer, A. & Bos, J. L. Ligand-mediated activation of the cAMP-responsive guanine nucleotide exchange factor Epac. *J Biol Chem* **278**, 38548-56 (2003).

162. Tasken, K. & Aandahl, E. M. Localized effects of cAMP mediated by distinct routes of protein kinase A. *Physiol Rev* **84**, 137-67 (2004).

163. Davare, M. A. et al. A beta2 adrenergic receptor signaling complex assembled with the Ca2+ channel Cav1.2. *Science* **293**, 98-101 (2001).

164. Arslan, G., Kull, B. & Fredholm, B. B. Signaling via A2A adenosine receptor in four PC12 cell clones. *Naunyn Schmiedebergs Arch Pharmacol* **359**, 28-32 (1999).

165. Chen, C., Nakamura, T. & Koutalos, Y. Cyclic AMP diffusion coefficient in frog olfactory cilia. *Biophys J* **76**, 2861-7 (1999).

166. Olson, A. & Pugh, E. N., Jr. Diffusion coefficient of cyclic GMP in salamander rod outer segments estimated with two fluorescent probes. *Biophys J* **65**, 1335-52 (1993).

167. Podzuweit, T., Nennstiel, P. & Muller, A. Isozyme selective inhibition of cGMP-stimulated cyclic nucleotide phosphodiesterases by erythro-9-(2-hydroxy-3-nonyl) adenine. *Cell Signal* **7**, 733-8 (1995).

168. Mery, P. F., Pavoine, C., Pecker, F. & Fischmeister, R. Erythro-9-(2-hydroxy-3-nonyl)adenine inhibits cyclic GMP-stimulated phosphodiesterase in isolated cardiac myocytes. *Mol Pharmacol* **48**, 121-30 (1995).

169. Freedman, N. J. & Lefkowitz, R. J. Anti-beta(1)-adrenergic receptor antibodies and heart failure: causation, not just correlation. *J Clin Invest* **113**, 1379-82 (2004).

170. Mobini, R. et al. Probing the immunological properties of the extracellular domains of the human β1-adrenoceptor. *J. Autoimmun.* **13**, 179-186. (1999).

171. Jahns, R. et al. Direct evidence for a β1-adrenergic receptor directed autoimmune attack as a cause of idiopathic dilated cardiomyopathy. *J. Clin. Invest.* **113**, 1419-1439 (2004).

172. Jahns, R. et al. Autoantibodies activating human beta1-adrenergic receptors are associated with reduced cardiac function in chronic heart failure. *Circulation* **99**, 649-54 (1999).

173. Mobini, R. et al. Probing the immunological properties of the extracellular domains of the human beta(1)-adrenoceptor. *J Autoimmun* **13**, 179-86 (1999).

174. Staudt, A. et al. Potential role of autoantibodies belonging to the immunoglobulin G-3 subclass in cardiac dysfunction among patients with dilated cardiomyopathy. *Circulation* **106**, 2448-53 (2002).

175. Christ, T. et al. Autoantibodies against the beta1 adrenoceptor from patients with dilated cardiomyopathy prolong action potential duration and enhance contractility in isolated cardiomyocytes. *J Mol Cell Cardiol* **33**, 1515-25 (2001).

176. Christensen, A. E. et al. cAMP analog mapping of Epac1 and cAMP kinase. Discriminating analogs demonstrate that Epac and cAMP kinase act synergistically to promote PC-12 cell neurite extension. *J Biol Chem* **278**, 35394-402 (2003).

177. Dostmann, W. R. et al. Probing the cyclic nucleotide binding sites of cAMP-dependent protein kinases I and II with analogs of adenosine 3',5'-cyclic phosphorothioates. *J Biol Chem* **265**, 10484-91 (1990).

178. Sugita, S., Baxter, D. A. & Byrne, J. H. cAMP-independent effects of 8-(4-parachlorophenylthio)-cyclic AMP on spike duration and membrane currents in pleural sensory neurons of Aplysia. *J Neurophysiol* **72**, 1250-9 (1994).

179. Connolly, B. J., Willits, P. B., Warrington, B. H. & Murray, K. J. 8-(4-Chlorophenyl)thio-cyclic AMP is a potent inhibitor of the cyclic GMP-specific phosphodiesterase (PDE VA). *Biochem Pharmacol* **44**, 2303-6 (1992).

180. Ogreid, D., Ekanger, R., Suva, R. H., Miller, J. P. & Doskeland, S. O. Comparison of the two classes of binding sites (A and B) of type I and type II cyclic-AMP-dependent protein kinases by using cyclic nucleotide analogs. *Eur J Biochem* **181**, 19-31 (1989).

181. Ogreid, D. et al. (Rp)- and (Sp)-8-piperidino-adenosine 3',5'-(cyclic)thiophosphates discriminate completely between site A and B of the regulatory subunits of cAMP-dependent protein kinase type I and II. *Eur J Biochem* **221**, 1089-94 (1994).

182. Berman, H. M. et al. The cAMP binding domain: an ancient signaling module. *Proc Natl Acad Sci U S A* **102**, 45-50 (2005).

183. Sopory, S., Balaji, S., Srinivasan, N. & Visweswariah, S. S. Modeling and mutational analysis of the GAF domain of the cGMP-binding, cGMP-specific phosphodiesterase, PDE5. *FEBS Lett* **539**, 161-6 (2003).

184. Butt, E. et al. Analysis of the functional role of cGMP-dependent protein kinase in intact human platelets using a specific activator 8-para-chlorophenylthio-cGMP. *Biochem Pharmacol* **43**, 2591-600 (1992).

185. Su, J., Scholz, P. M. & Weiss, H. R. Differential effects of cGMP produced by soluble and particulate guanylyl cyclase on mouse ventricular myocytes. *Exp Biol Med (Maywood)* **230**, 242-50 (2005).

186. Rich, T. C. et al. A uniform extracellular stimulus triggers distinct cAMP signals in different compartments of a simple cell. *Proc Natl Acad Sci U S A* **98**, 13049-54 (2001).

187. Houslay, M. D. & Adams, D. R. PDE4 cAMP phosphodiesterases: modular enzymes that orchestrate signalling cross-talk, desensitization and compartmentalization. *Biochem J* **370**, 1-18 (2003).

188. Rochais, F. et al. Negative feedback exerted by cAMP-dependent protein kinase and cAMP phosphodiesterase on subsarcolemmal cAMP signals in intact cardiac myocytes: an in vivo study using adenovirus-mediated expression of CNG channels. *J Biol Chem* **279**, 52095-105 (2004).

189. Rich, T. C., Tse, T. E., Rohan, J. G., Schaack, J. & Karpen, J. W. In vivo assessment of local phosphodiesterase activity using tailored cyclic nucleotide-gated channels as cAMP sensors. *J Gen Physiol* **118**, 63-78 (2001).

190. Rich, T. C. & Karpen, J. W. Review article: cyclic AMP sensors in living cells: what signals can they actually measure? *Ann Biomed Eng* **30**, 1088-99 (2002).

191. Nikolaev, V. O., Bunemann, M., Hein, L., Hannawacker, A. & Lohse, M. J. Novel single chain cAMP sensors for receptor-induced signal propagation. *J Biol Chem* **279**, 37215-8 (2004).

192. Schlossmann, J. & Hofmann, F. cGMP-dependent protein kinases in drug discovery. *Drug Discov Today* **10**, 627-34 (2005).

193. Soeki, T. et al. C-type natriuretic peptide, a novel antifibrotic and antihypertrophic agent, prevents cardiac remodeling after myocardial infarction. *J Am Coll Cardiol* **45**, 608-16 (2005).

194. Rademaker, M. T. & Richards, A. M. Cardiac natriuretic peptides for cardiac health. *Clin Sci (Lond)* **108**, 23-36 (2005).

195. Lipworth, B. J. Phosphodiesterase-4 inhibitors for asthma and chronic obstructive pulmonary disease. *Lancet* **365**, 167-75 (2005).

196.   O'Donnell, J. M. & Zhang, H. T. Antidepressant effects of inhibitors of cAMP phosphodiesterase (PDE4). *Trends Pharmacol Sci* **25**, 158-63 (2004).

197.   Nikolaev, V. O., Gambaryan, S., Engelhardt, S., Walter, U. & Lohse, M. J. Real-time monitoring of the PDE2 activity of live cells: hormone-stimulated cAMP hydrolysis is faster than hormone-stimulated cAMP synthesis. *J Biol Chem* **280**, 1716-9 (2005).

Liste eigener Publikationen zum Thema der Doktorarbeit

1.   Nikolaev, V. O., Bunemann, M., Hein, L., Hannawacker, A. & Lohse, M. J. Novel single chain cAMP sensors for receptor-induced signal propagation. *J Biol Chem* **279**, 37215-8 (2004).

2.   Nikolaev, V. O., Gambaryan, S., Engelhardt, S., Walter, U. & Lohse, M. J. Real-time monitoring of the PDE2 activity of live cells: hormone-stimulated cAMP hydrolysis is faster than hormone-stimulated cAMP synthesis. *J Biol Chem* **280**, 1716-9 (2005).

3.   Landa, L. R., Jr., Harbeck, M., Kaihara, K., Chepurny, O., Kitiphongspattana, K., Graf, O., Nikolaev, V. O., Lohse, M. J., Holz, G. G. & Roe, M. W. Interplay of Ca2+ and cAMP signaling in the insulin-secreting MIN6 beta -cell line. *J Biol Chem* **280**, 31294-31302 (2005).

Summary

The cyclic nucleotides cAMP and cGMP are two ubiquitous important second messengers, which regulate diverse physiological responses from vision and memory to blood pressure and thrombus formation. They act in cells via cAMP- and cGMP-dependent protein kinases (PKA and GK), cyclic nucleotide-gated channels and Epac. Although the concept of cyclic nucleotide signalling is well developed based on classical biochemical studies, these techniques have not allowed to analyze cAMP and cGMP in live cells with high temporal and spatial resolution.

In the present study fluorescence resonance energy transfer was used to develop a technique for visualization of cAMP and cGMP in live cells and *in vitro* by means of fluorescent biosensors. Ligand-induced conformational change in a single nucleotide-binding domain flanked with green fluorescent protein mutants was used for dynamic, highly sensitive measurements of cAMP and cGMP. Such biosensors retained binding properties and chemical specificity of unmodified domains, allowing to image cyclic nucleotides in a physiologically relevant range of concentrations. To develop cAMP-sensors, binding domains of PKA, Epac and cAMP-gated HCN-channel were used. cGMP-sensors were based on single domains of GK and phosphodiesterases (PDEs)

Sensors based on Epac were used to analyze spatio-temporal dynamics of cAMP in neurons and macrophages, demonstrating that cAMP-gradients travel with a high speed (~ 40 µm/s) throughout the entire cytosol. To understand the mechanisms of cAMP-compartmentation, kinetics properties of phosphodiesterase (PDE2) were, next, analyzed in aldosterone producing cells. PDE2 is able to rapidly hydrolyze extensive amounts of cAMP, so that the speed of cAMP-hydrolysis is much faster than that of its synthesis, which might serve as a basis of compartmentation. cAMP-sensors were also used to develop a clinically relevant diagnostic method for reliable detection of β_1-adrenergic receptor autoantibodies in cardiac myopathy patients, which has allowed to significantly increase the sensitivity of previously developed diagnostic approaches.

Conformational change in a single binding domain of GK and PDE was, next, used to create novel fluorescent biosensors for cGMP. These sensors demonstrated high spatio-temporal resolution and were applied to analyze rapid dynamics of cGMP production by soluble and particulate guanylyl cyclases as well as to image cGMP in mesangial cells.

In summary, highly sensitive biosensors for cAMP and cGMP based on single cyclic nucleotide-binding domains have been developed and used in various biological and clinically relevant applications.

Zusammenfassung

Die zyklischen Nukleotide cAMP and cGMP sind zwei ubiquitäre Botenstoffe, die verschiedene physiologische Prozesse regulieren, vom Sehen und Gedächtnis bis zu Blutdruck und Thrombusbildung. Sie wirken über cAMP- und cGMP-abhängige Kinasen (PKA und GK), Kanäle und Epac. Obgleich die Funktionen von zyklischen Nukleotiden in klassischen biochemischen Studien gut untersucht sind, ermöglichen diese Methoden nicht, cAMP und cGMP in lebenden Zellen mit hoher zeitlicher und räumlicher Auflösung zu analysieren.

In dieser Arbeit wurde Fluoreszenzresonanzenergietransfer benutzt, um eine Technik für die Visualisierung von cAMP and cGMP in lebenden Zellen und *in vitro* zu entwickeln. Ligand-induzierte Konformationsänderung in einer einzelnen, mit Grünfluoreszenzproteinmutanten fusionierten Bindungsdomäne diente als Grundlage für Biosensoren, die dynamische, hochsensitive Messungen von cAMP und cGMP ermöglichen. Bei solchen Sensoren wurden die chemischen und Bindungseigenschaften von unmodifizierten Domänen aufrechterhalten, was die cAMP- und cGMP-Messungen im physiologischen Konzentrationsbereich in lebenden Zellen ermöglicht. Für die Entwicklung der cAMP-Sensoren wurden die Domänen von PKA, Epac und von einem cAMP-gesteuerten HCN-Kanal benutzt. cGMP-Sensoren beruhen sich auf den Bindungsdomänen von GK und Phosphodiesterasen (PDEs).

Mit Hilfe der auf Epac-basierten Sensoren wurde die cAMP-Dynamik in Neuronen und Makrophagen zeitlich und räumlich aufgelöst. In diesen Zellen diffundiert cAMP mit hoher Geschwindigkeit (~ 40 µm/s) frei durch das ganze Zytosol. Um die Mechanismen der cAMP-Kompartimentierung besser zu verstehen, wurden die kinetischen Eigenschaften der PDE2 in aldosteronproduzierenden Zellen analysiert. PDE2 ist imstande, große Mengen von cAMP äußerst schnell zu hydrolisieren, so dass die Geschwindigkeit der cAMP-Hydrolyse viel höher ist als von cAMP-Synthese, was eine Grundlage der cAMP-Kompartimentierung sein könnte. cAMP-Sensoren wurden auch benutzt, um eine klinisch relevante diagnostische Methode zu entwickeln, die Autoantikörper gegen β_1-adrenergen Rezeptoren bei Herzinsuffizienzpatienten zuverlässig nachweist. Diese Methode hat ermöglicht, die Sensitivität der früher entwickelten Techniken zu verbessern.

Konformationsänderung in einzelnen Bindungsdomänen von GK und PDE wurde als nächstes benutzt, um ein Reihe neuer fluoreszierender Biosensoren für cGMP zu entwickeln. Diese Sensoren zeigten hohe räumliche und zeitliche Auslösung und wurden zur Analyse schneller Dynamik von cGMP-Synthese und für cGMP-Imaging in Mesangialzellen angewandt.

Zusammenfassend wurden hochsensitive Biosensoren für cAMP und cGMP auf Grund einzelner, mit Grünfluoreszenzproteinmutanten fusionierter Bindungsdomäne entwickelt und in verschiedenen biologischen und klinisch relevanten Applikationen eingesetzt.

Danksagung

Danke Herr Prof. Martin Lohse für die Bereitstellung des interessanten Themas und die umfassende Betreuung während dieser Doktorarbeit.

Danke Frau Prof. Ulrike Holzgrabe für die nette Betreuung an der Fakultät für Chemie und Pharmazie.

Danke Herr Dr. Moritz Bünemann, Dr. Stefan Engelhardt und Frau Annette Hannawacker für die intensive Beratung und die wertvollen Hinweise bei allen auftretenden Problemen.

Danke allen Mitarbeiter des Instituts für Pharmakologie und Toxikologie für ihre Hilfsbereitschaft und eine schöne Zeit während der Doktorarbeit.

Danke allen Verwandten und Freunden für ihre einfühlsame Unterstützung und Verständnis.

Lebenslauf

Persönliche Daten

Name	Viacheslav Olegowitsch Nikolaev
Geburtsdatum	18.03.1980
Geburtsort	Leningrader Gebiet, Smerdi
Staatsangehörigkeit	russisch
Familienstand	ledig

Ausbildung

1987-1992	Schule 200, Leningrad
1992-1995	Gymnasium 293, St. Petersburg
1995-1997	Gymnasium 272, St. Petersburg
	Abschluss: Abitur
1997-2002	Studium der Pharmazie and der St. Petersburger Staatlichen Chemisch-Pharmazeutischen Akademie
July 2002 – Dezember 2002	Wissenschaftliches Praktikum, Biozentrum der Martin-Luther-Universität Halle Betreuung: Prof. Dr. Dr. h.c. Meinhart H. Zenk
Seit Januar 2003	Promotion, Institut für Pharmakologie und Toxikologie der Julius-Maximilians-Universität Würzburg Betreuung: Prof. Dr. Martin J. Lohse